NATIONAL TELECOMMUNICATIONS AND INFORMATION ADMINISTRATION

Institute for Telecommunication Sciences
Boulder, Colorado 80303

Technical Evaluation of the 2.45 and 5.8 GHZ ISM Bands for Intelligent Vehicle Highway Systems

A. D. Spaulding

Table of Contents

List of Figures

List of Tables

Technical Evaluation of the 2.45 and 5.8 GHz ISM Bands for Intelligent Vehicle Highway Systems

A.D. Spaulding

1. Introduction

IVHS Electronic Toll and Traffic Management (ETTM) Systems will involve very large numbers of electronic equipment in vehicles and along the roadside. These systems and others will be used for communication, toll collection, traffic management, vehicle location, traveler information, and many other uses. Many current ETTM systems operate in the 902-928 MHZ band. This band is currently becoming crowded, and many compatibility problems with existing systems are arising. Other frequencies, up to around 6 GHz, need to be considered for the additional oncoming ETTM and related systems. The 5.8 GHz ISM band (5800 + 75 MHZ) appears to be a desirable alternative since currently it is little used, and not widely used geographically. Also, the European Common Market is proposing to operate their ETTM systems in this ISM band. The 2.45 GHz ISM band (2450 + 50 MHZ) may also be a suitable band. It is the purpose of this report to investigate the suitability of these ISM bands for ETTM and related systems. We start in the next section by looking at the natural and incidental radiation devices in these bands. A rather broad look at this has been given by Spaulding [1], and we repeat some of these results here for completeness and also include the ISM equipment currently used. ISM devices are not covered in [1]. Next, section 3, we look at the spectrum usage (intentionally radiated signals) in and near these two bands, giving various measurement examples. It is the combination of all these radiations, natural, incidental and intentional, that combine to form the interference environment in which the new (e.g., ETTM) systems must operate.

As is shown in Section 3, the main source of interference from licensed emitters to IVHS systems in the two ISM bands, is from radars located above the 2400-2500 MHZ band and below the 5725-5875 MHZ band. Section 4 gives an EMC analysis concerning the effects of

these radars on an IVHS generic system. This analysis relies heavily on the Monte Carlo simulation software ACOLADE (software for design, simulation, and analysis of communication systems). The Irregular Terrain Propagation Model (ITM), which is extensively used in the ITS Telecommunication Analysis Services, is also used. The analysis is to determine under worse case situation the distance separation required from the out-of-band radars. Inside this distance, a case by case EMC analysis is required using the actual antenna coupling appropriate and the actual terrain profile, etc. An example of this is also given.

In order to analyze or design communications systems for the real world non-Gaussian interference, such as exists in the two ISM bands, an appropriate interference model is required. This study includes a summary of a model designed to represent the entirety of the interference background. Also, measurement techniques required to specify the physical-statistical parameters of the model are given. Examples of generic system performance using the model are included.

2. Summary of the natural and man-made noise environment

In this section we want to briefly review the natural background noise and man-made noise levels in our two bands of interest. The natural noise is included for completeness, and to eliminate it from consideration as a "problem." The man-made noise of concern to us is automotive ignition noise and the ISM equipment. The roadway natural and man-made noise environment has been treated in detail recently for IVHS systems by Spaulding [1] for the main frequency ranges of 100 MHZ and 0.9-3 GHz. The appropriate results are included here (for the 2.45 GHz band) with additional information to try to cover the 5.8 GHz band. In addition we will consider ISM equipment in these two bands.

Figure 1, from [1], shows the overall background of natural sources from 100 MHZ to 100 GHz. The noise levels are given in terms of F_a (and t_a) F_a is the antenna noise figure due to

external noise, and is the parameter normally used to express the external noise level. Precise definitions are given in [1]. The noise temperature t_a is related to F_a via the reference temperature t_0 (300 K, see [l]). For our purposes here, the conversion of F_a to rms field strength (for a short vertical monopole) is given by:

$$E_n = F_a + 20 \log f_{MHz} + B - 95.5 dB(uV/m) \qquad (1)$$

where:

En is the field strength in bandwidth b (B = 10 log b), and

f_{MHz} is the center frequency in MHZ.

Note that for our frequencies, any natural noises are below the cosmic background of 2.7 K (F_a = -20 dB) and certainly are of no concern to us. To further illustrate this, a F_a of -20 dB converts to a field strength in a 1.5 MHZ bandwidth (the minimal bandwidth of the "standard" dedicated, short-range, two-way vehicle to roadside communications receiver) at a frequency 2.45 GHz, say, of 14 dB (uV/m) or about 5 u V/m. The only natural noise not included in Figure 1 is nearby lightning. Figure 2 from [2] shows a summary of lightning peak field strength at 1 mile distance. It was pointed out in [l] that nearby lightning can be quite disruptive at lower frequencies (e.g. 100 MHZ), but not at our frequencies of interest here. If we convert the peak value at 2.45 GHz from Figure 2 (-12 dB uV/m, 1 kHz bandwidth) to F_a using (1) (the rms value is lower than the peak value by at least 10 dB) we obtain an "F," of -14.3 dB, of no concern to us (i.e., the true F_a is at least -24 dB).

Figure 1 also includes a curve giving the estimated median business area man-made noise level. This noise is almost entirely due to automotive ignition noise. The individual trend continues and Figure 1, curve A, gives a high automotive density area background noise level

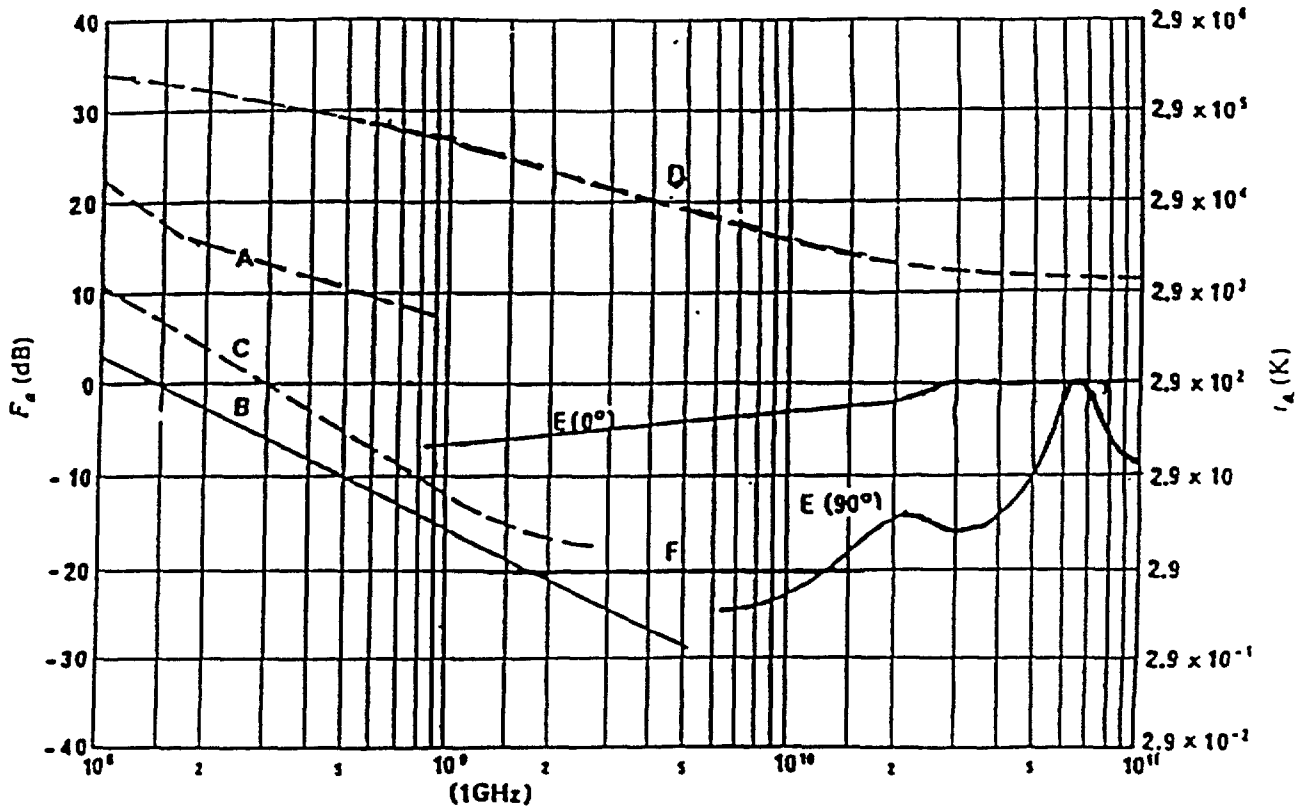

Figure 1. F_a versus frequency (100 MHz to 100 GHz)

A. Estimated median business area man-made noise
B. Galactic noise
C. Galactic noise (toward galactic center with infinitely narrow beamwidth)
D. Quiet sun (1/2 degree beamwidth directed at sun)
E. Sky noise due to oxygen and water vapor (very narrow beam antenna; upper curve 0° elevation angle, lower curve, 90° elevation angle
F. Cosmic background, 2.7K

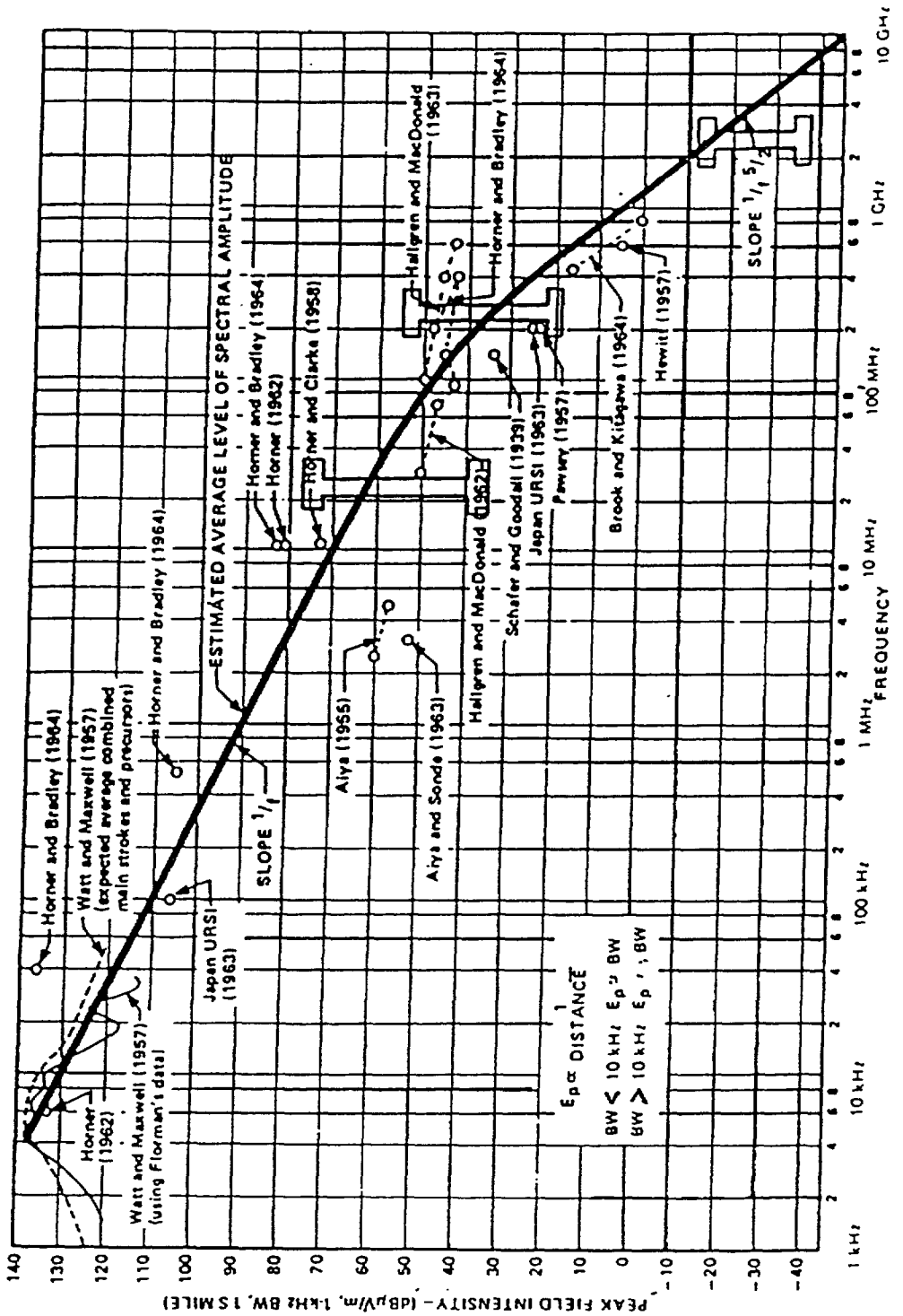

Fig. 2. Lightning emission peak field strength, 1 mile distant (from Shumpert, et. al., 1982).

of approximately F_a = 3 dB at 2.45 GHz and F_a = -2 dB at 5.8 GHz. These results are based on measurements made in the mid 1970's, and [2] has shown that the automotive ignition noise level is now substantially lower in general, but probably only about 5 dB lower at our frequencies. F_a gives the rms level and ignition noise is an impulsive process, so even if the rms level is low, perhaps some high level impulse could be a problem. Recently, Yamanaka and Sugiura [3] presented an extensive set of noise measurements in urban areas (general streets and metropolitan expressways in Tokyo) in the l-3 GHz range. These are apparently the only recent measurements available in our frequency range of interest, and are summarized in [1]. Figure 3 shows one ignition noise measurement from [3] of the received noise envelope. The measurement is the exceedance probability (termed amplitude probability distribution, or APD). The measurement is at 2.335 GHz in a 100 kHz bandwidth. The RMS level is at 20 dB uV/m, (100 kHz bandwidth) for this distribution. This gives an F_a of -1.9 dB. Note that high level impulses, occurring with a probability of 10^{-5} (e.g.), can be 20 dB or more higher than this in the 100 kHz bandwidth. The noise process will have a much wider dynamic range in our ETTM bandwidth of 1.5 MHZ How much higher the pulses might be in a 1.5 MHZ bandwidth is unknown at our frequencies.

The only other applicable measurement results are those made by Stanford Research Institute in 1975. SRI conducted a very extensive study of vehicle ignition radiation for the Motor Vehicle Manufacturing Association (MVMA). In this study, approximately 10,000 individual vehicles (in motion) were measured. The measurement was of peak field strength. Figure 4, from Shepherd et al. [4] shows measurement results at 2 GHz and 7 GHz, and Figure 5 summarizes the individual vehicle measurements. The measurement antennas were 10 meters from the vehicles at a 3m elevation in all cases. Finally, Figure 6 from [4], shows the distribution of peak field strength at an intersection with a traffic density of 10-60 vehicles per minute. Note that the "modem" single measurement given on Figure 3 indicates a peak field

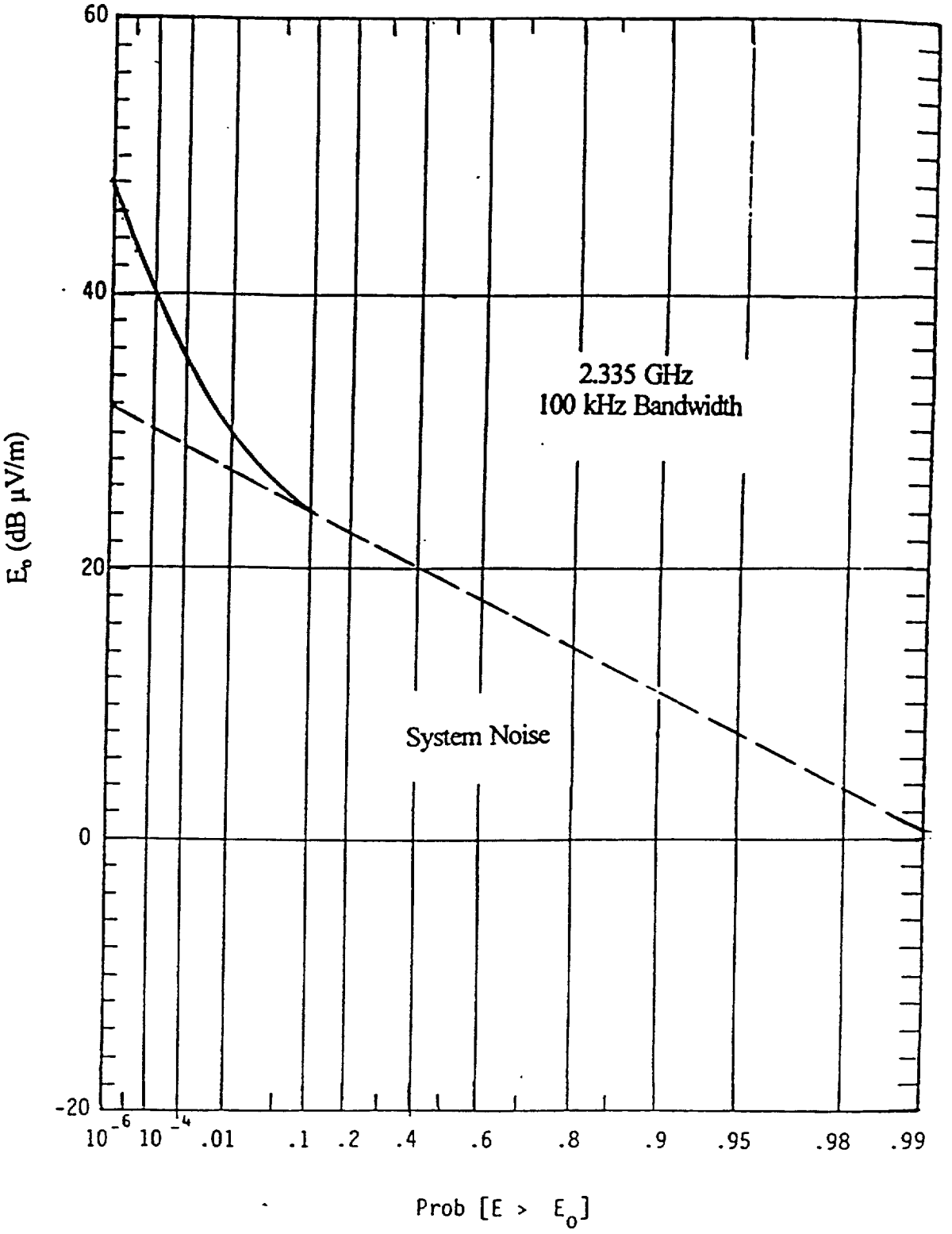

Figure 3. Amplitude probability distribution (ADP) of system noise and ignition noise

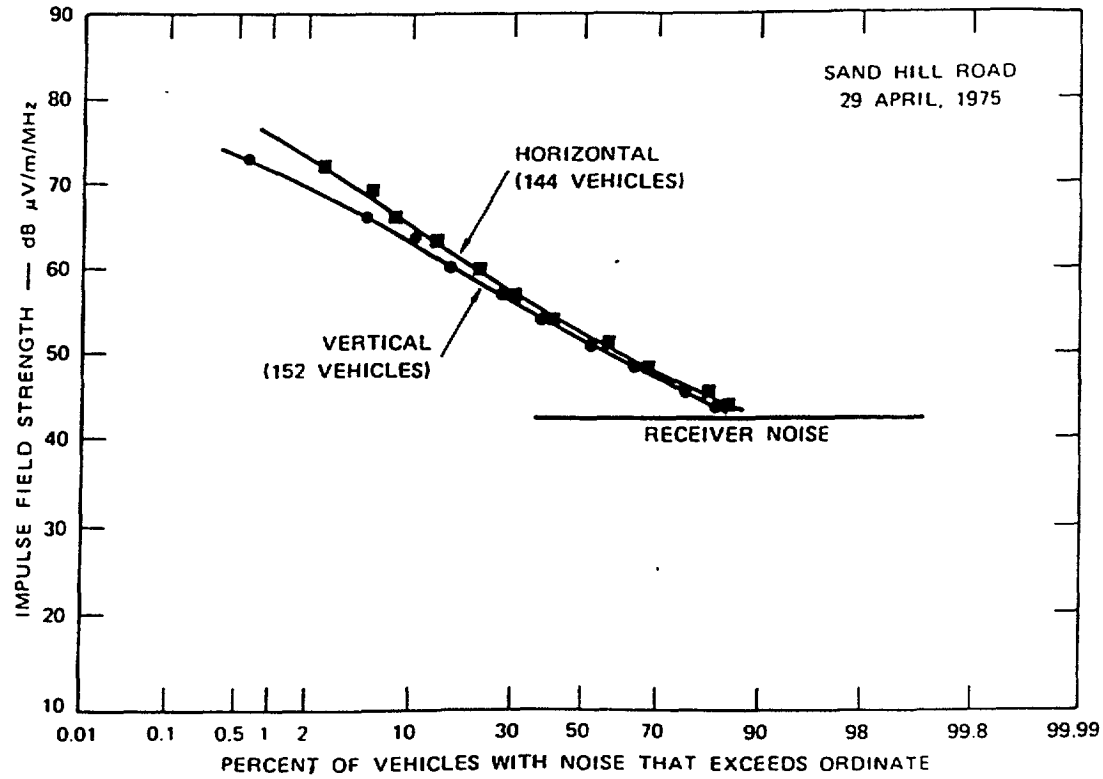

Figure 4a. Distributions of peak field strength from individual vehicles at 2GHz

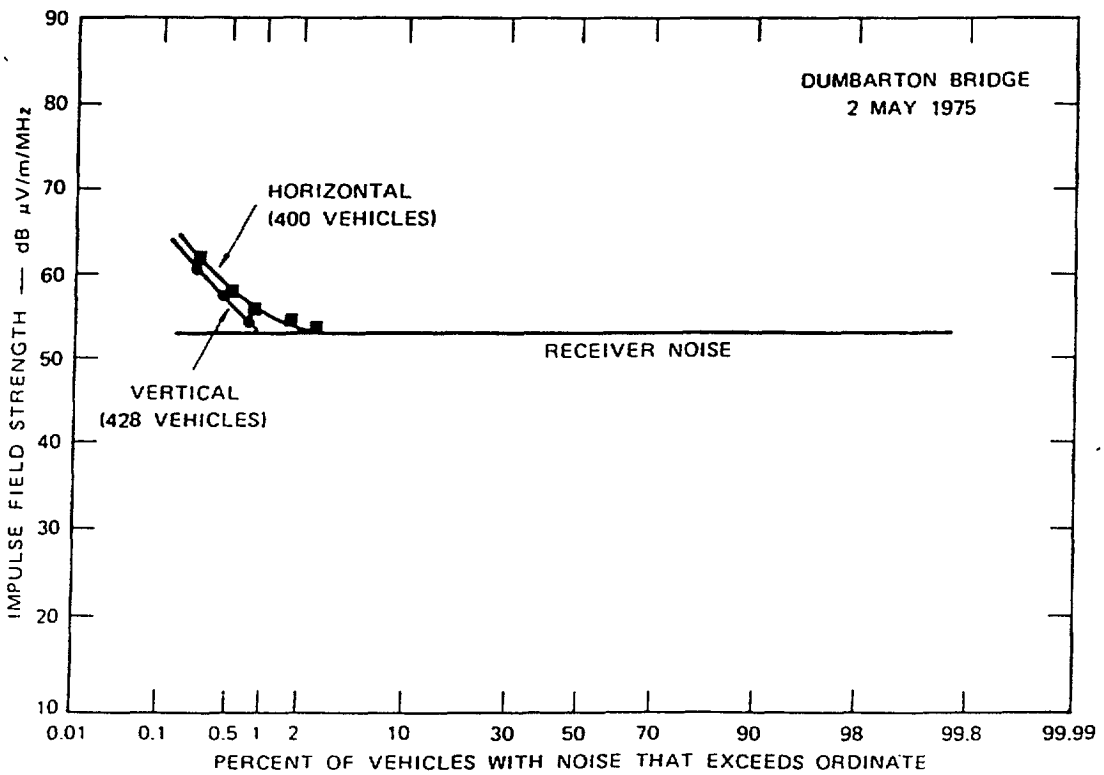

Figure 4b. Distributions of peak field strength from individual vehicles at 7GHz

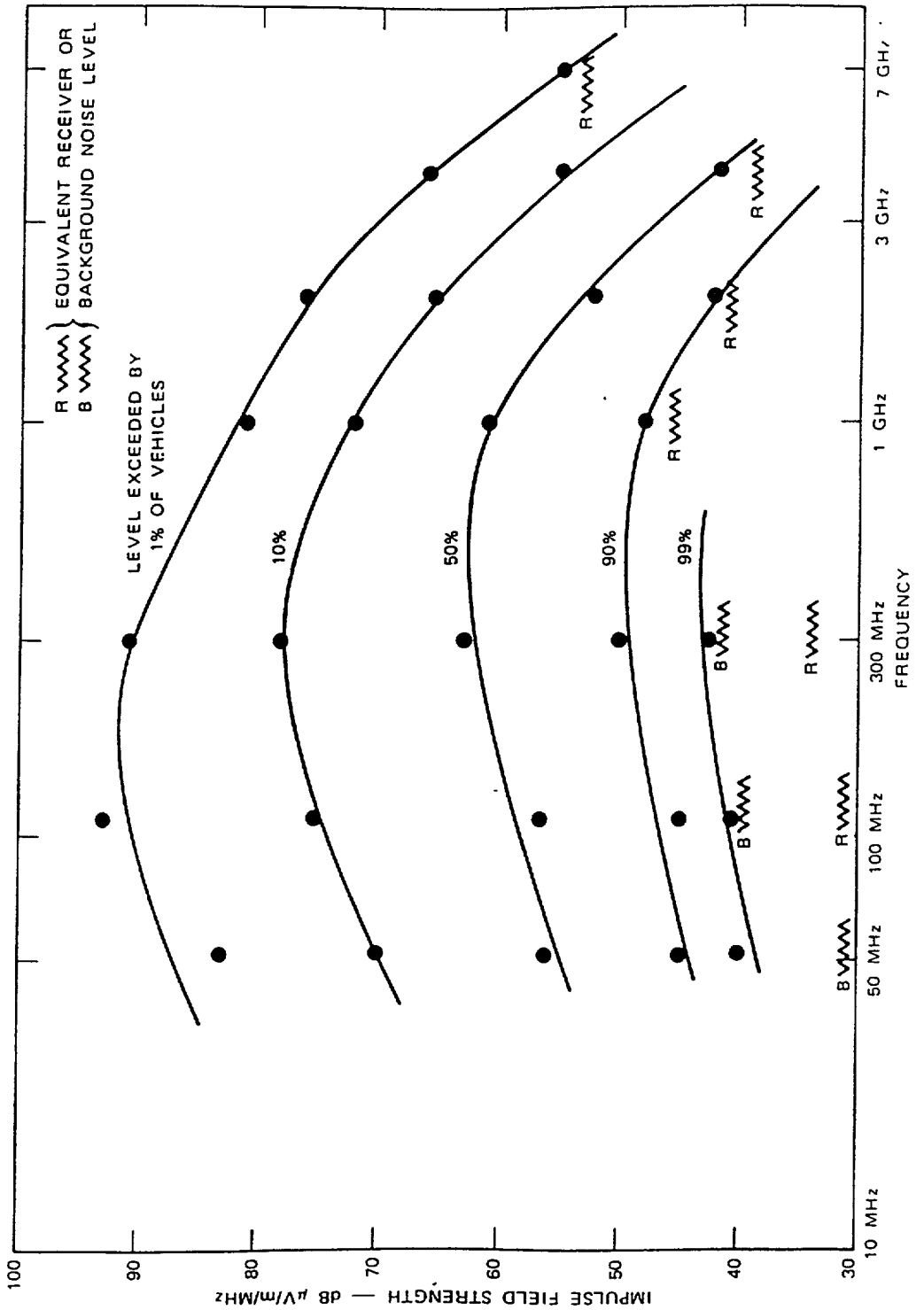

Figure 5. Ignition peak field strength from individual vehicles

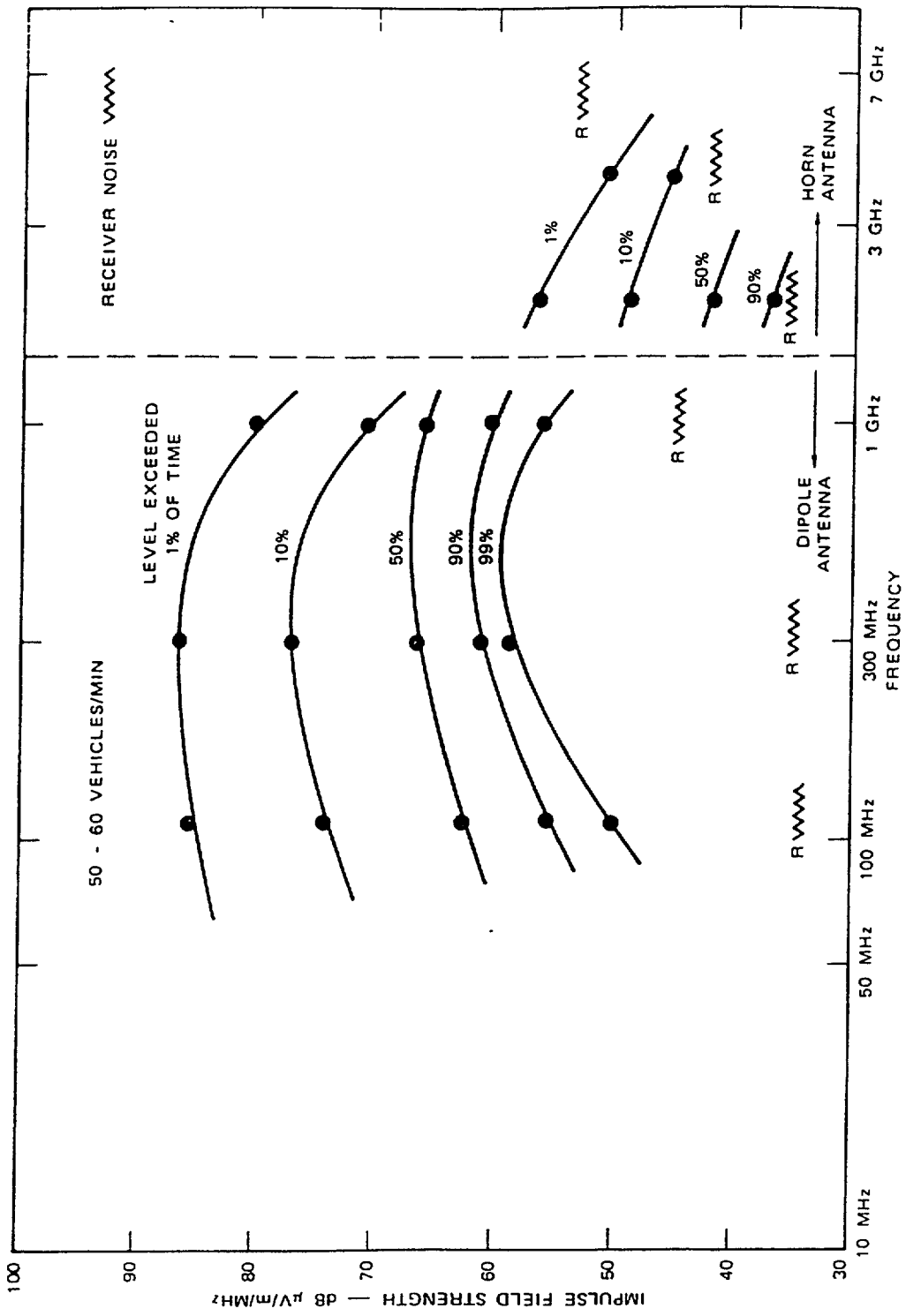

Figure 6. Ignition noise at an intersection

20 years apart. Figure 5 shows that 1% of the vehicles exceed the median vehicle by at least 20 dB at 2 GHz. This super noisy vehicle phenomena is discussed in [1] and the references therein. Figure 5 shows measurements of individual vehicles, i.e., the parameter is "percent of vehicles," whereas Figure 6 shows "percent of time" for an interaction. Figure 6 is therefore more characteristic of the overall background. On Figure 6 the curves are discontinuous at about 1.5 GHz. At the lower frequencies, the receiving dipole antenna illuminated most if not all of the intersection. The horn antennas used at the upper frequencies, however, had narrower beams that included a much smaller portion of the intersection and therefore saw a smaller number of the vehicles at one time.

Above, we have presented what information is available concerning ignition noise in our bands of interest. A method was developed some time ago to calculate the automotive ignition noise level from propagation and the distribution of radiated power from individual vehicles. This is summarized in [1], but, again, the required input data for modem vehicles and our frequency of interest is unknown. The other incidental radiation devices in our band of interest are ISM equipment, and we treat them next.

The "rules" for ISM equipment, for our purposes, are quite simple. In any of the designated ISM bands, any authorized radio service must accept any harmful interference from in-band equipment. However, if harmful interference is caused by ISM operation to any authorized service outside the ISM frequency limits, then the operator of the ISM equipment must take the necessary steps to eliminate the interference. Miscellaneous ISM equipment (e.g., microwave ovens) have no limit on in-band radiated electric field, but there are standards for any harmonic or other spurious radiation outside the frequency limits.

The FCC requires Part 18 compliance certification of consumer ISM equipment through testing by a qualified laboratory. However, only one unit must be tested for each model to demonstrate compliance. The FCC also specifies compliance for non-consumer ISM equipment. This requires manufacturers to have the equipment tested. Records are maintained

only by the manufacturer, available for verification by the FCC. Therefore, the FCC does not have complete information on the number of ISM units in use or their distribution. However, an estimate of the number of ISM units to date in the US would be well over 100 million [5,6]. The vast majority of these units are in the 2400-2500 MHZ band.

The majority of the microwave ovens, especially those manufactured in the U.S. operate at 2450 MHZ with an allowed tolerance of + 50 MHZ. Most of these ovens operate at a range of power of 700-1000 watts. Even though those ovens are constructed efficiently to prevent microwave energy from escaping the metal cavity, they still radiate energy. The FCC Laboratories have recorded a peak field strength of 1135 uV/m (61 dB uV/m) at 300 meters from a typical microwave oven.

Recently, NTIA concluded an extensive series of measurements of the emission spectra and waveforms of microwave ovens [7,8]. Figure 7 shows a typical measured microwave oven spectrum at a distance of 3 meters. The ovens "antenna pattern" is essentially omnidirectional. Figure 8 shows results from a 1993 spectrum survey by NTIA in Denver, Colorado. Note the contrast between the 2400-2500 MHZ ISM band and outside the band. On Figure 8, the peak received signal level of -70 dBm, for the measurement system and antenna used, corresponds to a peak field strength of 72 dB &V/m). This can be contrasted with the intersection peak ignition noise levels shown on figure 6. The microwave ovens etc. noise background is approximately equal to the ignition noise peak level exceeded 50% of the time. The Denver results are typical as shown by Figure 9, which shows spectrum survey measurements from Chicago in 1980 and Atlanta in 1988. In addition to microwave ovens, other ISM equipment in this band consists mainly of industrial heaters (microwave) ranging in power from 2.5 kW to 150 kW and medical diathermy devices. An estimated total of 35 million units of all types of industrial heaters between lo-2500 MHZ were recorded by the National Institute of Occupational Safety and Health (NIOSH) [9]. The majority of these devices are in the 902-928 MHZ ISM band, however. In the future there could be large scale microwave

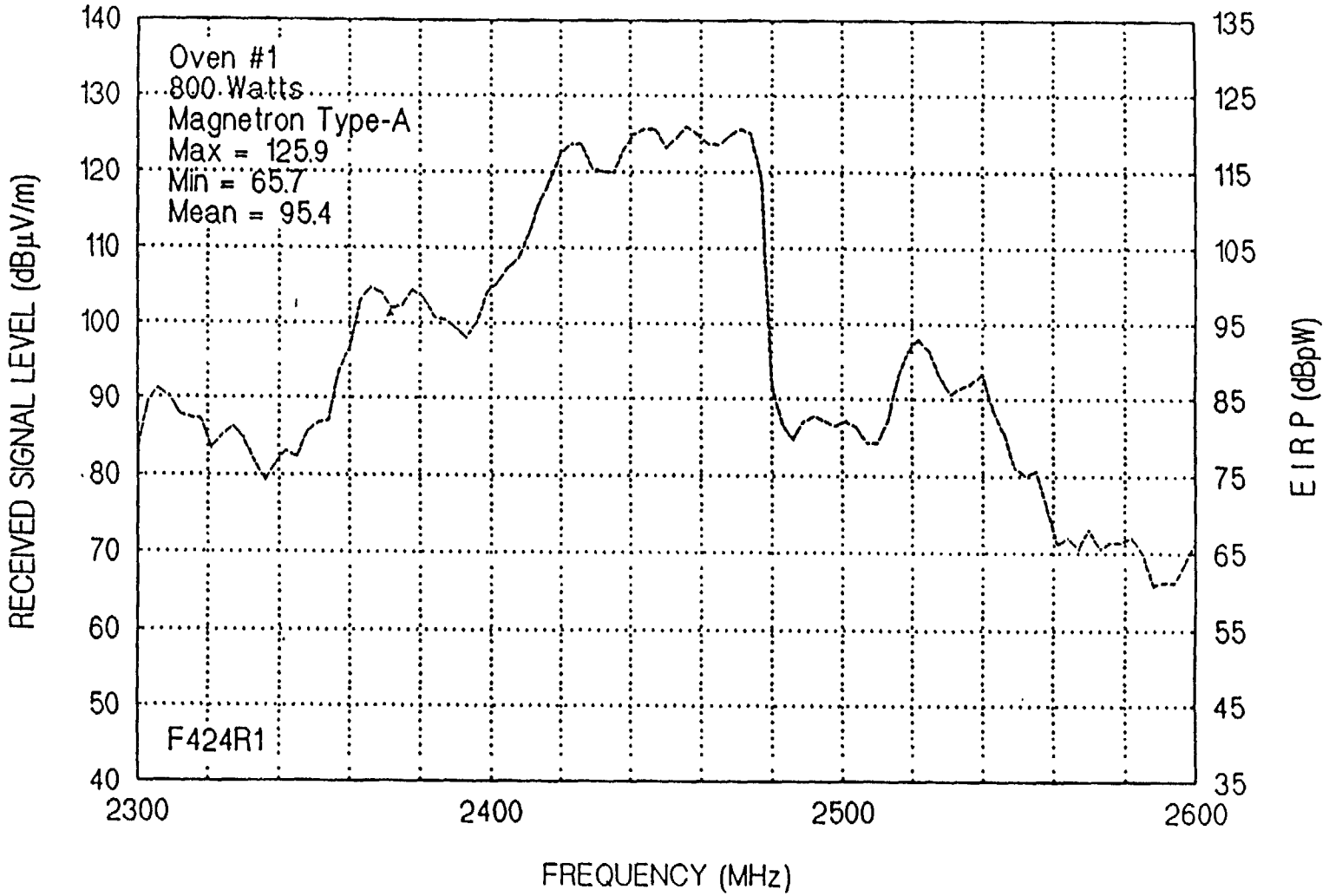

Figure 7. Measured peak emission spectrum of a microwave oven, 3 meter measurement distance

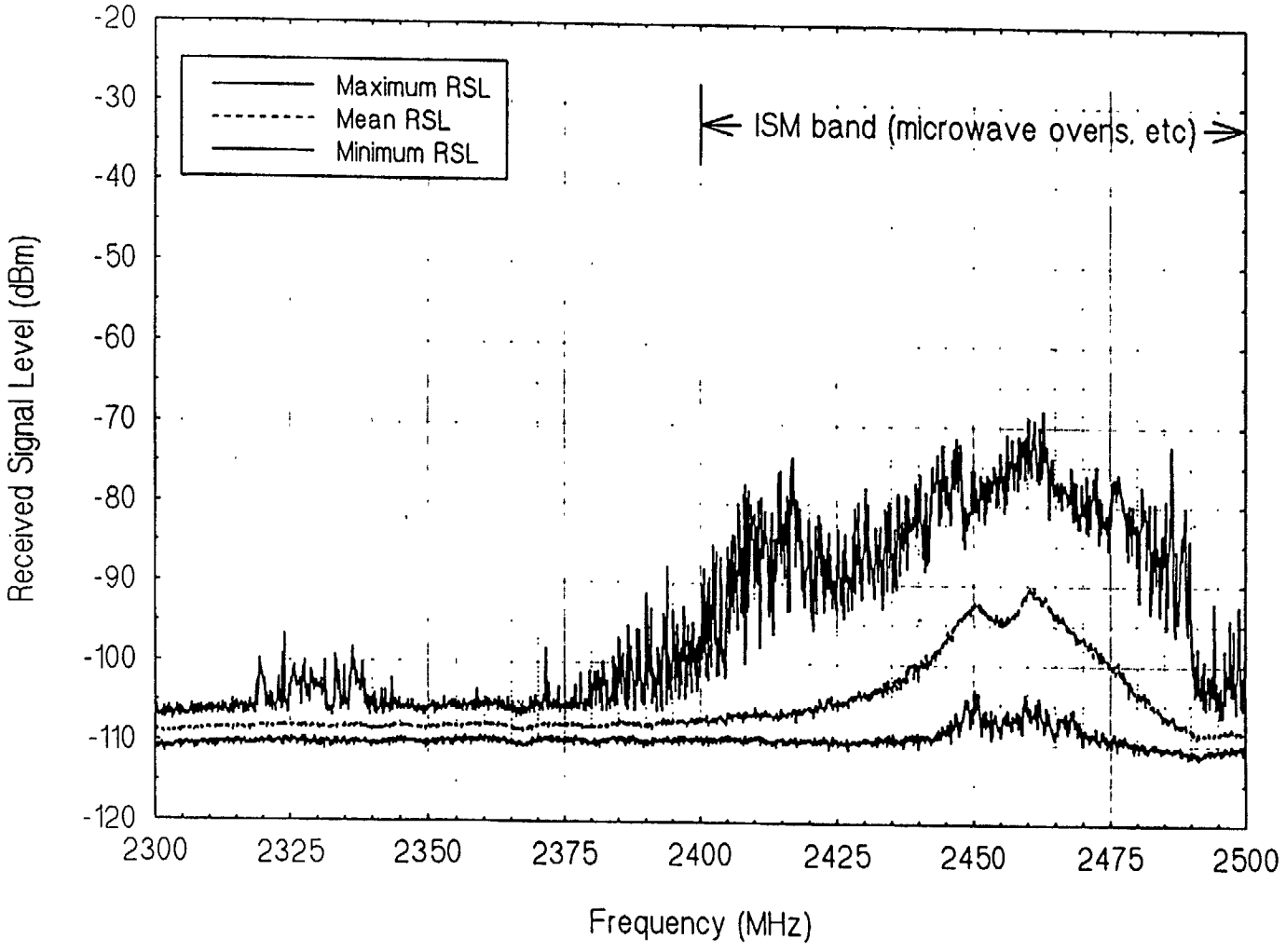

Figure 8. Data from Denver, CO., spectrum survey 1993

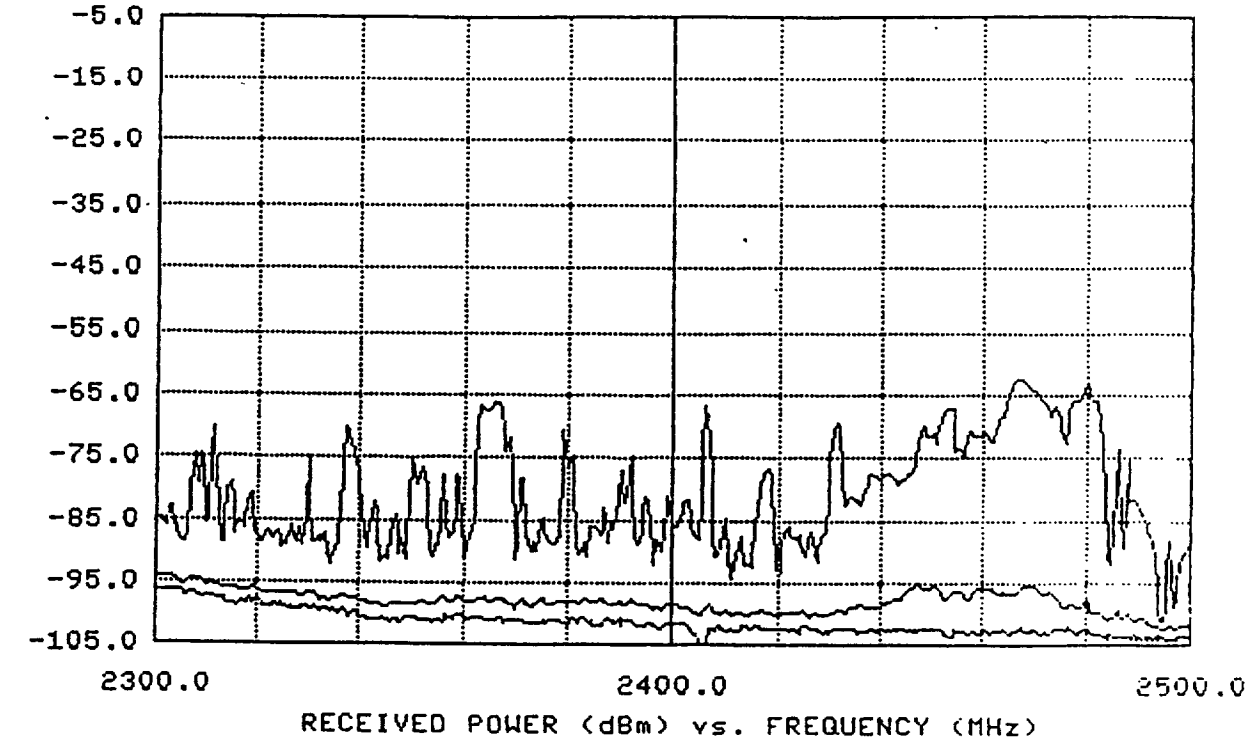

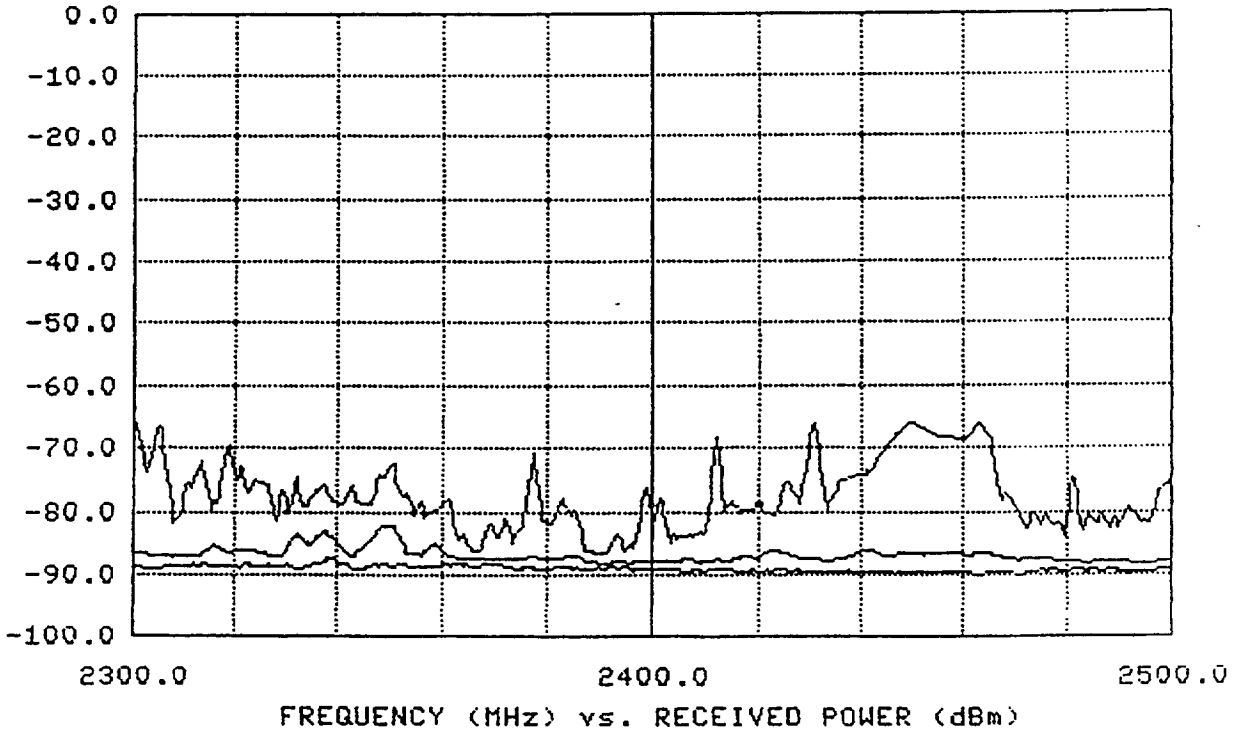

Figure 9. Data from spectrum surveys - top figure is for Chicago, 1989, and bottom figure is for Atlanta, 1988.

applications requiring free radiation. This band was “scheduled” for use, for example, in the solar-power satellite system studies some time ago. Retorting of oil shale and radiant heating in homes are other possible examples. Currently, projects related to these applications are at a standstill.

Of main interest here is that there are no indications that ISM equipments are operating in the 57255875 MHZ ISM band. Use of this band will probably come in time.

In this section we have summarized the natural background noise level and man-made noise levels in our two bands of interest. The background noise in the 2400-2500 MHZ band is due to automotive ignition systems and microwave oven (and other ISM devices) radiations. In urban areas, the peak levels in this band are some 10-20 dB higher than adjacent to this band (see figure 8 and 9). Even so, these levels are not high enough to cause any appreciable interference to short range directional communication systems such as those envisioned by IVHS. The background is quite low in the 5725-5875 MHZ band, especially since there is currently no ISM equipment operating in the band.

Interference to IVHS systems in these two ISM bands can only come from intentionally radiated signals and the above background, but the background is likely to contribute little to the overall process, especially at 5.8 GHz. The interference environment from intentional signals within and near to these bands is covered in the next section.

3. The interference environment

As noted above, unacceptable interference, if any, to IVHS systems in the two ISM bands of concern will arrive from intentionally radiated signals (licensed transmissions) or a combination of the background and these transmissions. We will note, however, the wariness of fixed services users in the 2.45 GHz band concerning the possibility of interference from microwave ovens. As well as licensed assignments within the bands, interference is possible

(more likely, as we will see) from transmissions outside the bands, primarily radars. Here, we want to detail the band usage for the two ISM bands and also, primarily via spectrum surveys, note possible interference from outside the bands. Because, presently, there is no simple and accurate way of representing the equipments used in a band, the number of assignments is the main criterion used to assess band usage. A summary compilation has been given by Hoffman et al [10] for portions of the RF spectrum of potential interest to IVHS. The ISM band assignments were not covered however. It should be pointed out that the number of assignments does not necessarily equal the number of equipments in the band. The use of an assignment is usually associated with numerous equipment. We now look at our bands, one at a time.

3.1 The 2400-2500 MHZ band

In the U.S. the 2400-2500 MHZ band frequency range has three sub bands. The 2400-2450 is allocated to the Federal Government for radiolocation service on a primary basis and to non-government for amateur service on a secondary basis. The Government radiolocation is limited to the military services. These radars are located in remote areas and operate intermittently. The segment 2450-2483.5 is allocated to non-government for fixed and mobile services on a primary basis and for radiolocation on a secondary basis. This segment is used for fixed and portable transmissions of video for T.V. for remote news events. The segment is mainly used for fixed service radio relay transmissions of voice and data. There are 441 U.S. assignments (1991) in this segment. The geographical location of licensed fixed stations is shown on figure 10 (from [11]). This geographical location, mainly in the Gulf of Mexico, shows the wariness of users concerning the possibility of interference from ISM equipment, mainly microwave ovens. As we saw in the previous section, it is in this position of this ISM band where the microwave oven “transmission“ are most prevalent. The FCC has recently allowed spread spectrum communications in this segment with up to 1 watt of power (without licensing or protection) and many experiments are underway for wireless LAN, PCS, etc..

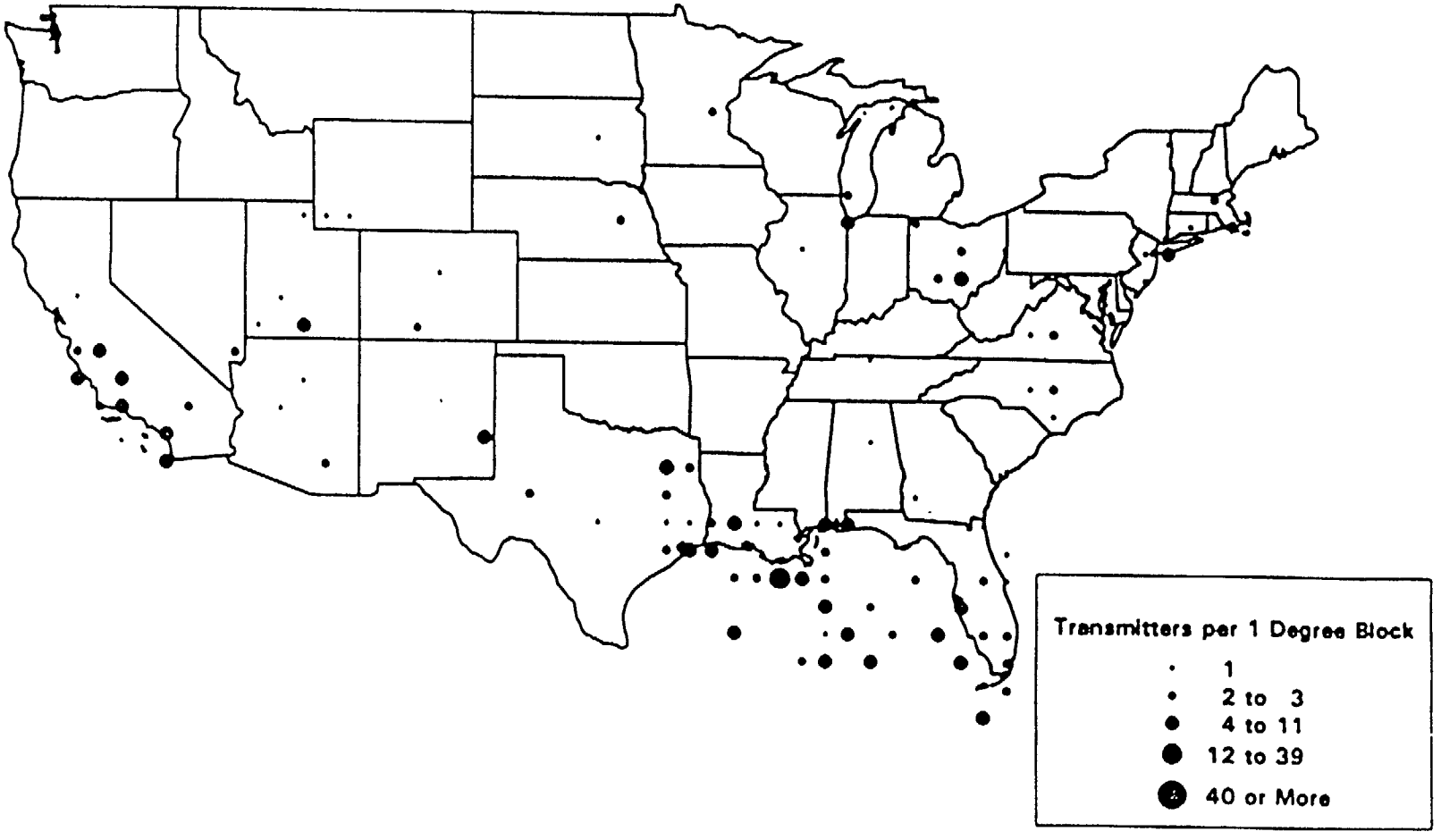

Figure 10. Density of assignments per degree in the 2450-2483 MHz bands

The number of the unlicensed users using spread spectrum technology will grow rapidly until additional bands are allocated for low power wireless devices. Interference problems will discourage the use of this segment in many urban environments, especially for systems for which reliable operation is important (e.g., IVHS).

The 2483.5-2500 MHZ is allocated for primary use by the non-Government for radio determination-satellite service with operations limited to space-to-earth transmission. The 2450-2500 (top two segments) is also allocated to the Government for radio location on a secondary, non-interference basis.

The 2400-2500 MHZ region is relatively quiet as far as radars are concerned. There are only a few high powered radars, all of which are located in remote sites and operate intermittently. There are a total of 55 assignments, 4 non-government, 5 NASA, and the rest DOD, primarily the Air Force (29). The frequency distribution of these assignment is shown on Figure 11. This is in addition to the 2450-2483.5 MHZ fixed and mobile assignments noted earlier.

Immediately above this ISM band, are numerous S-band weather radars, e.g., the new Next Generation Radar (NEXRAD) system at 2700-2900 MHZ. Figure 12 shows a measured spectrum for NEXRAD. The NEXRAD system is the first radar built that complies with the new Radar Emission Criteria (RSEC) which has more stringent spurious emission level limits than the "old" RSEC. Clearly, NEXRAD will produce no interference in the 2400-2500 MHZ band, but will become important when we discuss the 5725-5875 MHZ band. Many other S-band radars, however, can produce interference in the band, especially the upper portion. Figure 13 shows a measured WSR-74S weather radar (very common). Note that they easily can cause interference in the ISM band. Figure 14 shows an additional WSR-74S radar measurement. The measurement was taken l/2 mile from the radar. At 2450 MHZ, the -55

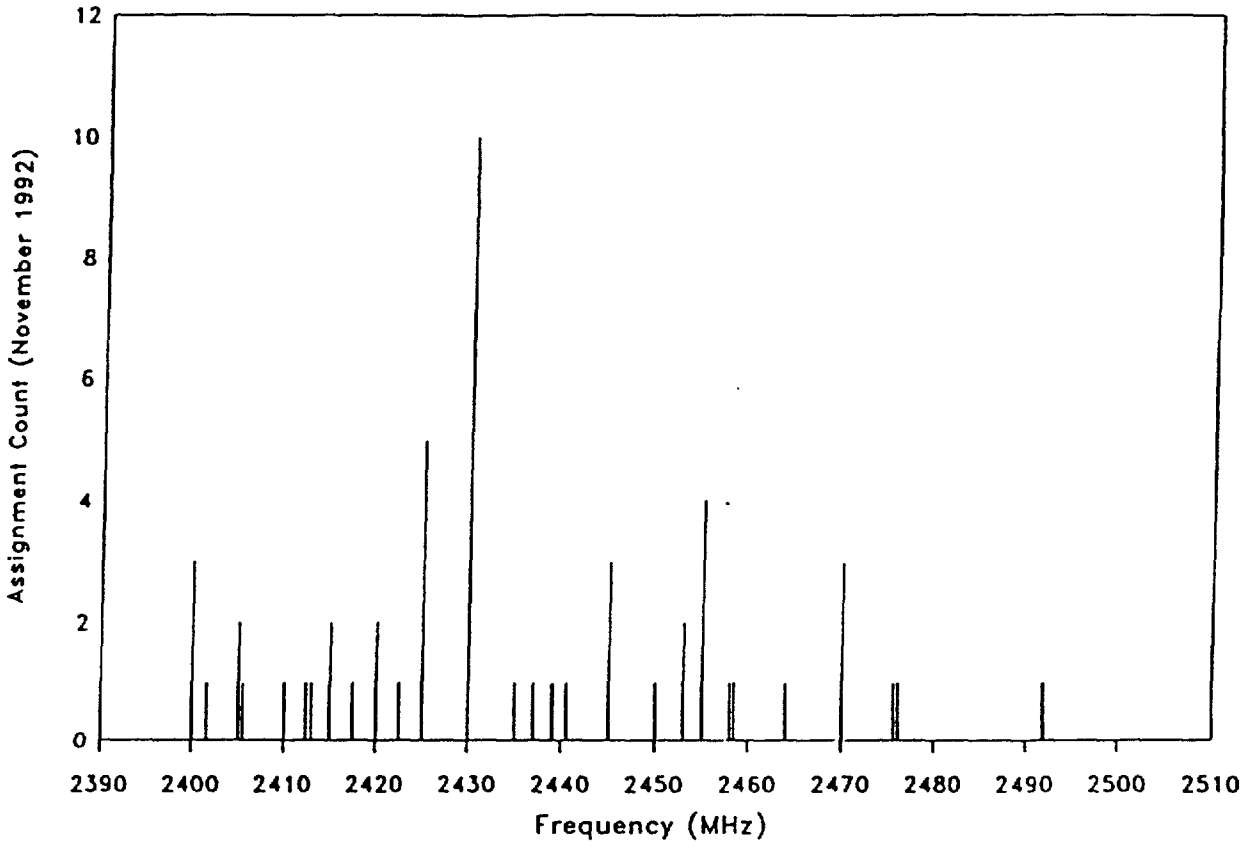

Figure 11. Frequency assignment distribution in the 2400-2500 MHz band.

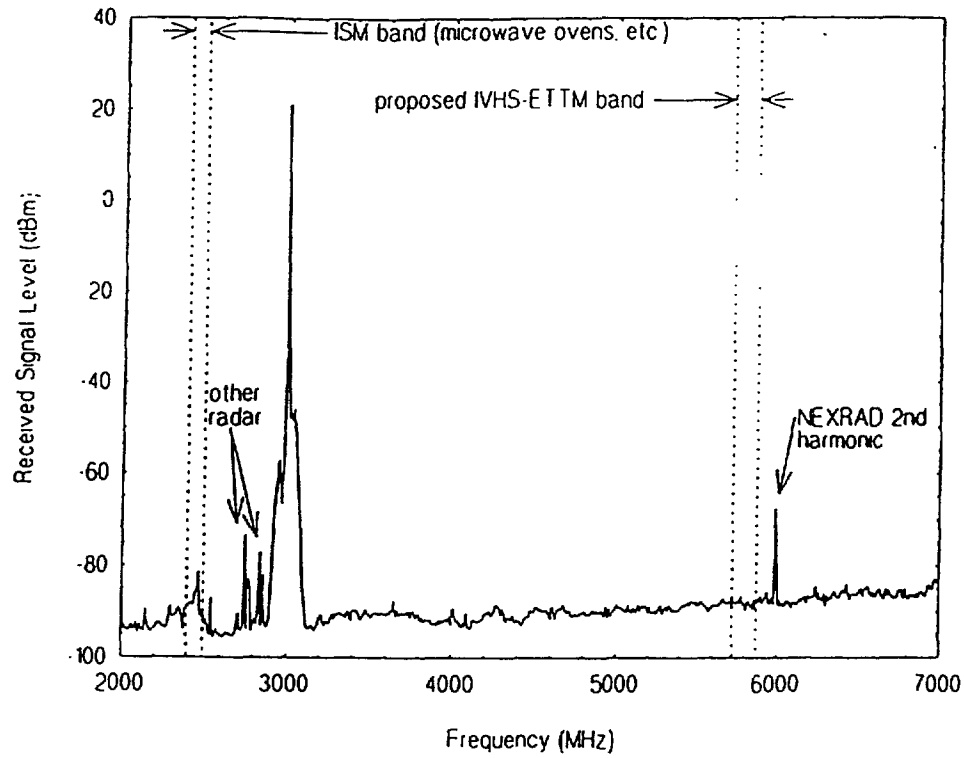

Figure 12. Measured spectrum, NEXRAD (WSR-88D), 1/2 mile distance

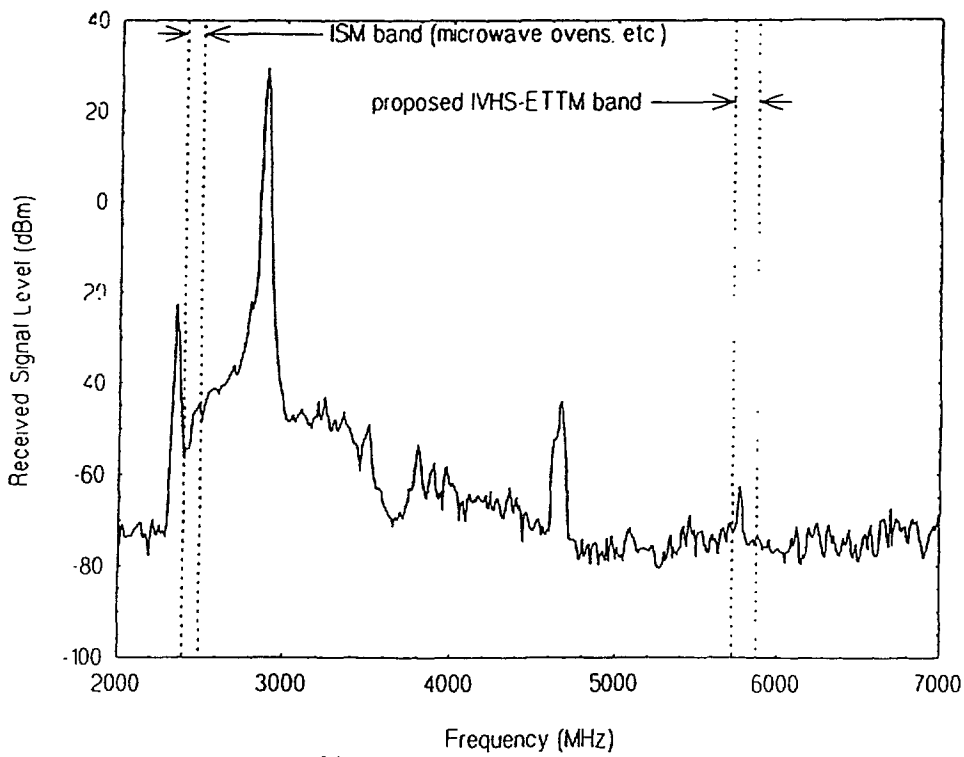

Figure 13. Measured spectrum, NWS (WSR-74S), 1/2 mile distance

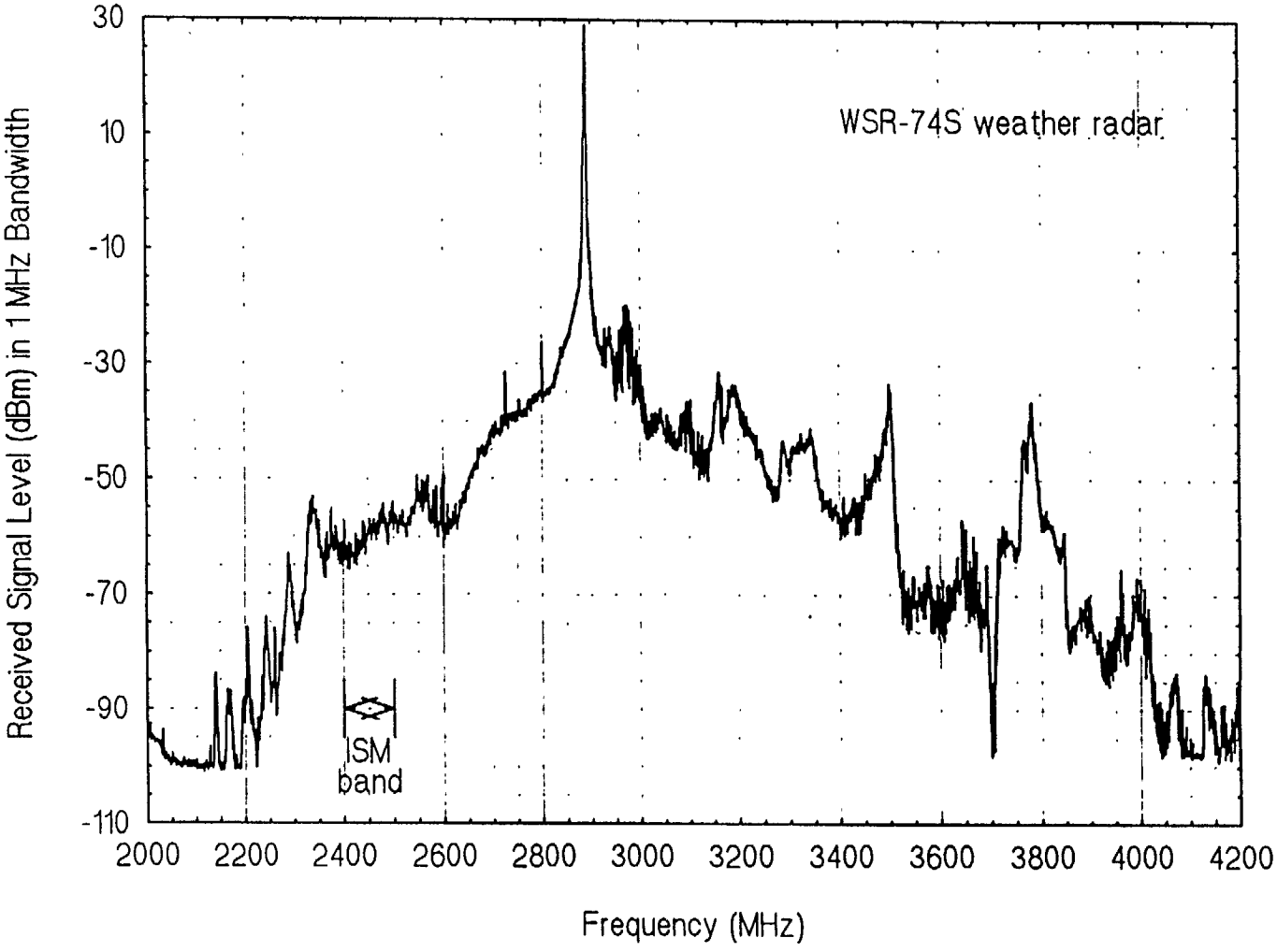

Figure 14. Measured spectrum of a WSR-74S meteorological radar, 1/2 mile distant

dBm measurement corresponds to a field strength of 70 dB uV/m In the 1994-1997 time frame, the NWS (National Weather Service) WSR-74S radars are scheduled to be moved and declared surplus Government property and replaced by the NEXRAD (WSR-88D) radar.

Additional radars exist above (and below) the 2400-2500 MHZ, band. Figure 15 shows the measurements given previously in Figure 9 (Atlanta portion) but now with some of the emitters identified. Finally, Figures 16 and 17 show two additional radar measurements. Figure 16 is a FPS-90 height finding radar and Figure 17, below our band, is a long-range air search radar. For this radar, the 2nd harmonic appears just above our band. In general, depending on the center frequency, the 2nd harmonic could be in our band (as well as the spurious emissions).

If IVHS systems use the 2400-2500 MHZ ISM band, they should stress using the lower segment. This is demonstrated above and by means of numerous spectrum surveys. After the NWS S-band WSR-74S are replaced, the upper segment of this band should be much more usable.

3.2 The 5725-5875 MHZ ISM band.

In the U.S., the 5725-5875 MHZ ISM band is allocated to the radiolocation service for the Federal Government on a primary basis and to the amateur service on a secondary basis. Government radiolocation applications, however, are limited to the military services (although a few are operated by NASA and DOE). Space-to-Earth application in the amateur satellite service is permitted in the frequency segment 5850-5850 MHZ. The upper portion of the frequency range (i.e., 5850-5875 MHZ) is allocated to the fixed-satellite service for uplink transmissions on a primary basis with radiolocation service. The majority of systems deployed in this band can be broadly classified as radars (ship-borne and ground-based) and radar activated transponders [12]. Presently, there are only two ship-borne radar system types in this frequency band. These Navy systems are deployed worldwide, along the coastal waters

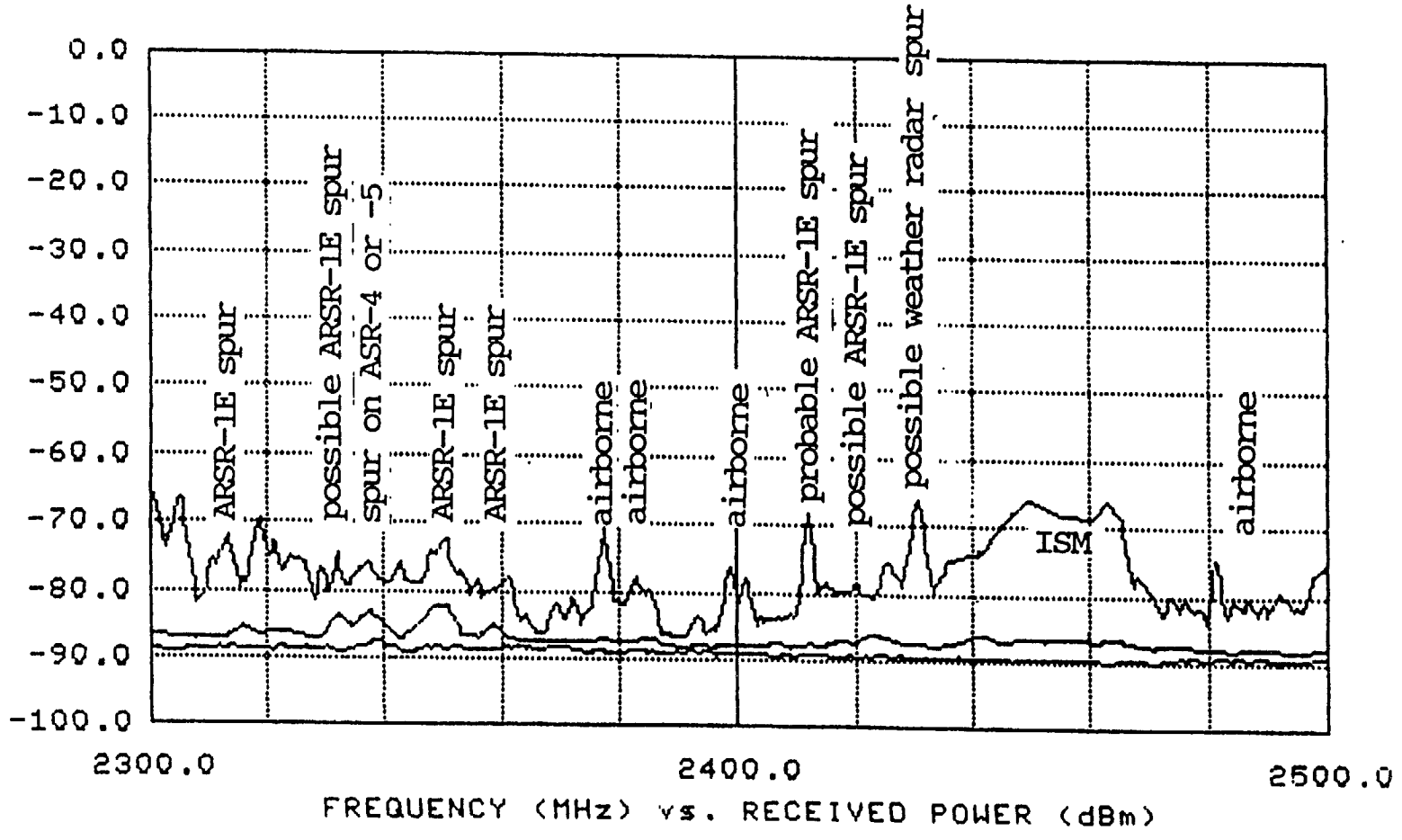

Figure 15. Data of figure 9 (Atlanta, GA.) showing probable emitters

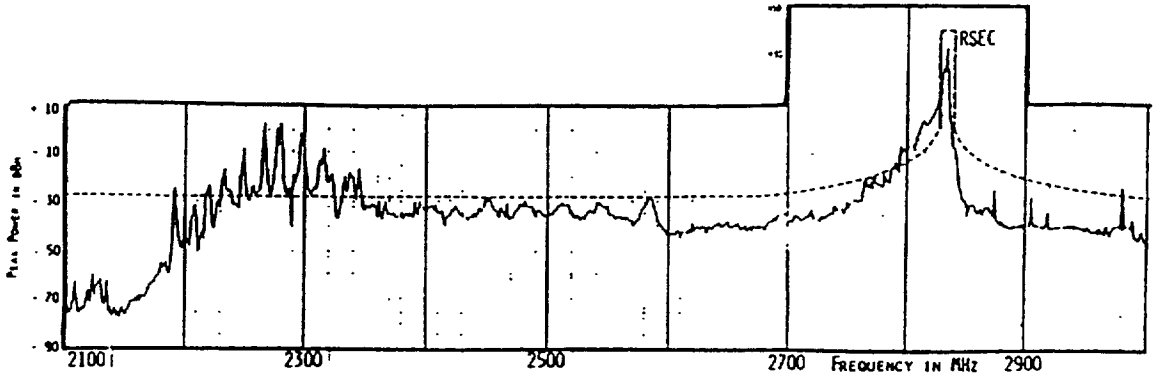

Figure 16. A FPS-90 height finding radar

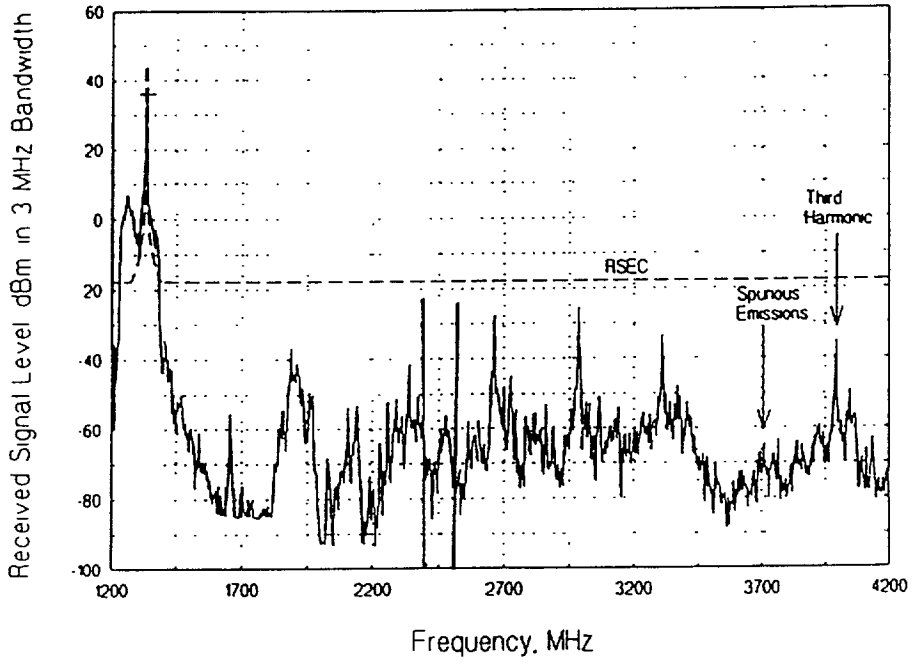

Figure 17. Emission spectrum of a long-range air search radar

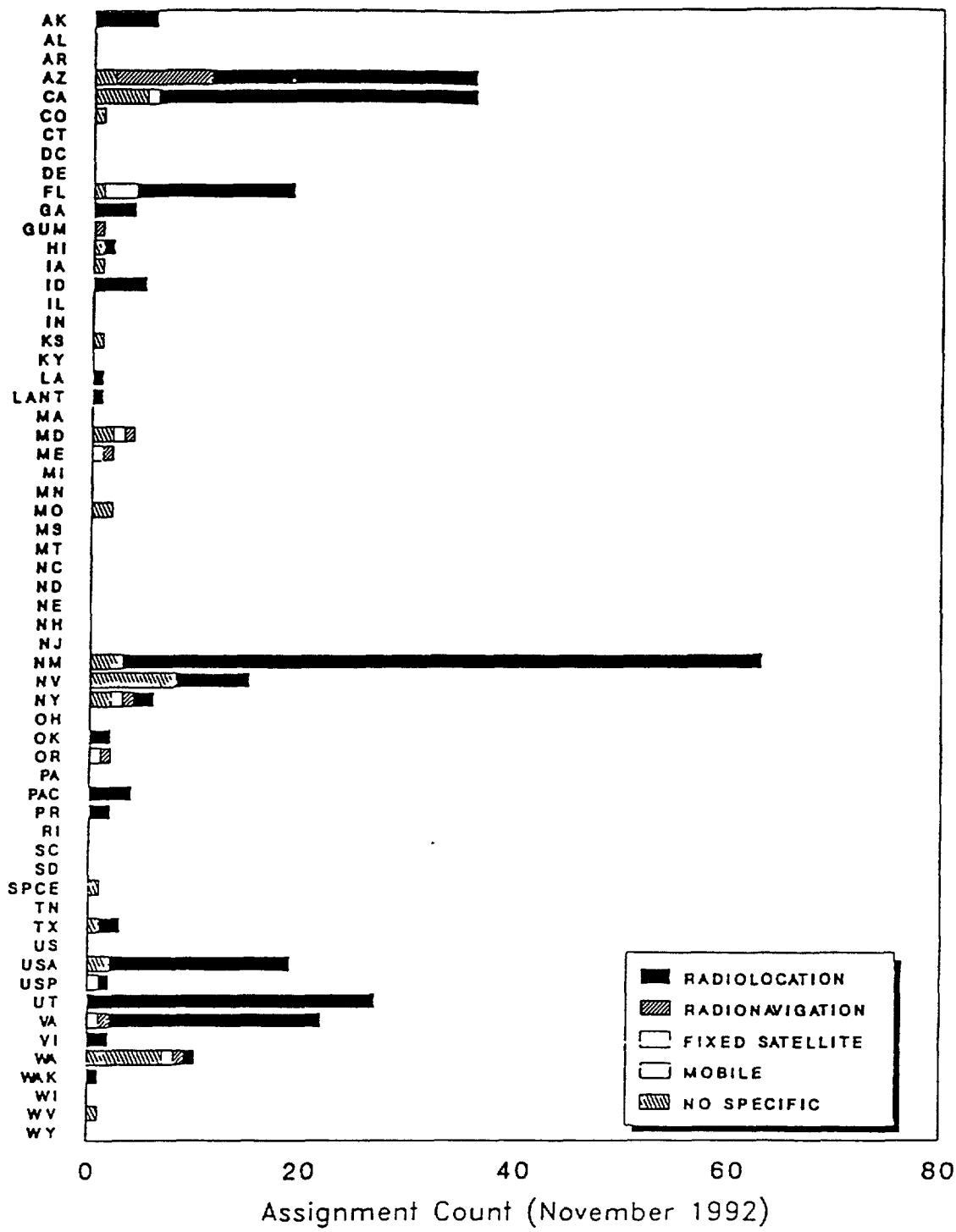

Figure 18. Geographic distribution of assignments per state in the 5725-5875 MHz ISM band.

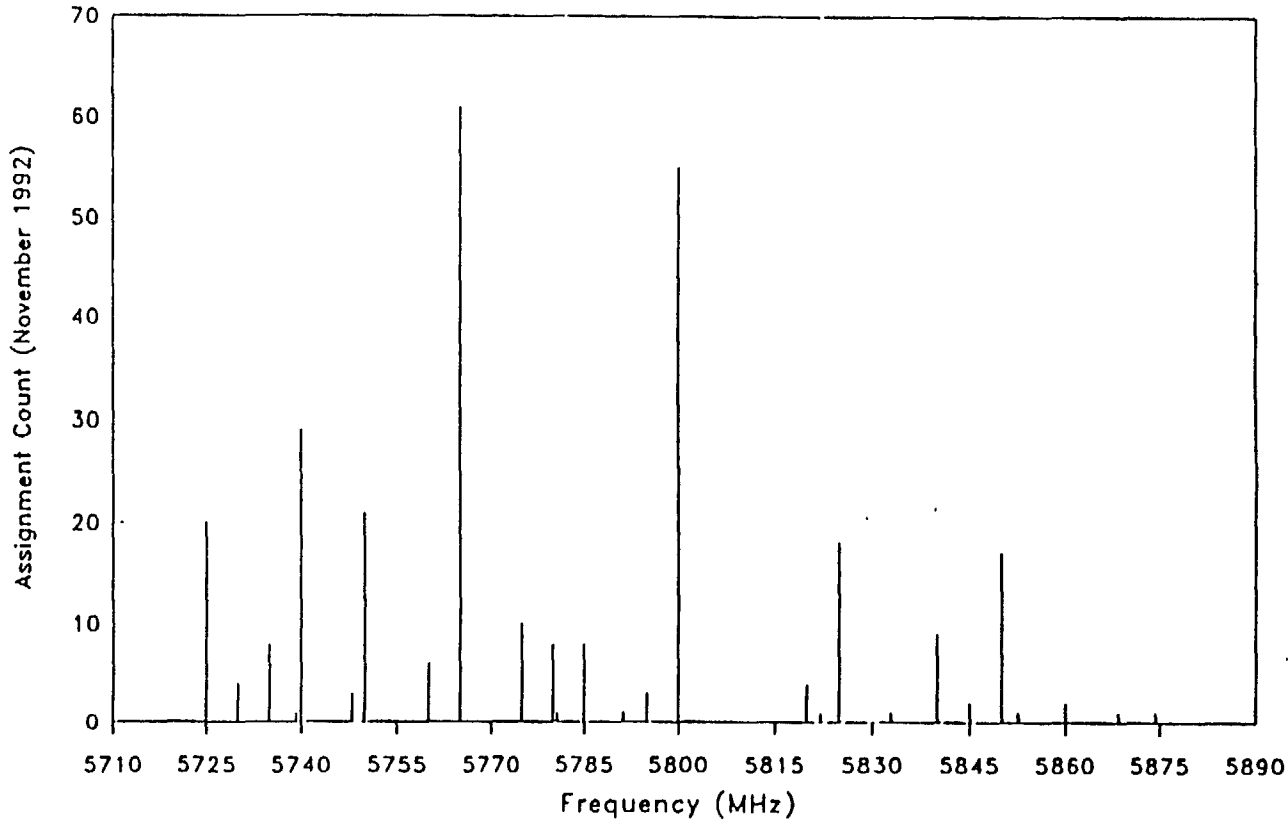

Figure 19. Frequency assignment distribution in the 5725-5875 MHz ISM band

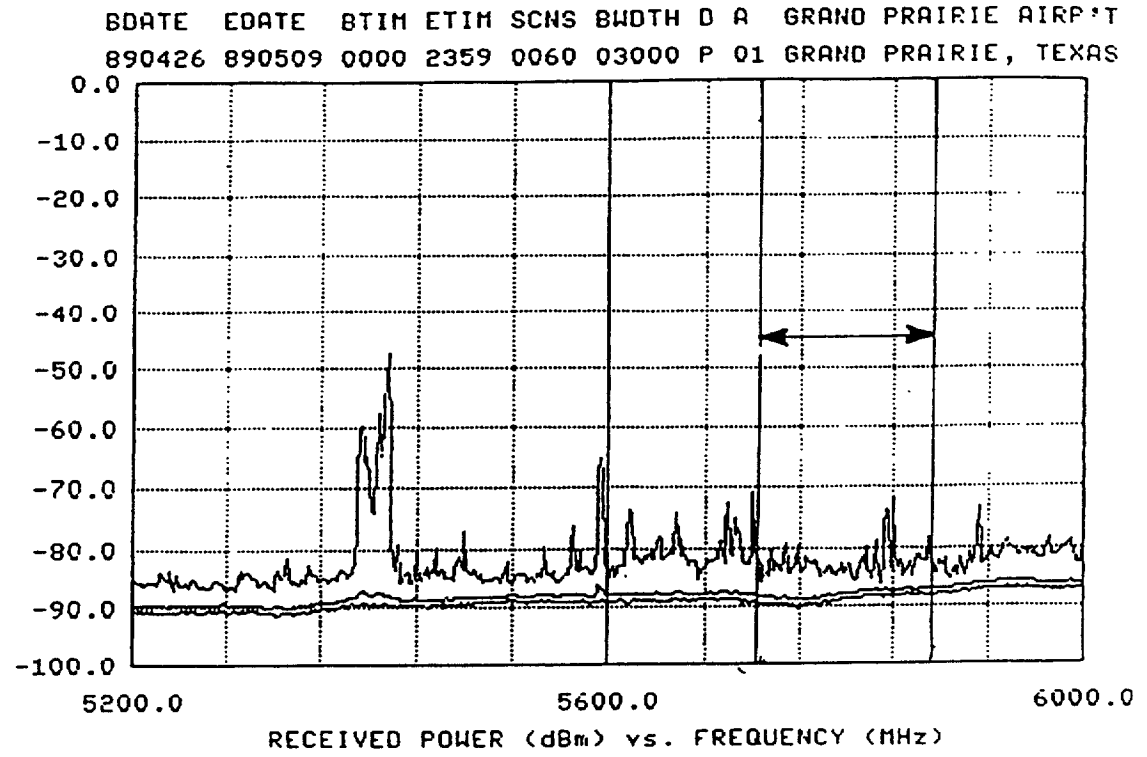

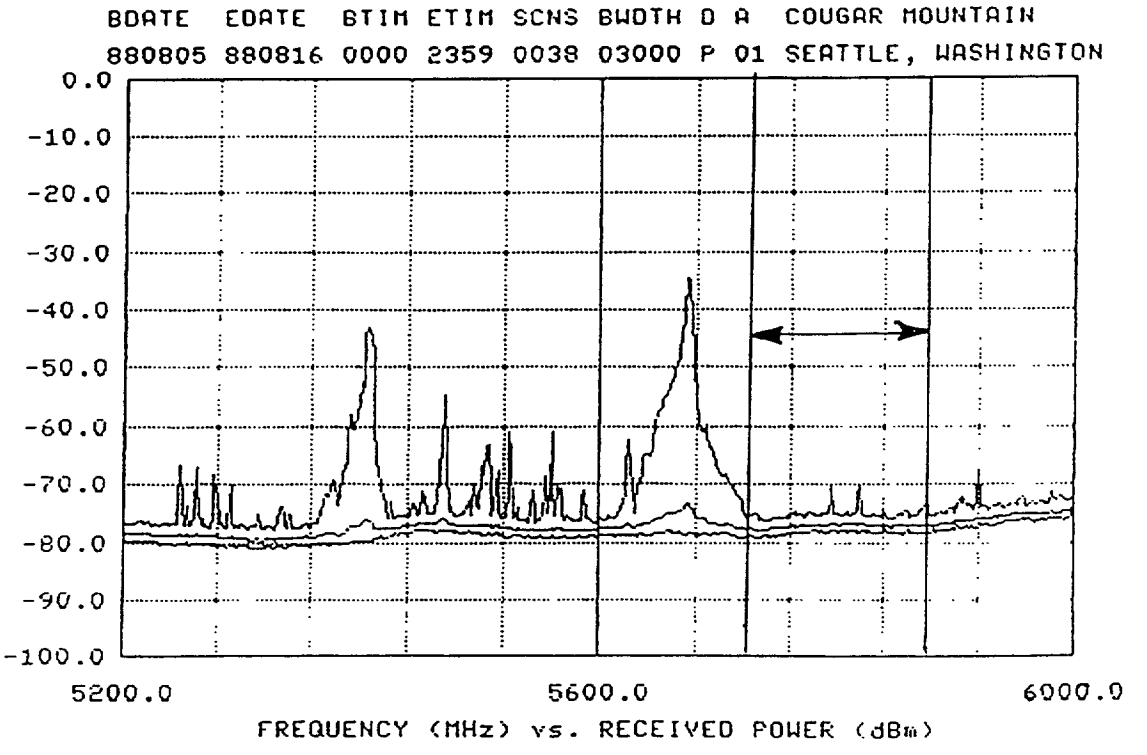

Figure 20. Minimum, mean, and maximum received power spectrum surveys; Dallas, Texas and Seattle, Washington

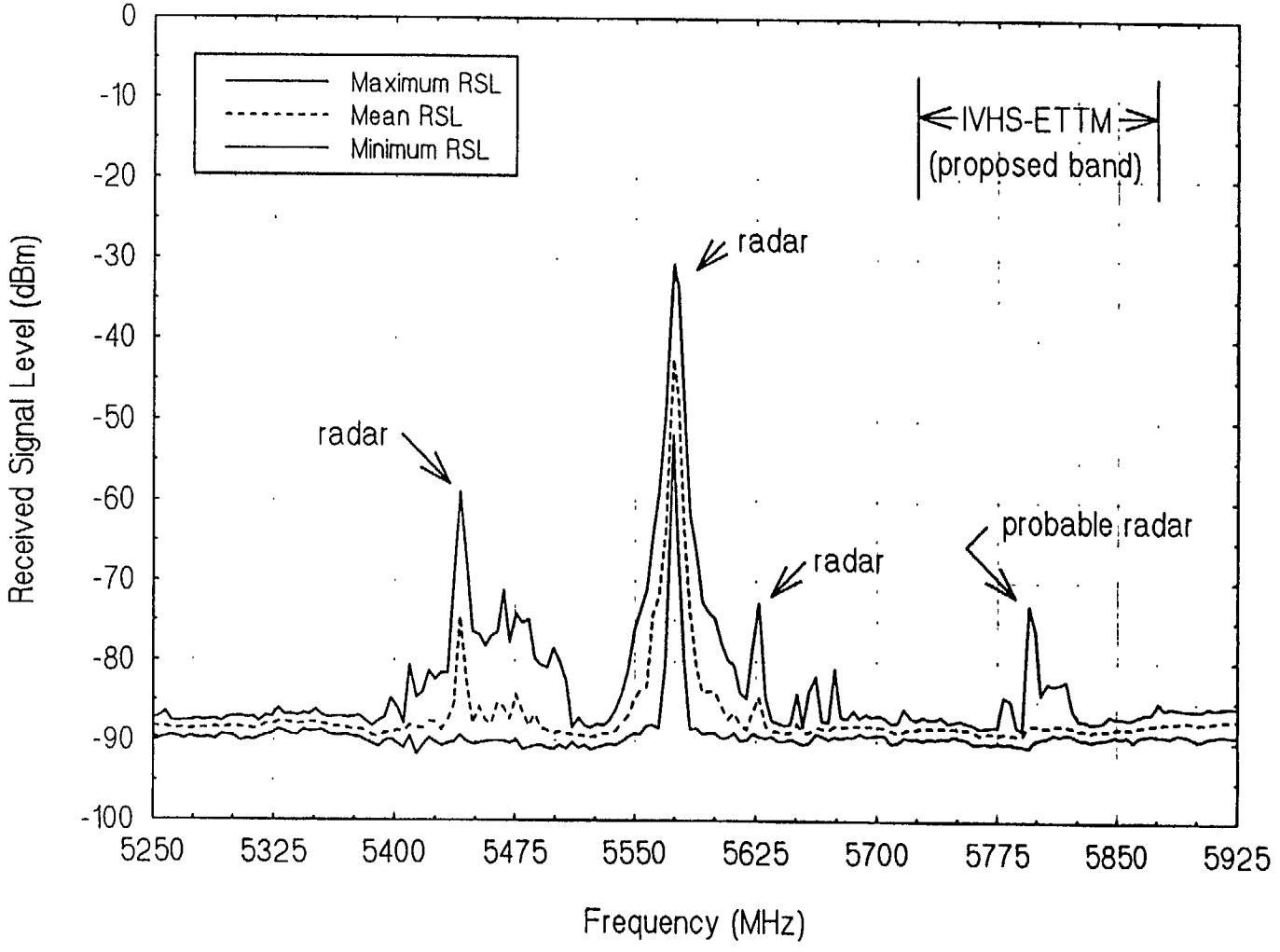

Figure 21. Spectrum survey results for Denver, CO.

of the continental U.S., and in Navy bases. The ground based radar systems operating in this . frequency range are a mixture of tracking and/or instrumentation radars. The majority of these radars are located at the various national missile test ranges. Figure 18 shows the geographical distribution per state and the assignment count (November 1992). Figure 19 shows the frequency assignment distribution in the 5725-5875 MHZ ISM band. This band, in general, is "quiet" (except, of course, at remote military base locations). Figure 20 shows the results of two spectrum survey measurements, one for Dallas and one for Seattle. Figure 21 shows the same for Denver. Note that on these surveys the ISM band (which is marked) has little activity. While these three results are fairly typical, interference within the band can occur, primarily from adjacent band radars. Figure 22 shows two surveys, one for San Francisco and the other for Atlanta. Figure 23 shows the Atlanta results with the emitters identified.

While the 5725-5875 MHZ band does not have a large number of emitters within the band, there are many C-band radars situated just below the band that can produce interference energy within the band. These radars operate in the vicinity of 5600-5650 MHZ. Figure 24 shows the measured spectra of three WSR-74C meteorological radars at Tulsa (top), Topeka (middle) and Kansas City. Note that these radars typically produce spurious emissions in our ISM band. Figure 25 shows a measured spectra of another WSR-74C radar over a wide frequency range. This measurement was taken 1.5 miles from the radar. Figure 26 shows the locations of the Government (primarily National Weather Service) meteorological radar stations while Figure 27 shows the locations of non-Government meteorological radar stations in the vicinity of 5600-5650 MHZ. The FAA has deployed 52 Terminal Doppler Weather Radar (TDWR) systems for weather forecasting, wind-shear and micoburst detection within 10-12 miles from airport runways. There are options for an additional 50 or so more TDWRs. These radars operate in the 5600-5650 band. Figure 28 shows the locations of the existing TDWRs. The TDWR system uses the technology developed for the NEXRAD system. What this means from our standpoint, is that these radars will produce little, if any, interference in the 5725-

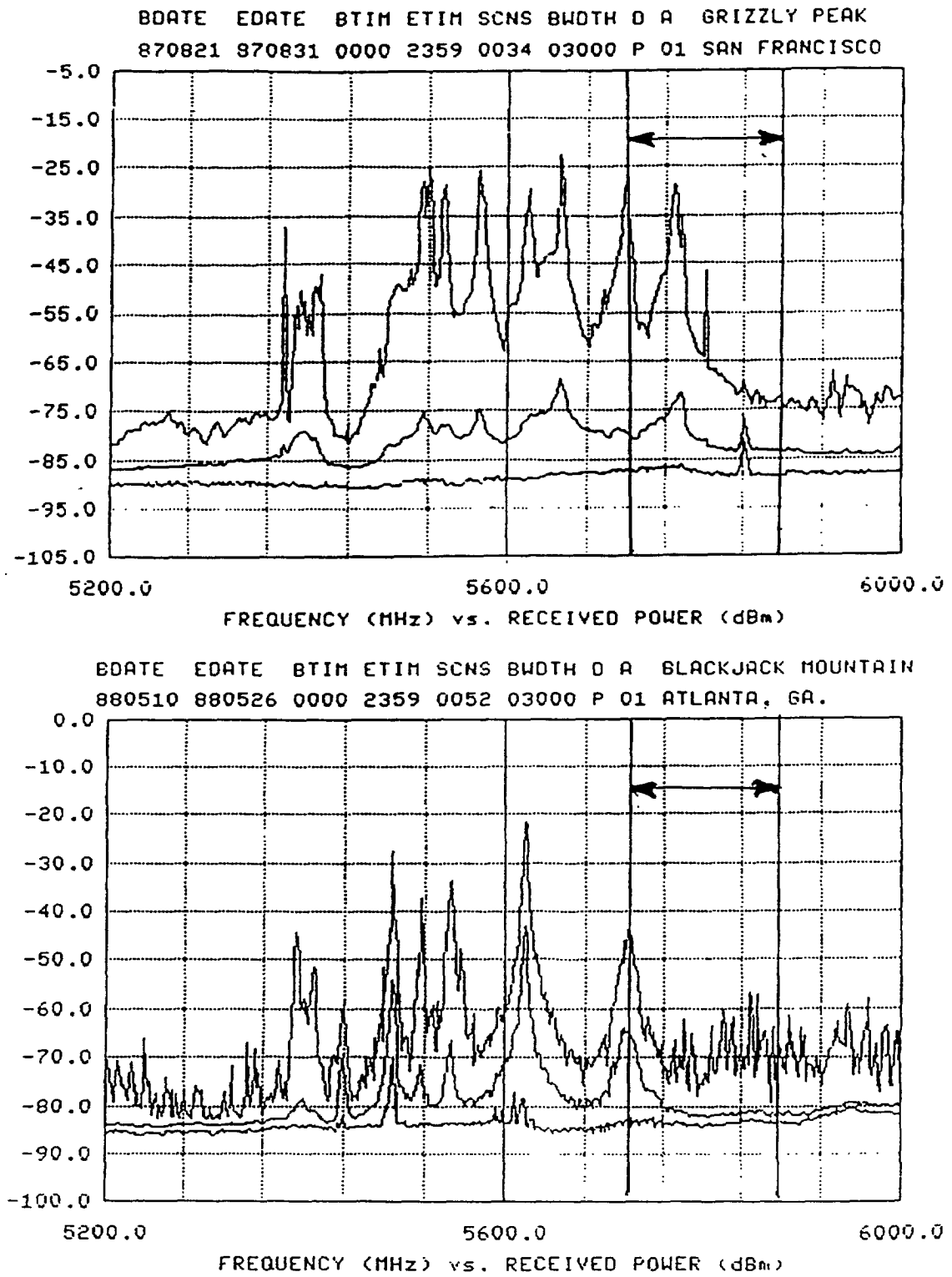

Figure 22. Minimum, mean, and maximum received power spectrum surveys; San Francisco, California and Atlanta, Georgia.

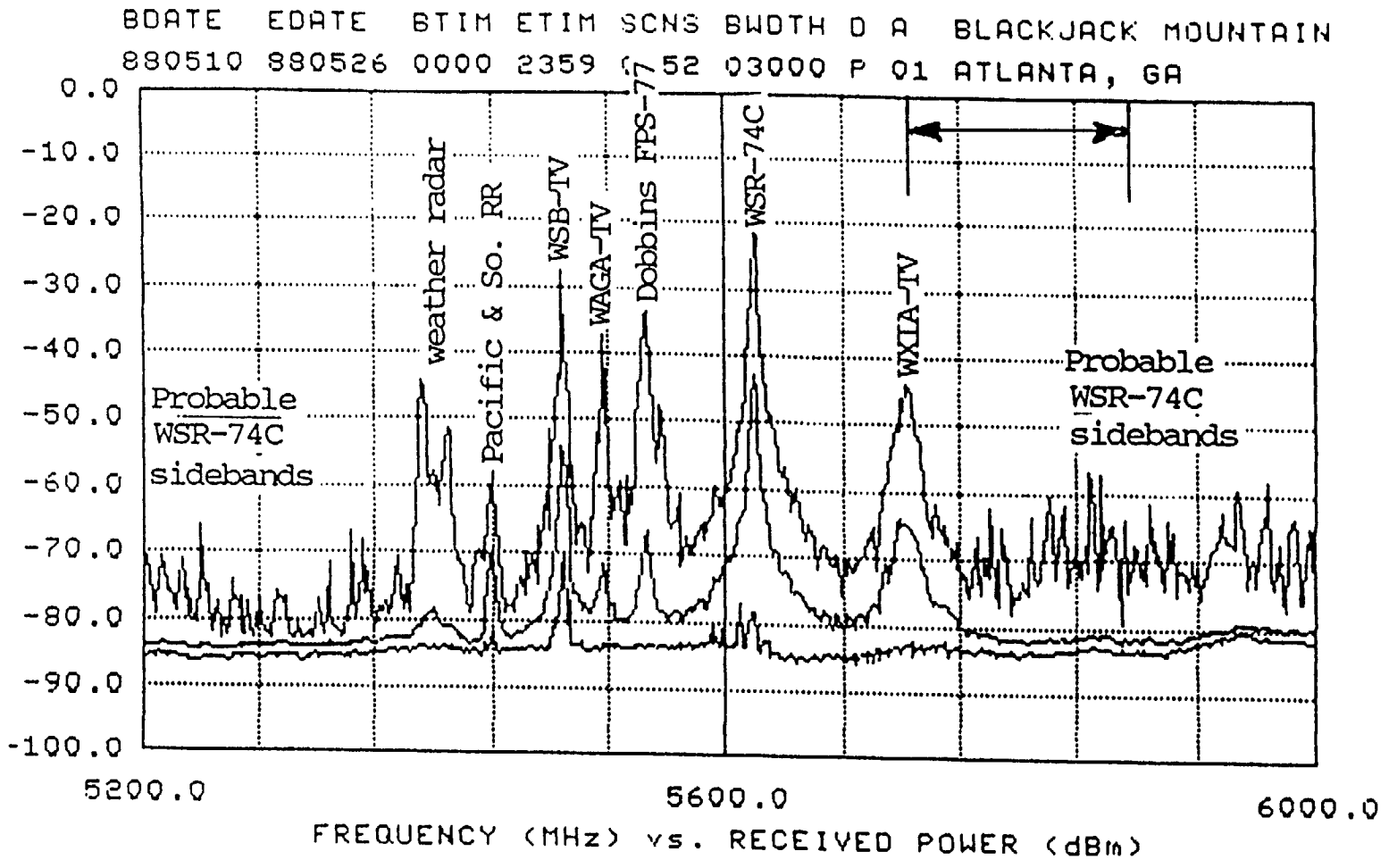

Figure 23. The Atlanta, GA. spectrum survey results showing probable emitters

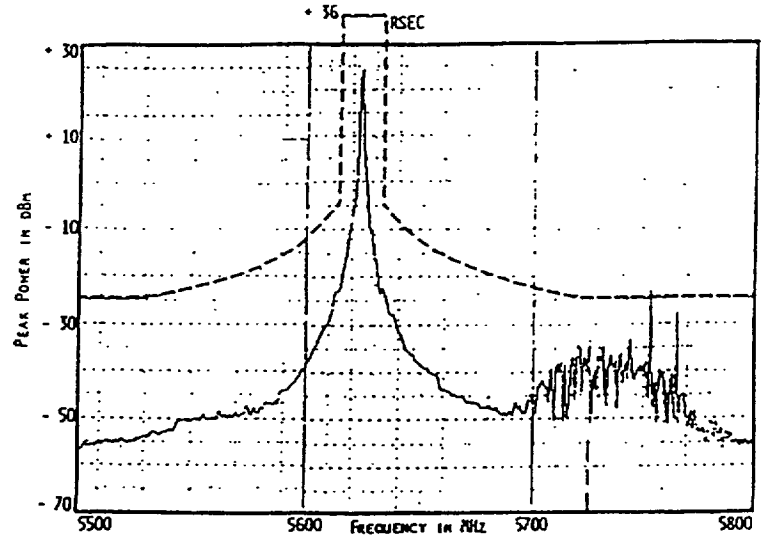

a. WSR-74C coaxial magnetron.

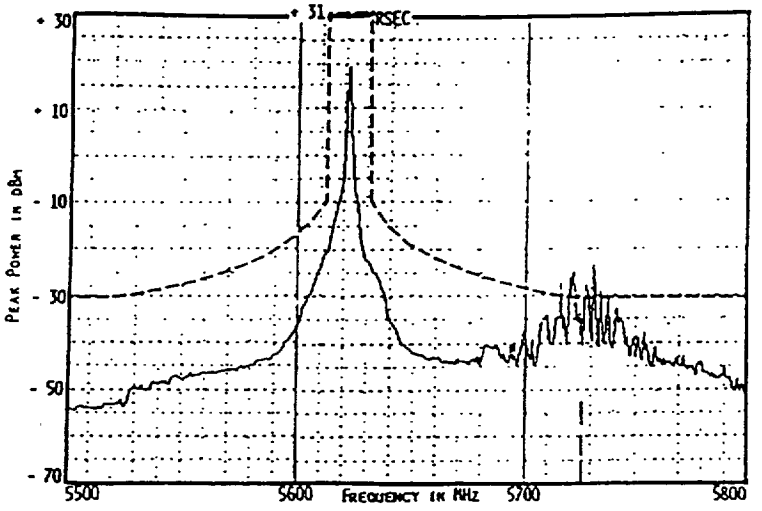

b. WSR-74C, coaxial magnetron.

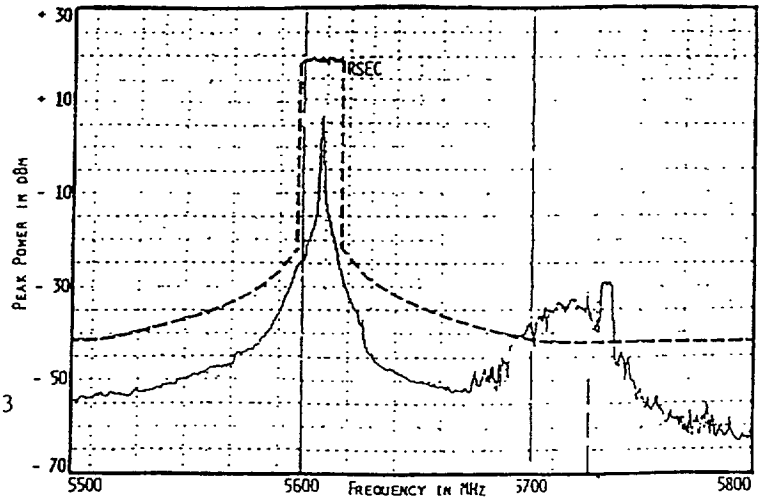

c. WSR-74C, coaxial magnetron (measurement error at 5733 MHz).

Figure 24. Measured spectrum for WSR-74C meteorological radars at Tulsa, OK., (top), Topeka, KS., (middle), and Kansas City, MO

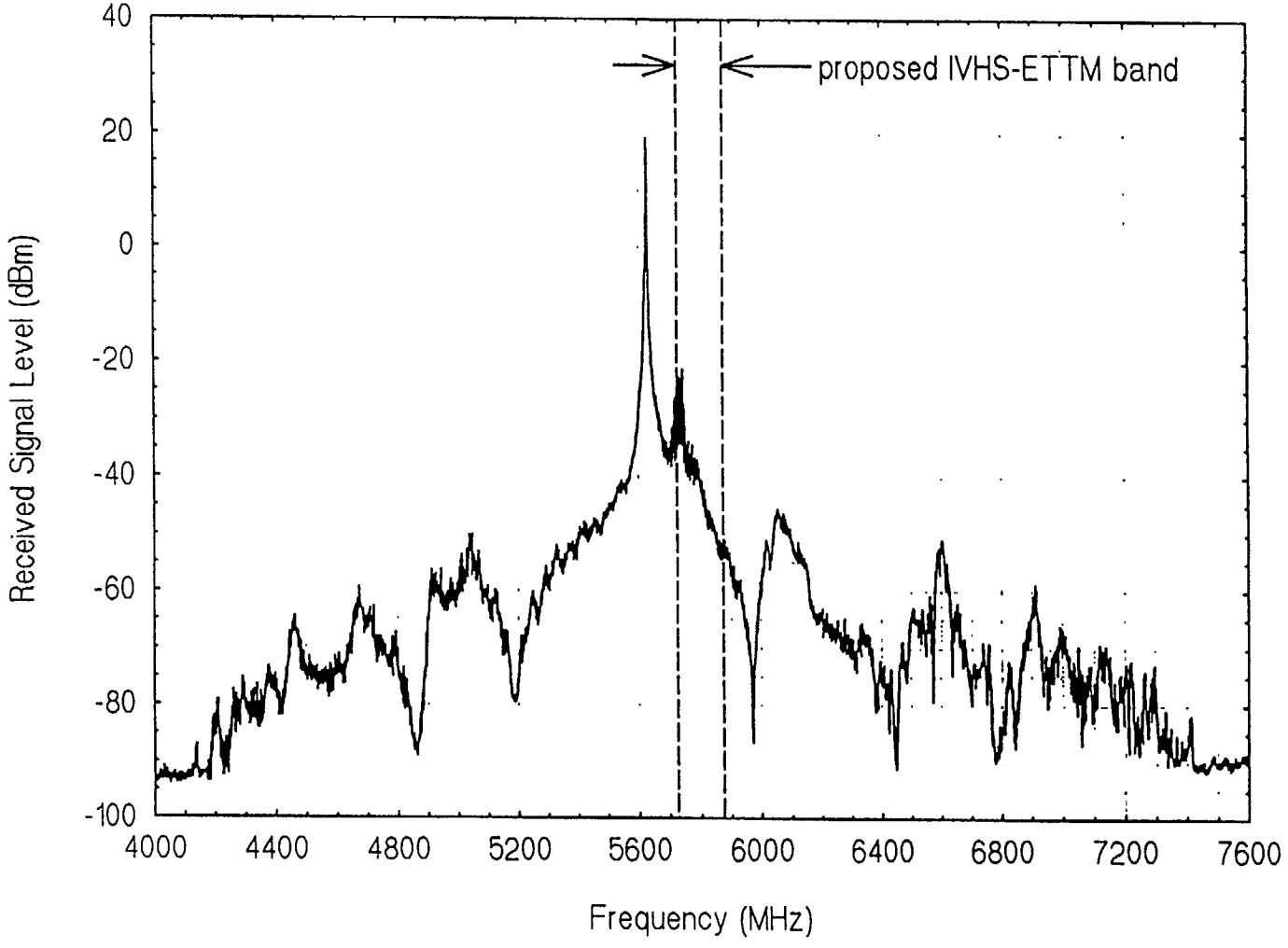

Figure 25. A measured spectrum of a WSR-74C meteorological radar, 1.5 mile distance

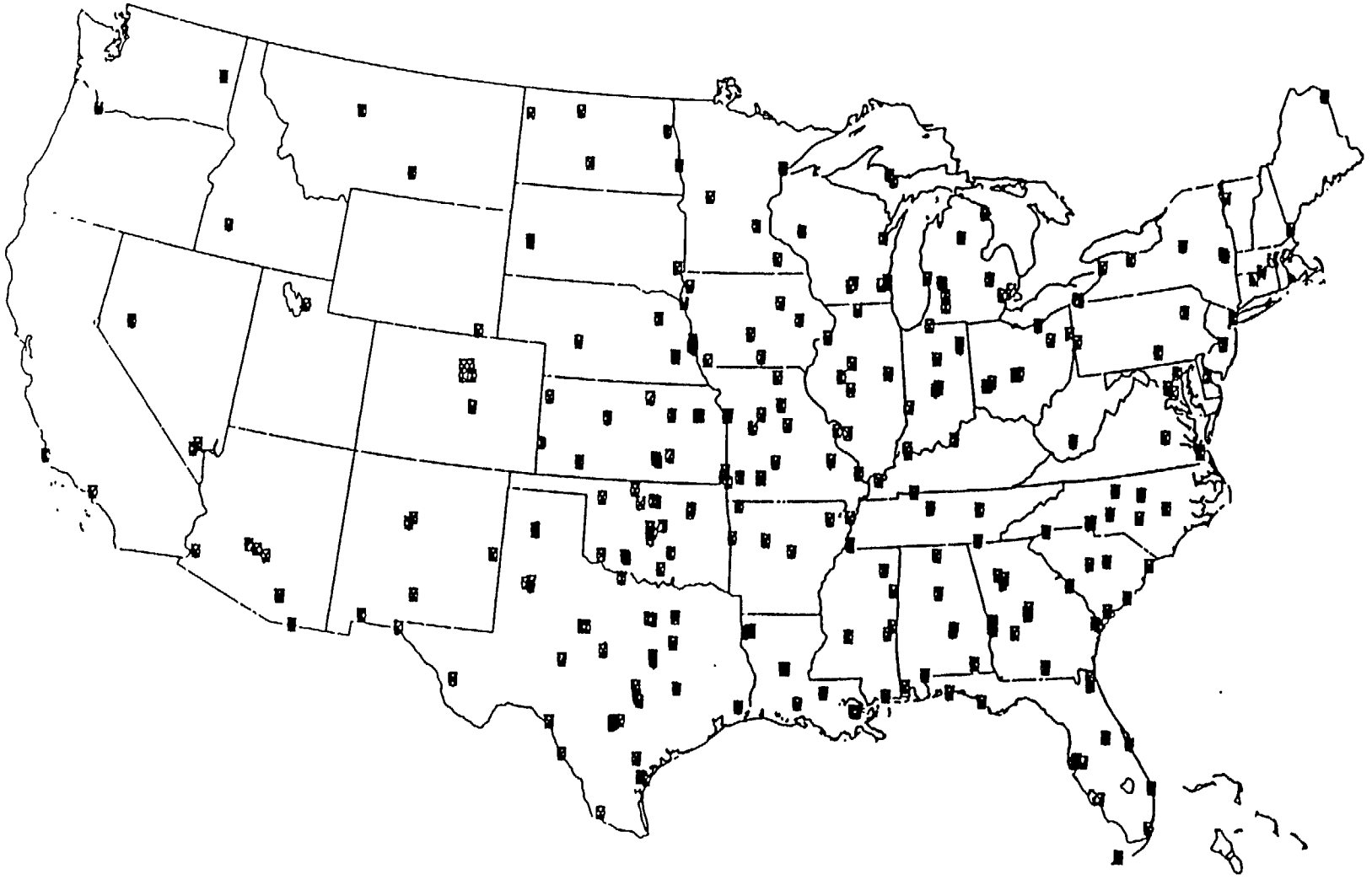

Figure 26. Government meteorological radar station locations in and in the vicinity of 5600-5650 MHz

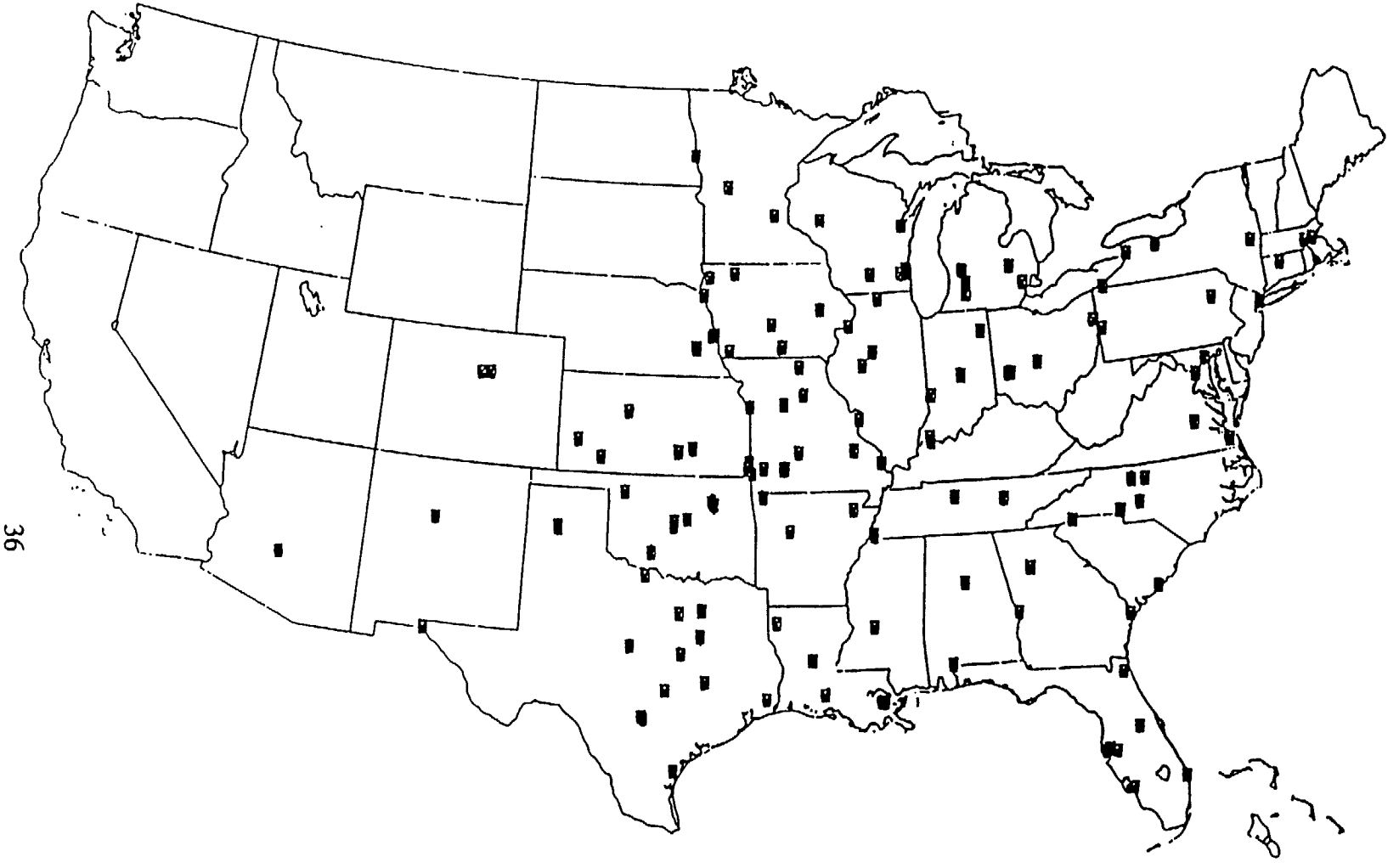

Figure 27. Non-government meteorological radio station locations in the vicinity of 5600-5650 MHz

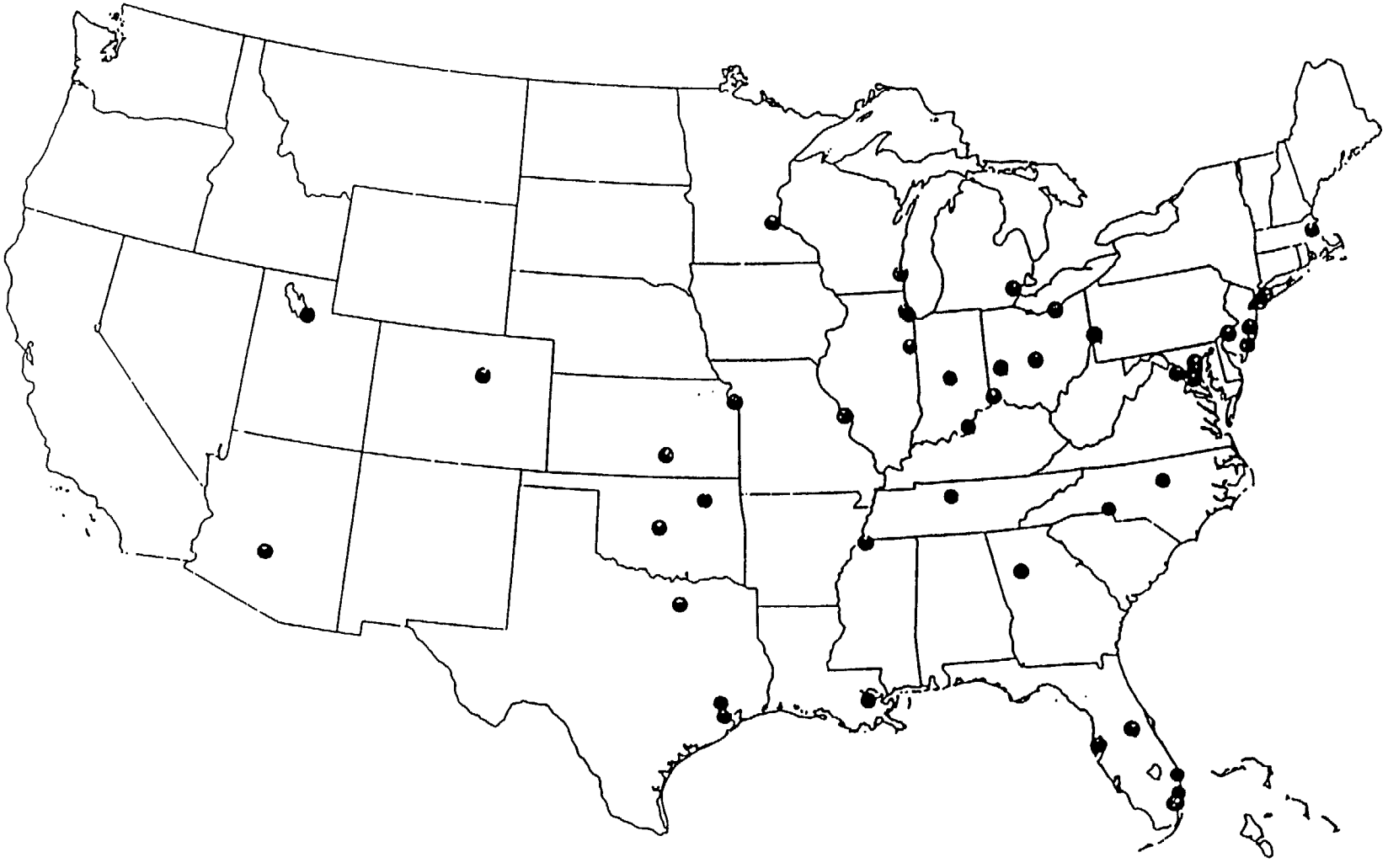

Figure 28. FAA TDWR radar locations in the 5600-5650 MHz band

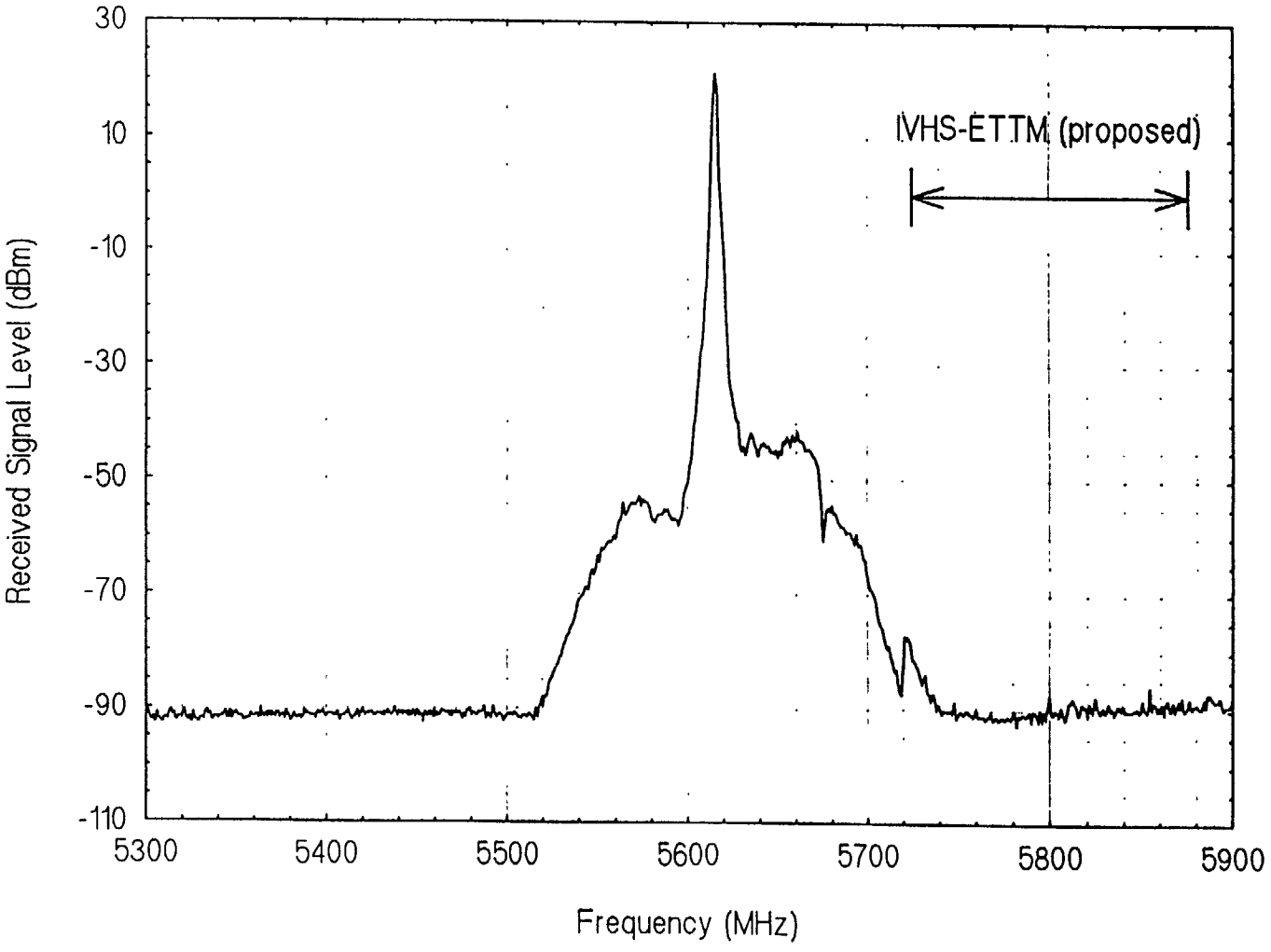

Figure 29. A synthesized spectrum for the Denver, CO. FAA TDWR radar

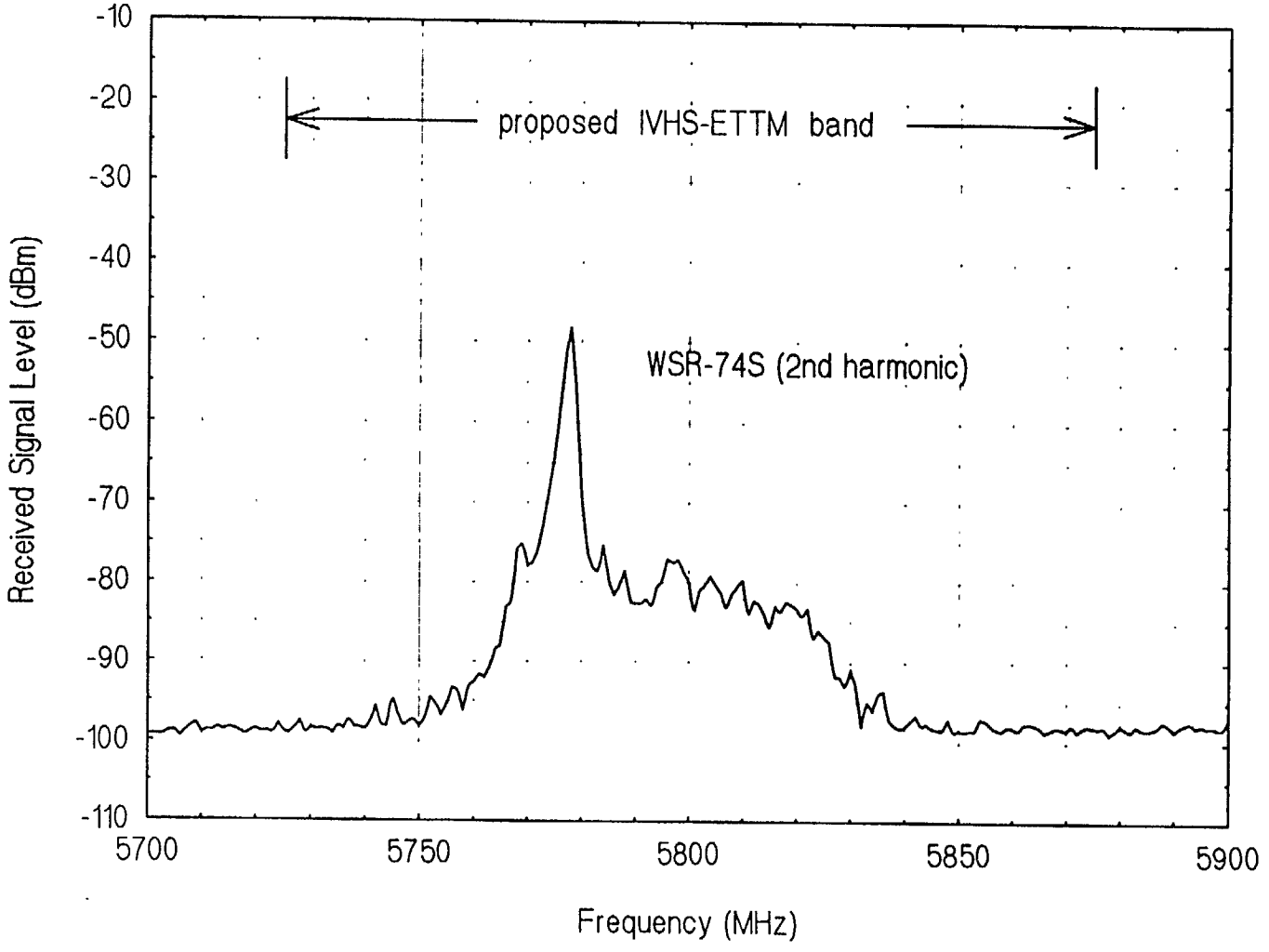

Figure 30. Measured 2nd harmonic of a WSR-74S, 1/2 mile distant

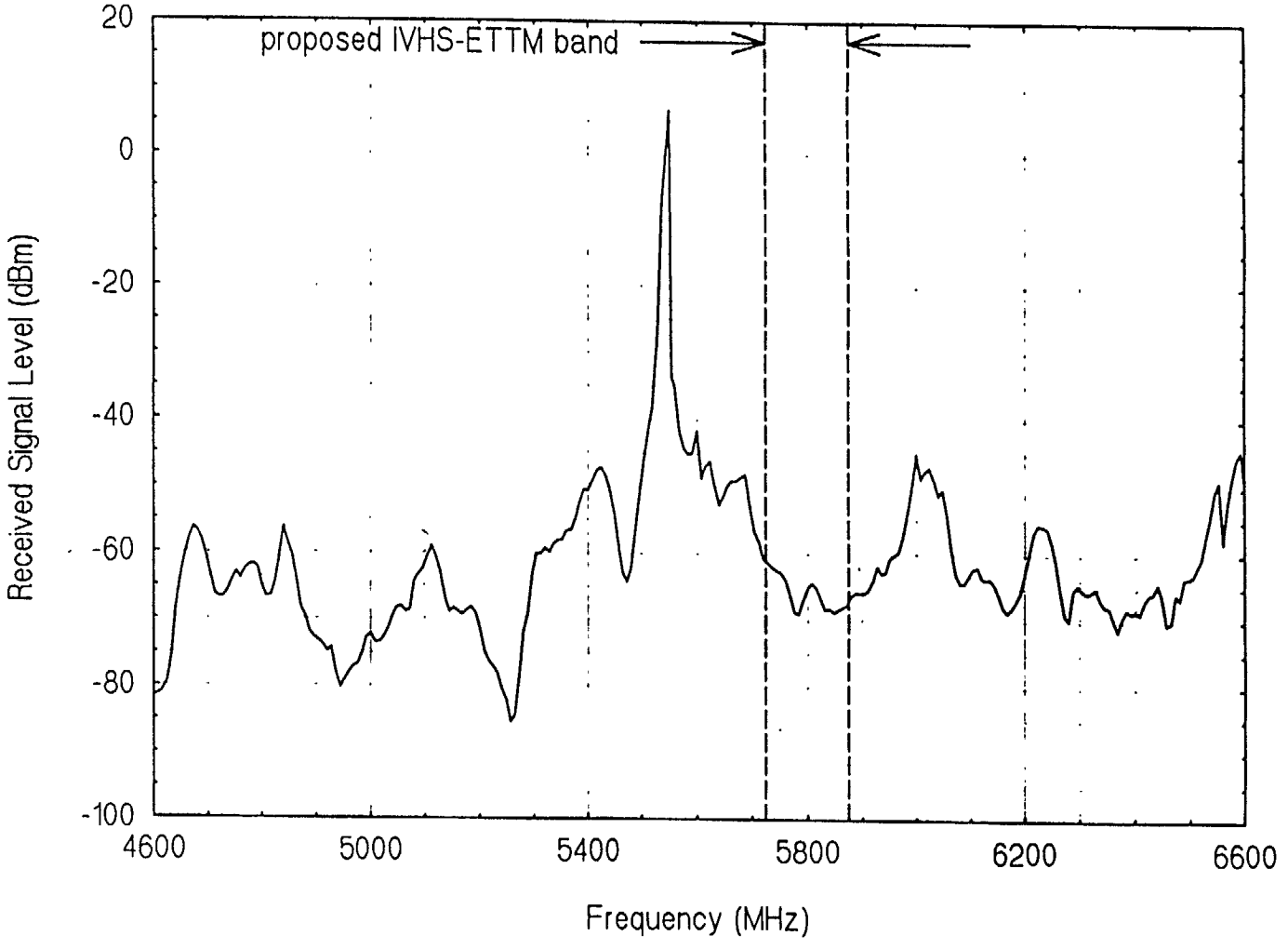

Figure 31. Measured spectrum of the radar WDSR-88CTV/KOTV in Tulsa, OK.

5875 MHZ band. Figure 29 shows a synthesized spectrum for the Denver FAA TDWR radar. For completeness, Figure 30, shows a measurement of the 2nd harmonic of a WSR-74S in our ISM band.

As noted above, both the WSR-74S and WSR-74C radars are being replaced by NEXRAD at 2700-2900 MHZ. In the 1995-1997 time frame, it is estimated that the number of Government meteological radar stations in the band in the vicinity of 5600-5650 MHZ will decline approximately 60% within CONUS, and that the number in the 2700-2900 MHZ band will increase approximately 130%. The remaining C-band radars are primarily non-Government. Figure 31 shows a measured spectrum of a WDSR-88C. These also are designated WDSR-88CTV and WDSR-9OCTV and are probably increasing in number. They can operate over the frequency range 5450-5825 MHZ, but as noted earlier, frequencies within our band are reserved for the U.S. military. The radar shown in Figure 31 is WDSR-88CTV/KOTV measured in Tulsa, Oklahoma. The next section gives an EMC analysis concerning the effects of this type of radar on generic IVHS systems.

4. Compatibility of IVHS systems and ground-based weather radars.

As noted in the last section, out-of-band radars are the main source of possible interference to IVHS systems operating in the 5.8 GHz ISM band. Radars operating above the 2.45 GHz ISM band can also result in interference to IVHS systems in this band. In this section, we want to perform an EMC analysis of the pulsed interference (radar) effects on a standard IVHS system. We start by determining a frequency-distance separation criteria under worst-case conditions. That is, no off-frequency rejection, direct antenna coupling and smooth Earth propagation. If a proposed installation meets this criterion, then no further analysis would be required. As we shall see, most possible installations probably will have enough distance separation to meet the criteria, especially when the off frequency rejection is added in. Those that don't, i.e., are within the criteria distance, require a case by case study. The actual antenna coupling and actual terrain between the radar and IVHS receiver would need to be

taken into account. The procedure is the same, and an example is included here to show the procedure to follow in actual cases.

The EMC analysis is based on a required propagation loss between the radar and the victim receiver. This required propagation loss, Lp, is given by:

$$Lp = CII - C + P_T + G_T + G_R - I, - I_R + FDR \qquad (2)$$

where:

Lp = Median propagation path loss between the transmitting and receiving antennas, in dB.

C/I = Carrier-to-interference ratio necessary to maintain an acceptable performance criteria.

C = Nominal receiver carrier level at the receiver input, in dBm.

P_T = Peak transmitted power of interfering radar system, in dBm.

G_T = Radar antenna gain.

G_R = Receiver antenna gain.

I, = Insertion loss for the radar.

I_R = Insertion loss for the receiver.

FDR = Frequency dependent rejection (off-frequency rejection) between the radar and the receiver.

Once the Lp is determined, it can be related to distance via appropriate propagation models. Of course, the major part of the analysis is determining the terms, especially the required C/I ratio, in (2).

Table 1 gives the technical characteristics of the radars of concern, i.e., those noted in the previous section. These radars are out-of-band radars and the measurements given in the last section showed some appropriate FDR values, i.e., dB below main beam. We assume the inband radars, which are DoD radars operating at remote missile test ranges, at sea, etc., will not be a problem to IVHS receivers. Even so, we start the analysis with FDR = 0, essentially

placing the radars inband, on frequency. **This** way the military counterparts of the meteorological radars are also covered. And the techniques given can be applied to "any" radar.

TABLE 1. METEOROLOGICAL RADAR CHARACTERISTICS

Model	WSR-74S
Manufacturer	Enterprise Electronics Corporation
Frequency Range	2700-2900 MHZ
Output Tube	Coaxial Magnetron
Peak Power	500 kW (87dBm)
Duty Cycle	0.000545@ 1.0 us 0.000648@ 4.0 us
Pulse Width	1 or 4 us
Pulse Repetition Rate	539 PPS@ 1.0 us 162 PPs@ 4.0 us
RX Noise Figure	9 dB
Min. Discemable Signal	-110 dBm
Antenna: Diameter	12 feet, parabolic dish
Mainbeam Gain	38 dBi
Beamwidth	2.0"
Elevation Angle	-2" to +60^{o}
Azimuth Scan Time	17 to 20 seconds

Model	**DWSR-88S "Doppler"**
Manufacturer	Enterprise Electronics Corporation
Frequency Range	2700-2900 MHZ
Output Tube	Coaxial Magnetron (locked for coherent processing)
Peak Power	500 kW (87 dBm)
Duty Cycle	0.00085@ 0.8 us 0.00085@ 2.0 us
Pulse Width	0.8 or 2.0 ,us
Pulse Repetition Rate	1063 PPS@ 0.8 us 300 PPS@ 2.0 us
RX Noise Figure	5 dB
Min. discemable Signal	-109 dBm
Antenna: Diameter	12, 14, 20 feet, parabolic dish
Mainbeam Gain	38, 39, 42dBi
Beamwidth	2.0," 1.7," 1.2"

Elevation Angle	0” to +60°
Azimuth Scan Time	20 seconds@ 0.8 us , 60 seconds@ 2.0 us
Model	**WSR-74C (WR100-2 OR -5 prior to 1974) and AN/FPQ-21**
Manufacturer	Enterprise Electronics Corporation
Frequency Range	5450-5825 MHZ
Output Tube	Coaxial Magnetron
Peak Power	250 kW (84 dBm)
Duty Cycle	0.000777
Pulse Width	3 us
Pulse Repetition Rate	259 PPS
RX Noise Figure	9 dB
Min. Discernable Signal	-104 dBm
Antenna: Diameter	8 feet (WSR-74C) 12 feet(AN/FPQ-2 1) dish
Mainbeam Gain	40 dBi 44 dBi
Beamwidth	1.5” 1,l°
Elevation Angle	-2” to +60°
Azimuth Scan Time	17 to 20 seconds and manual slewing
Model	**DWSR-88C,-88TV and -90CTV "Doppler”**
Manufacturer	Enterprise Electronics Corporation
Frequency Range	5450-5825 MHZ
Output Tube	Coaxial Magnetron (locked for coherent processing)
Peak Power	250 kW (84 dBm), max 300 kW (84.7 dBm)
Duty Cycle	0.00085
Pulse Width	0.8 us
Pulse Repetition Rate	1063 PPS
RX Noise Figure	3.5 dB
Min. Discernable Signal	-106 dBm
Antenna: Diameter	6, 8, 12, 14 feet parabolic dish
Mainbeam Gain	37, 39, 44, 45 dBi
Beamwidth	2.0,” 1.6,” 1.1,” 0.95”
Elevation Angle	0” to +60° (manual operation from 0° to 90°)
Azimuth Scan Time	20 seconds
Model	**NEXRAD (WSR-88D)**
Manufacturer	UNISYS Corporation
Frequency Range	2700-3000 MHZ

Output Tube	Klystron
Peak Power	750 kW (88.8 dBm, normal), 1MW max. (90 dBm)
Duty Cycle	0.0021
Pulse Width	1.6 us and 4.7 us
Pulse Repetition Rate	318-1304 PPS @ 1.6 us 318-452 PPS@ 4.7 us
RX Noise Figure	2.1 dB
Min. Discernable Signal	-115 dBm
Antenna: Diameter	28 feet, parabolic dish
Mainbeam Gain	45 dBi
Beamwidth	0.89° to 0.95°
Elevation Angle	**-1**° to **45**°
Azimuth Scan Time	**20** seconds

Model	**Terminal Doppler Weather Radar (TDWR)**
Manufacturer	Raytheon
Output Tube	Klystron
Frequency Range	**5600-5650 MHZ**
Peak Power	**250** kW (84 dBm)
Duty Cycle	**0.0022**
Pulse Width	1.1 us
Pulse Repetition Rate	**2000** PPS
RX Noise Figure	1.8 dB
Min. Discemable Signal	109 dBm
Antenna: Diameter	25 feet, parabolic dish
Mainbeam Gain	50 dBi
Beamwidth	**0.5**°
Elevation Angle	-1° to +60°
Azimuth Scan Time	11 seconds

We now need the characteristics of the generic IVHS system required for input to (2) and for determination of the required C/I ratio. The characteristics we need were obtained from various publications and draft standards, as well as personal correspondence with IVHS equipment developers. The main source was from Draft 4 Standard Exxx-xx of the American Society for Testing and Materials (ASTM) committee [13]. Additional information, especially ETTM specific, is contained in the IVHS America (now ITS, Intelligent Transportation System, America) Draft Version 2.0 report [14], the National Institute of Standards and Technology (NIST) document by Scott, et al [15], the Lawrence Livermore National

Laboratory document by Davis [16], and the National Cooperative Highway Research Program (NCHRP) Synthesis 194 by Pietrzyk and Mierzejewski [17]. The Draft Standard [13] is intended to meet the requirements for many of the Vehicle-to-Roadside Communications (VRC) defined by the Intelligent Vehicle Highway Society of America for Commercial Vehicle Operations (CVO), Advanced Traveler Information Systems (ATIS), Advanced Vehicle Control Systems (AVCS), Electronic Toll and Traffic Management Systems (ETTM), Advanced Public Transportation Systems (APTS), and Advanced Transportation Management (Systems (ATMS).

The above documents, collectively, give a good set of specifications for IVHS systems, especially those we need for our EMC analysis, however, as noted above, some required information was obtained from equipment developers. Table 2 summarizes the basic IVHS characteristics.

TABLE 2. SUMMARY OF CHARACTERISTICS

PARAMETER	CHARACTERISTICS
Carrier Frequency	Country/Application Specific (Subject to assignment)
Carrier Modulation	Unipolar ASK (Manchester Encoded)
Data BIT Rate	500 kbps
Message Data	512 data bits per TDMA packet, single or multi-packet transactions
Technology Type	Two-way Active RF
Antenna Location	Application Specific
Protocol	TDMA/Adaptive slotted Aloha Access

The Manchester Coding means a 0 data bit is composed of a 0 bit (carrier off) followed by a 1 bit (carrier on) and a 1 data bit is composed at a 1 bit followed by a 0 bit. Note that the Manchester Code has a transition in the middle of every bit interval whether a one or a zero is being sent. This guaranteed transition provides synchronization and a clocking signal. The 500 kbps rate for all messages implies a minimum receiver band width of approximately 1.5 MHZ.

The VRC equipment is composed of two principle components: a Beacon (also referred to as a Reader) and a Transponder. The transponder is intended for, but no restricted to, installation in or on a vehicle. The Beacon activates the Transponder and reads from or writes to the Transponder, and assures message deliverability and validity. Here, we consider the Reader receiver the most vulnerable to the interference since it is in a fixed location and has a much higher gain antenna. The method of analysis used, however, could apply equally well to the Transponder receiver. The message includes a 16 bit cyclic redundancy check for error detection and a 7 bit linear sequence for link validation. The reader transmits at RF power levels allowed at the operating frequency for each country, region, and/or application. Currently, in the U.S., the VRC reader peak output power at 915 MHZ is 30 dBm or one watt. Typical U. S. installations use an antenna with 13 dB of gain, so the reader/antenna EIRP is 43 dBm or 20 watts. If one wants to maintain the same range at the higher frequencies, then the transponder sensitivity or the reader transmit power must be increased by 8.6 dB at 2.45 GHz and 16.0 dB at 5.8 GHz Of interest to us (required in (2)) is that the nominal receiver system carrier level at the reader receiver input must be > 165 uV/m or (-35 dBm). The transponder transmit amplifier and antenna shall operate at a field strength between 170 mV/m to 350 mV/m, when measured at one meter along the antenna boresight. The performance standard needed by us in order to determine the required C/I ratio is that the received bit error rate shall be no greater than 10^{-5}. The ETTM system has a separate criteria, namely, a bit error rate no greater than 10^{-7}. We will use the 10^{-5} threshold in our EMC analysis, but also give results (required C/I ratio) for the 10^{-7} case. We will also use the 13 dB reader antenna gain noted above, even though the gain could be somewhat different at the

higher frequencies. Also, system performance improvement can be achieved via appropriate signal processing and the use of specialized antennas, as covered in the next section on interference modeling.

The above has given the basic parameters of VRC systems. Table 2 summarizes the ones we need for the EMC analysis.

TABLE 3. RECEIVERPARAMETERS

Bandwidth	1.5 MHZ
Nominal Carrier Level at receiver input	-35 dBm
Receiver Antenna Gain	13 dBi
Required Error Rate	$< 10^{-5}$
Required Error Rate (ETTM)	$< 10^{-7}$

Next, we must determine the required C/I ratio. This, of course, is the difficult part of the analysis. Traditionally, this determination can take the form of 'closed form" analytical expressions, laboratory measurements, and numerical or "Monte Carlo" simulation. The analytical expressions, when they exist, are often not approximate for actual systems due to the necessity of making simplifying assumptions in the analysis to obtain tractable solutions. Also, a search of the literature showed no available analytical results applicable to our case. In 1990, NTIA performed an EMC analysis entitled "Ground-based weather radar compatibility with digital radio-relay microwave systems" [18]. For this study, the required C/I ratio was determined by AT&T laboratory measurements. The report (Weather Surveillance Radar Interference to Digital Common Carrier Microwave Systems, by Richard Callahan, AT&T Memorandum, AT&T Headqurters, Rt. 202-206, Bedminster, NJ, 01971) detailing these measurements was, apparently, never produced. Some of the radar information used here was obtained from [18].

In analyzing complex systems, numerical simulation has become the tool of choice. Simulation is also useful in checking analytical models of system performance, and vice versa. The great increase in computer computational power also makes simulation attractive. An example of the current state of simulation sophistication can be gleaned from [19]. In [19], the NASA/GSFC Communications Link Analysis and Simulation System (CLASS) is used. Developing a computer simulation of a complex communications system, however, often requires extensive and time consuming programming. The need to mitigate this programming requirement led to the development of the Advanced Communications Link Analysis and Design (ACOLADE) simulation environment. ACOLADE was originally developed for the DoD, but is now a commercial product. ITS has installed and added to the ACOLADE system and uses it for various system simulations. ACOLADE is a software tool that enables a user to quickly and easily design and implement a Monte Carlo simulation for a communications system of arbitrary complexity. Here, we use ACOLADE to analyze the effects of the radar pulsed interference on our IVHS receiver (reader).

As noted earlier, the DWSR-88C type radar will remain near the 5.8 GHz ISM band after the WSR-74C's are replaced by NEXRAD (WSR-88D). Therefore, we will use the DWSR-88C pulse structure (0.8 μs pulse, 1063PPS) in our simulation, but will also look briefly at the other radars. The ACOLADE system does not have Manchester encoding as one of its options. We model the ASK Manchester by BPSK at double the Manchester rate, that is at a bit rate of 1 MHZ in our 1.5 MHZ bandwidth. BASK at 1 MHZ is the actual system, but BASK is not an ACOLADE option, and BPSK and BASK are "identical" with a 3dB shift in signal-to-interference ratio. As we will see, this will not effect our analysis. We want to determine a signal-to-jammer (the radar signal being the jammer) ratio that results in no significant performance degradation to the IVHS reader. This is our C/I for equation (2). In the absence of the pulsed interference, we assume the system is operating in white Gaussian noise.

The interfering signal has a 0.8 usec pulse every 940.7 usec (1063 PPS). If we used this actual interfering signal for our simulation, much to much computer time will be required. That is, errors are infrequent, and if we want results for a probability of error of 10^{-5}, say, we require, for statistical significance, about 10 errors, or 10^{6} samples. Also, ACOLADE uses average interference power, and we require peak interference power in our C/I ratio, since peak transmitted radar power is used in (2). This requires programming a modification into ACOLADE . In the simulation, we will use a pulse every 4 usec (instead of every 940.7 usec). This will generate more errors by a factor of 293.72 (24.7 dB), requiring about one three hundredth of the computer time. Still, many hours of computer time are required to perform the Monte Carlo simulation. The results then can be scaled to determine performance in the actual interference. To cross check, we will also do a simulation using pulses every 8 usec. This is a factor of 130.54 or 21.2 dB.

Figure 32 shows our simulation topology as represented by the ACOLADE Graphical User Interface (GUI). The system consists of an equiprobable binary source, the BPSK modulator, the additive white Gaussian noise channel, the demodulator and error counter. The radar pulsed interference is added in as shown. Also, shown is the spectrum of the desired digital signal, the spectrum of the pulse interference, and the envelope of the interference, i.e., 0.8 usec pulses every 4 usec. Figure 33 shows the simulation results. The result for additive white Gaussian noise and no pulsed interference is labeled BPSKAWGN. This simulation result is extremely close to the theoretical (textbook) result, e.g., see Sklar [20]. The curves labeled jsr (jammer-to-signal ratio) are for the pulse interference being added. Note that as the jsr decreases, (signal-to-interference ratio increasing) the results approach the white Gaussian noise results. We want the jsr that essentially matches the Gaussian result, but for our actual interfering signal (1063 PPS). This is the required jsr that results in no noticeable degradation to the system. At the 10^{-5} probability of error level (an SNR of 9dB) we determine which jsr curve has 293.72 (24.7 dB) more errors. From Figure 33, this gives a jsr of -35.5 dB or a

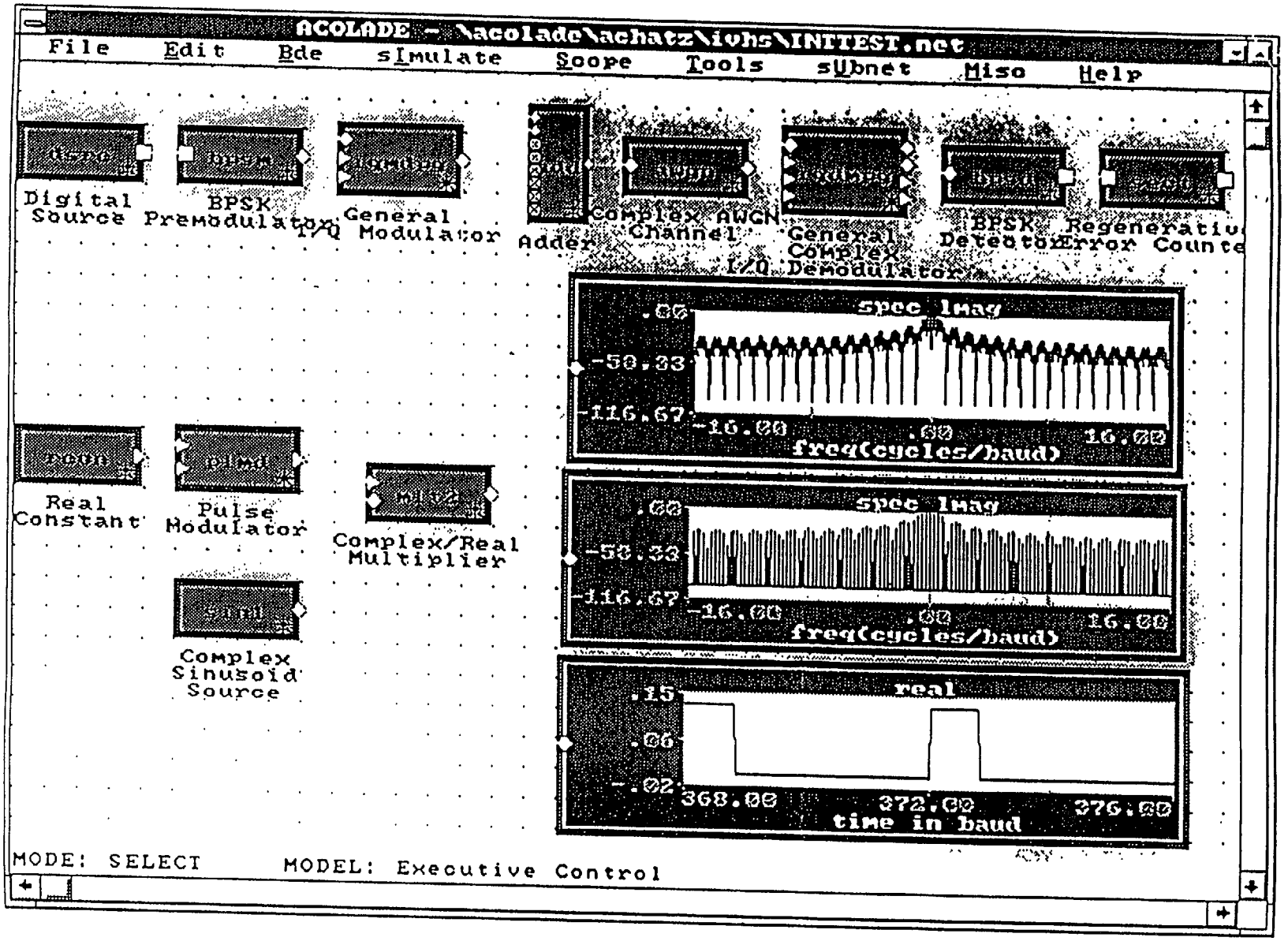

Figure 32. The simulation architecture as displayed by the ACOLADE Graphical User Interface

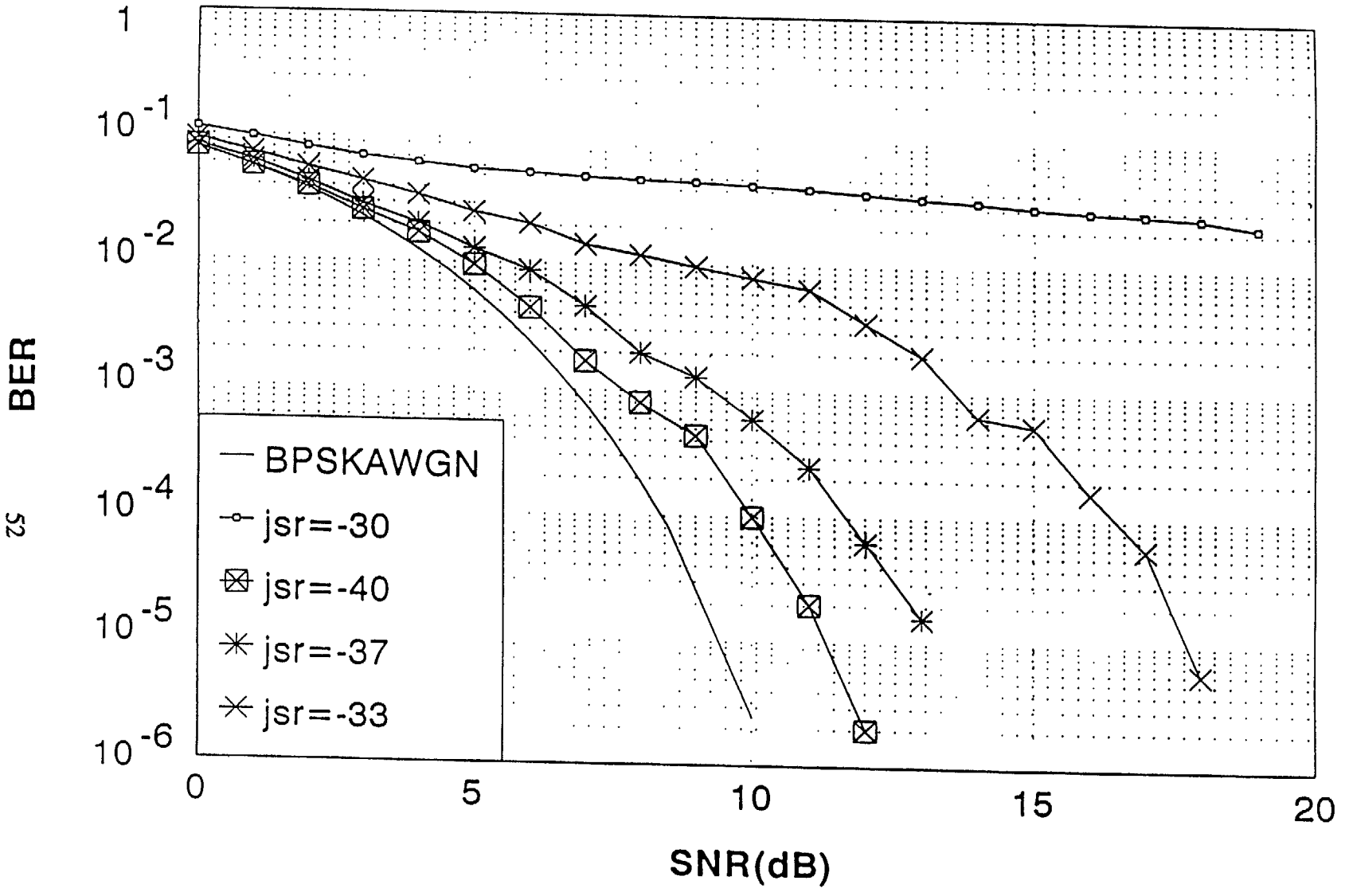

Figure 33. Simulation results for radar pulse interference, 0.8 μsec pulses every 4 μsec, BPSK system, 1 MHz bit rate, 1.5 MHz bandwidth

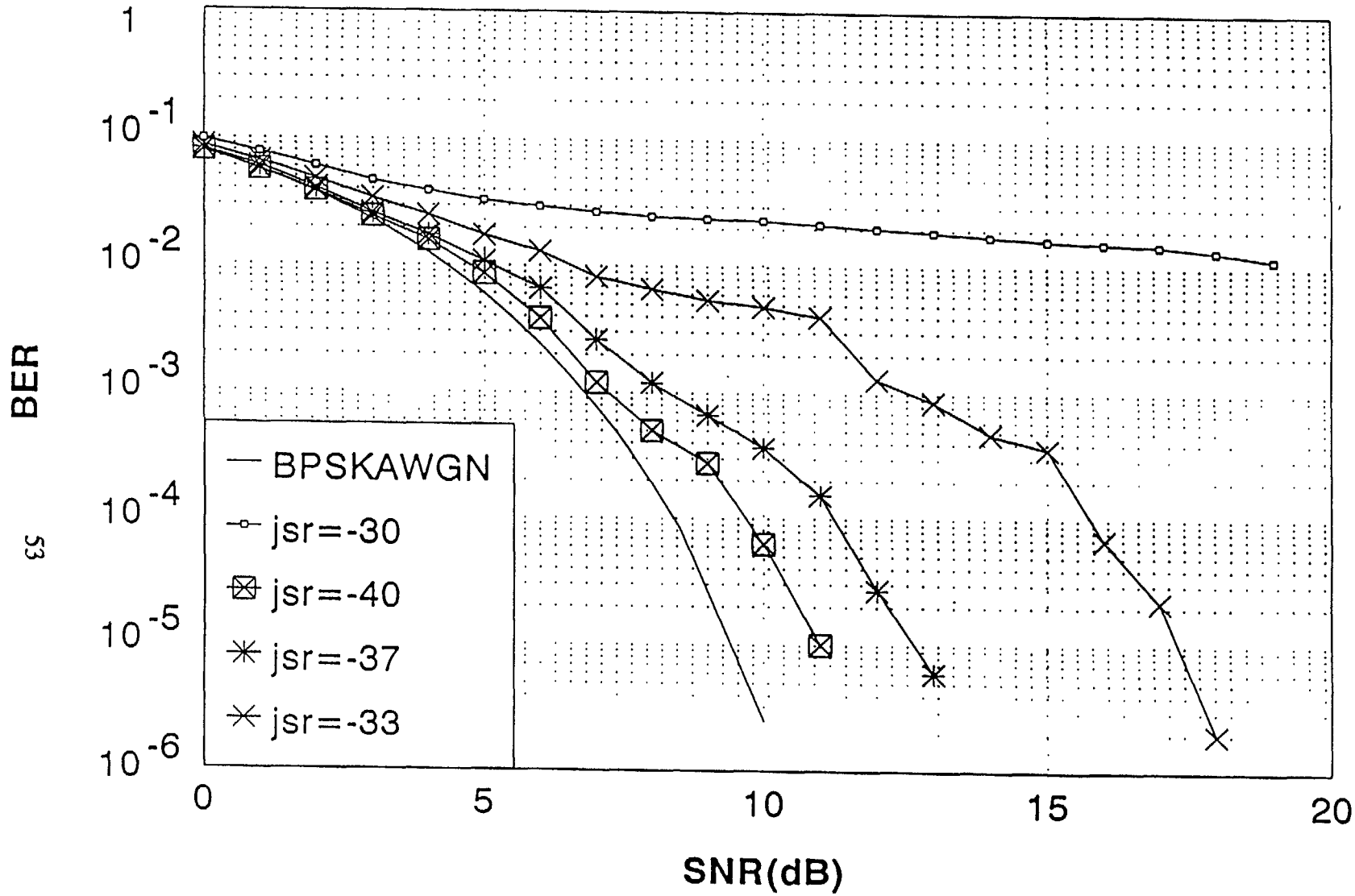

Figure 34. Simulation results for radar pulse interference, 0.8 μsecpulses every, 8 μsec, BPSK system, 1 MHz bit rate, 1.5 MHz bandwidth

required C/I ratio of 35.5 dB For the 10^{-7} probability of error requirement, the AWGN noise curve needs extrapolating. The 10^{-7} BER occurs at a SNR of 11 dB. Following the above procedure, we obtain a required C/I ratio of 39 dB.

Figure 34 shows the simulation results for the 0.8 usec pulses occurring every 8 usec Following the above procedure, we obtain a required C/I ratio of 36 dB for the 10" BER case and a required C/I ratio of 39 dB for the 10^{-7} BER case. We now have the required C/I values for (2). We will use 36 dB for the 10^{-5} BER case. As noted above, the scaling procedure used is only appropriate (reasonable accurate) at low BER.

We now have the information required for (2). For the insertion losses, I_T and I,, we will use the typical values of 2dB for the radar (IT) and 3 dB for the reader (I_R). Using the parameters given in Table 1 for the DWSR-88CTV radar and Table 2 for the IVHS receiver, we obtain, for 10^{-5} BER threshold:

$$Lp = 36 + 35 + 84 + 44 + 13 - 3 - 2 + FDR \ dB,$$
$$L_P = 207 + FDR \ dB \qquad (3)$$

The result (3) indicates that under worse case conditions of direct antenna coupling (mainbeam to mainbeam) and the radar at the same frequency as the receiver (FDR = 0) we require a path loss of 207 dB to be assured of no interference from a DWSR-88CTV radar. It remains now to determine what distance corresponds to the required path loss. Figure 35 shows propagation loss versus distance for the two frequencies 5800 MHZ (lower curve) and 2450 MHZ (upper curve). The results of Figure 35 were obtained using the Irregular Terrain Model (ITM) [21] via the ITS Telecommunications Analysis (TA) Services [22]. The purpose of the TA services is to provide analysis techniques in the form of easy-to-use time-sharing computer programs to interested agencies and organizations. The propagation parameters used for Figure 35 are given below in Table 4.

TABLE 4. PROPAGATION PARAMETERS

Model	Smooth Earth
Output Option	Basic Transmission loss
Frequency	2450 MHZ 5800 MHZ
Conductivity	0.27 S/m
Dielectric constant	15.0
Climate Zone	Continental Temperate
Xmtr ant Height	50 Ft.
Rcvr ant Height	3.00 m (9.84 ft.)
Analysis radius	300 mi

From Figure 35, at 5800 MHZ, we see that a Lp of 207 dB requires a distance separation of 40 miles (FDR= 0). This is the worst case possible, direct mainbeam coupling and Smooth Earth propagation. We can probably safely assume the IVHS systems will be a least 40 miles from the military inband radars, located at remote DoD test sites. For a case of more interest to us, consider the WSDR-88C radar of Figure 31. For this radar at 5800 MHZ, we have an FDR of approximately -70 dB That is, the radar power at 5800 MHZ is 70 dB below the mainbeam power at 5550 MHZ. Now, we require an Lp of 207-70 or 137 dB. From figure 35, an Lp of 137 dB corresponds to a distance separation of 7 miles. This is still for worst case conditions of mainbeam coupling and Smooth Earth propagation.

Even though the WSR-74C radars are scheduled to be replaced as noted earlier, some may still be used past 1997. As a further example of the compatibility analysis, consider the WSR-74C radar of Figure 25. This radar ha a 3us pulse width and 259 PPS. It has the same peak power (84 dBm) and Mainbeam gain (44 dB) as the DSWR-88C treated above (Table 1). Note that the pulse width is 3.75 times the pulse width of the DSWR-88C and the pulse rate is 4.15

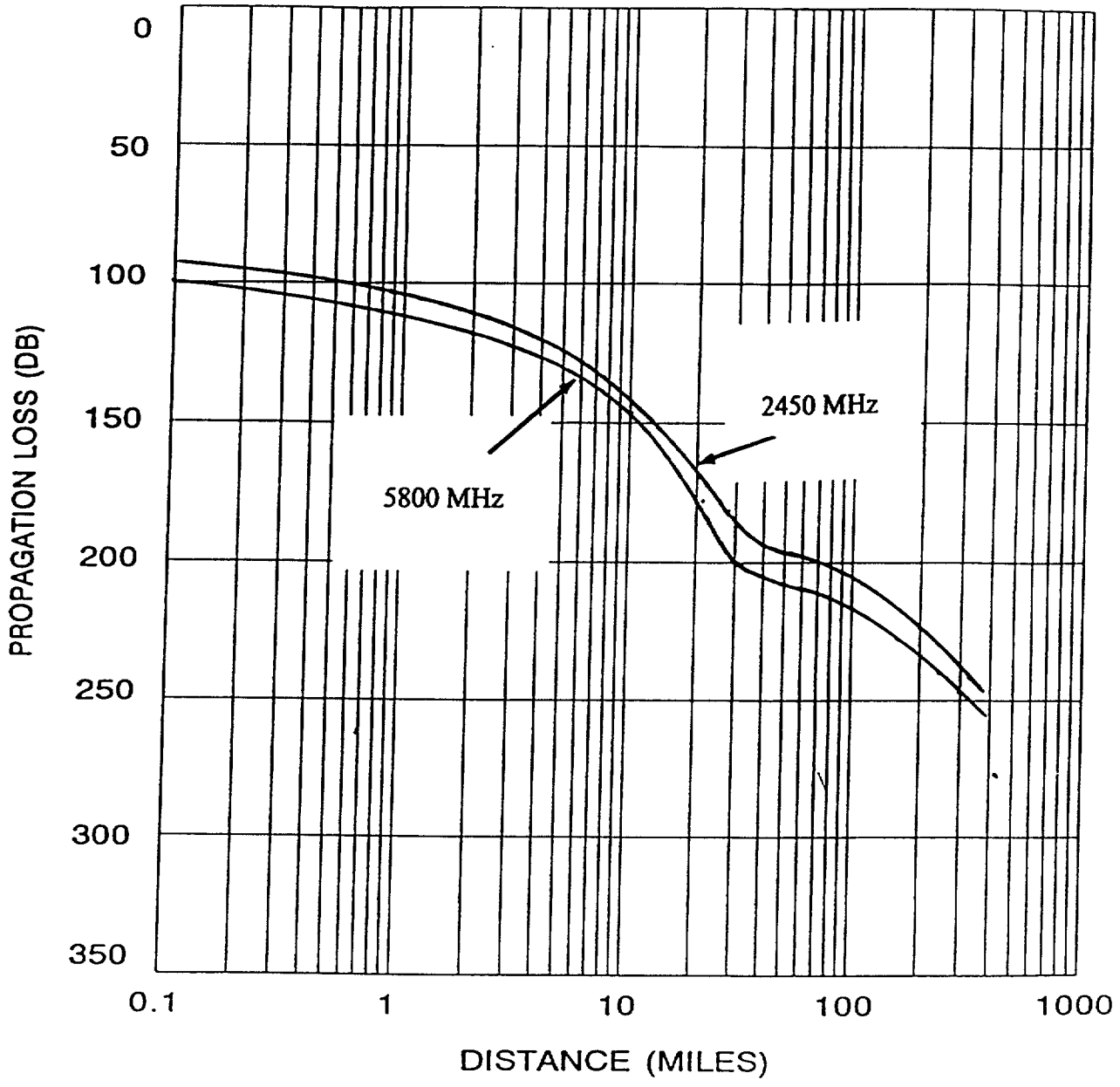

Figure 35. Basic transmission loss versus distance, smooth Earth, soft transmitting antenna height and 3 meter (9.84 ft.) receiving antenna height

times less. This means that the WSR-74C will cause essentially the same number of errors as the DSWR-88C. We can therefore approximate the required C/I ratio by 36 dB (for the BER of 10^{-5} threshold) for the WSR-74C. Since the parameter values for use in (2) are the same as before, the required path loss for the WSR-74C is 207 + FDR dB. From figure 25, this particular WSR-74C has an FDR of between -40 and -65 dB, depending where our IVHS system is located in the 5.8 GHz ISM band. Using the -40 dB, we require a Lp OF 167 dB. From Figure 35, this corresponds to a required distance separation of approximately 17 miles.

The 17 mile separation distance derived above is worst case Smooth Earth propagation. If our particular IVHS system is within 17 miles of this particular WSR-74C radar, a more detailed analysis is required. Our example radar (Figure 25) is located near the Worcester Municipal Airport in Massachusetts at 42" 16' 2.1" North latitude and 71 0 52' 24.5" West longitude. Figure 36 shows a map of the area around this radar. The terrain in this area is rather hilly. Figure 37 shows an output from TA services using the same lTM propagation model, but this time using actual 3 second digital terrain data rather than Smooth Earth. Figure 37 is for a 30 mile area around the radar. Note that our required 167 dB basic transmission loss is achieved throughout most of the area, even quite near to the radar. Any IVHS system in the shaded areas of Figure 27 will meet our criteria. Note further, we still are considering worst case direct antenna mainbeam coupling. Of course, the same propagation parameters (except for Smooth Earth and analysis distance) given in Table 3 were used. The WSR-74C has an 8 foot dish with a 1.5" beam width and can have an elevation of -2" to 60. 0 Suppose for our case of interest, we will not have direct mainbeam coupling, but 20 dB less. It takes very little off mainbeam of the 12 ft. dish to reduce the field by 20 dB Our required transmission loss is now 147 dB (167-20). Figure 38 shows the same as Figure 37, but now for the 147 dB criteria. Even more of the area is now available to us. This example has been to illustrate an EMC analysis procedure for a particular case. Such an analysis is required when we find ourselves within the "basic" general purpose criteria derived above for various radar types.

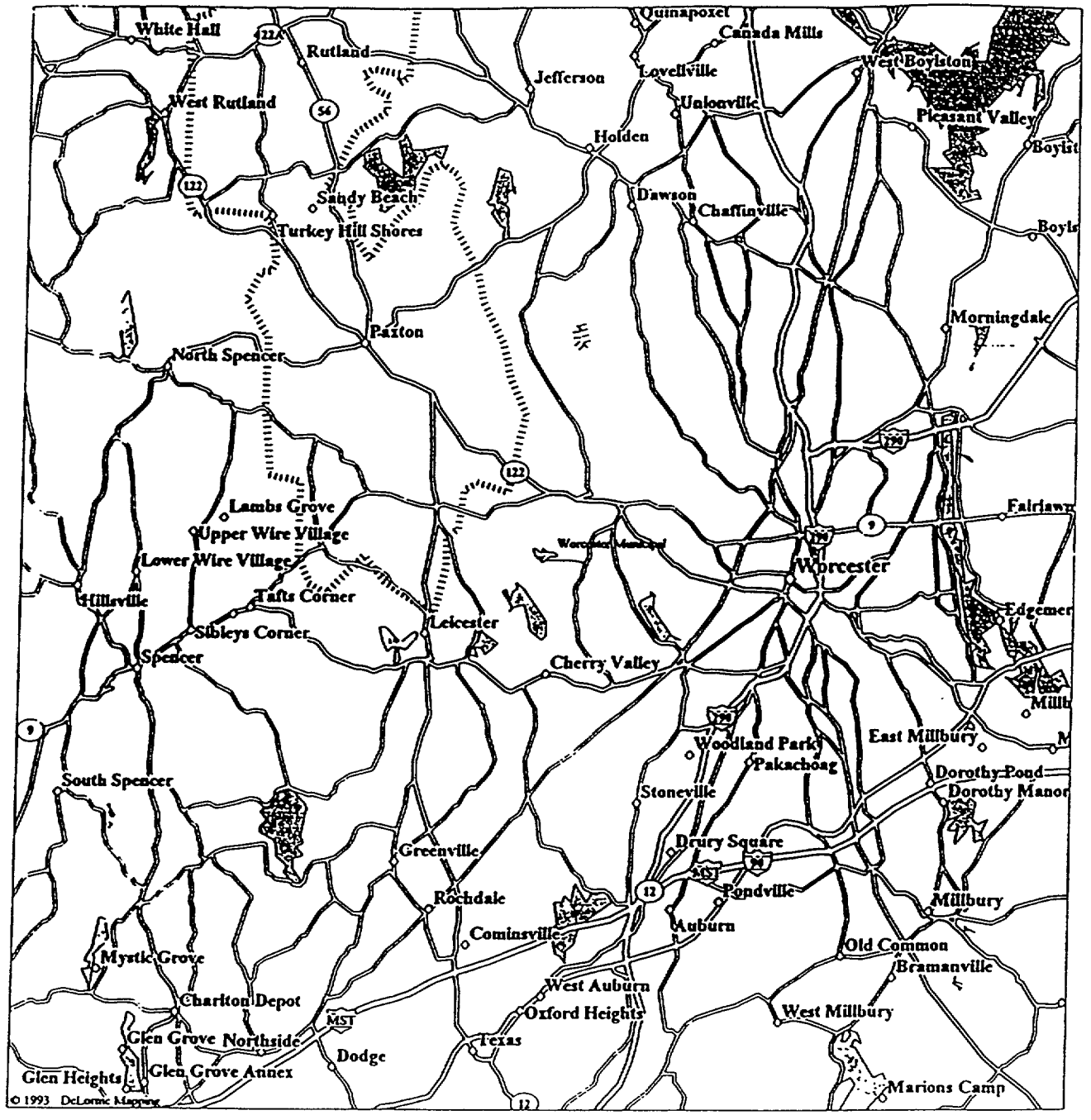

LEGEND

- Population Center
- State Route
- Town, Small City
- Large City
- Interstate, Turnpike
- Airfield
- County Boundary
- Major Street/Road
- State Route
- Interstate Highway
- US Highway
- Airfield
- Open Water
- Contour

Scale 1:125,000 (at center)

2 Miles

2 KM

Mag 12 00

Figure 36. Map of area ground Worcester Municipal Airport

For completeness, we will give one more example. Consider the WSR-74S radar of Figure 14 located above the 2400-2500 ISM band. We want to determine a Lp threshold and a worst case separation distance for this radar and an IVHS system in the 2400-2500 ISM band. As noted earlier, the WSR-74S radars are scheduled to eventually be replaced by NEXRAD (WSR-88D). From table 1, this radar type has a peak power of 87 dBm and a mainbeam gain of 38 DB. The mode of operation for the radar of Figure 14 was a pulse width of 1 us and 539PPS (Table 1). Compared to our simulation radar (DWSR-88C) with a pulse width of 0.8 us and 1063PPS, the WSR-74S will produce approximately twice as many errors. We, therefore, can reasonally approximate the required C/I ratio as 39 dB (for our BER threshold of 10"). That is, 3 dB more than the 36 dB derived earlier. From Figure 14, FDR is -90 dB for the 2400-2500 ISM band frequencies. We, therefore, obtain:

$$Lp = 39 + 35 + 87 + 38 + 13 \quad -3 \; -2 \quad -90 = 117 \text{ dB} \quad (4)$$

from Figure 35, for a frequency of 2450 MHZ, this corresponds to a required separation distance of 2.5 miles.

The above has covered an EMC analysis concerning the main form of possible interfering discrete signals (radars) to IVHS systems in the 2400-2500 and 5725-5875 MHZ ISM bands. The next section of this report reviews modeling of the overall non-Gaussian interference environment and signal processing means (both spatial and temporal) of improving performance.

5. Interference Modeling

In the previous sections, we summarized the contributors to the interference environment, especially in the 2450 and 5800 MHZ ISM bands, and presented EMC analysis procedures for

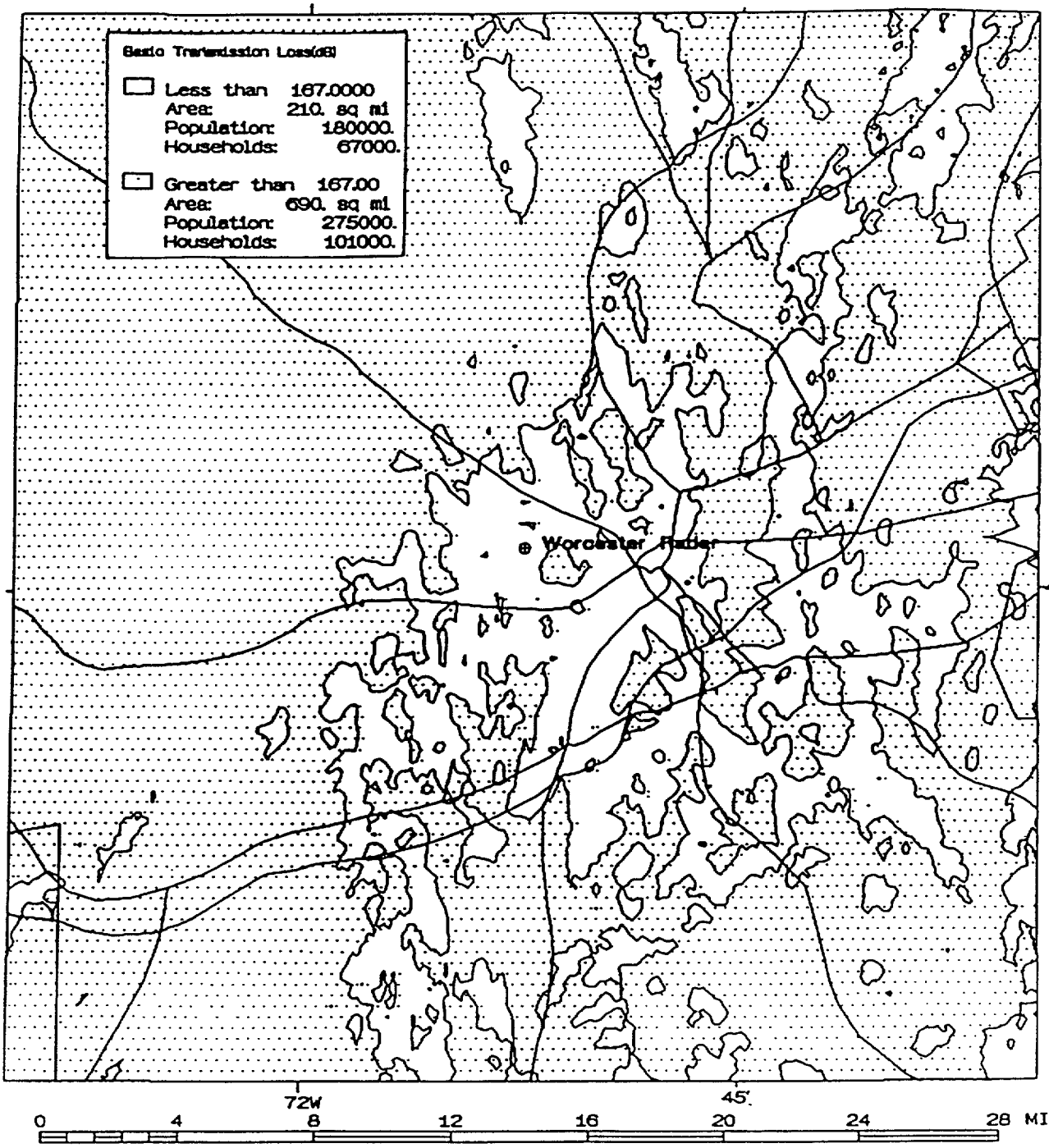

Figure 37. Propagation loss from the Worcester WSR-74C radar exceding 167 dB

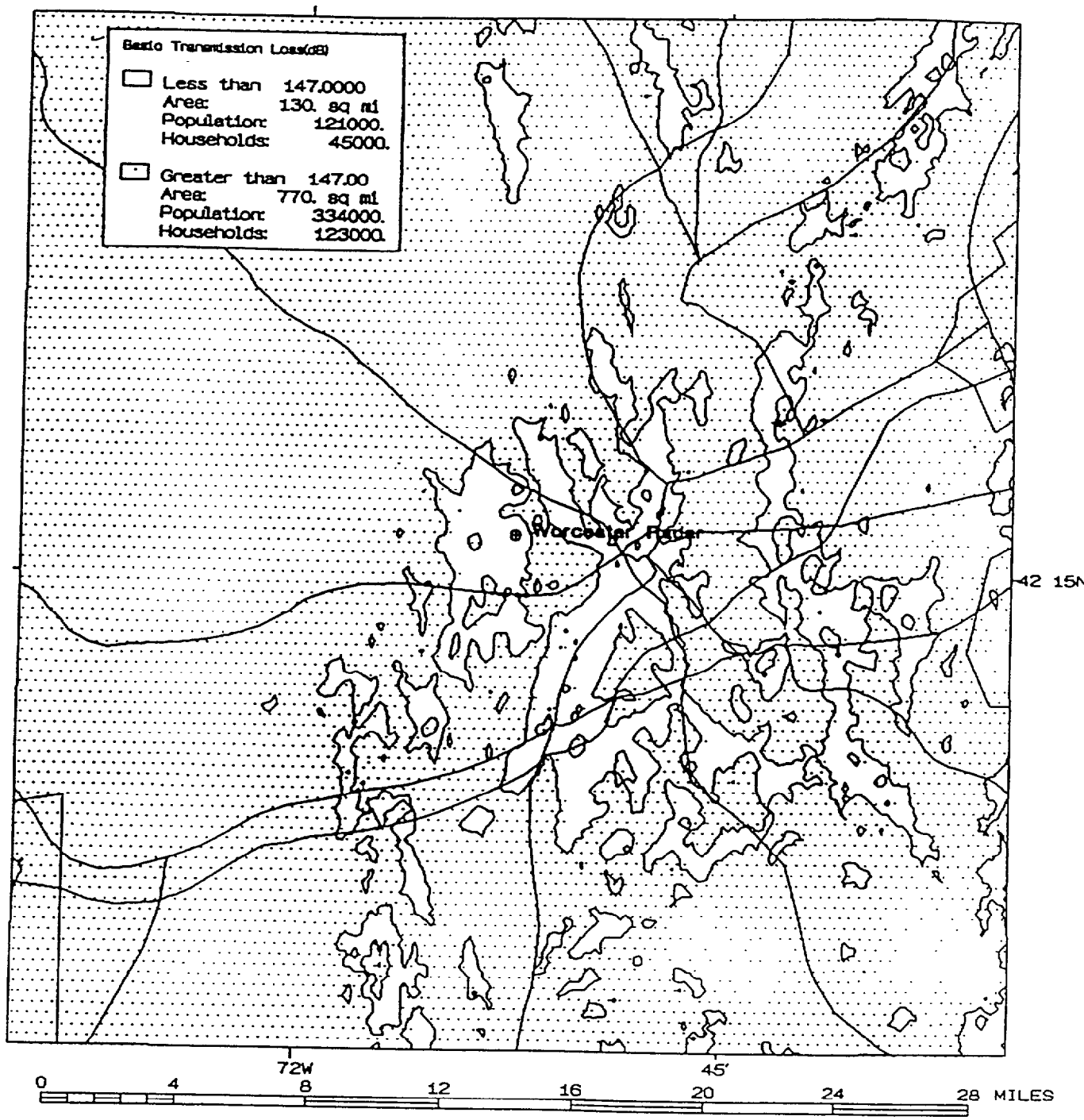

Figure 38. Propagation loss from the Worcester WSR-74C radar exceeding 147 dB

a single interfering signal. This signal was a coherent pulse train from radars, likely to be the main single source of interference to the proposed IVHS systems in the ISM bands. In this section, we want to summarize an interference model designed to represent the entire interference environment. In our case, as we saw earlier, the interference environment is likely to be composed of numerous narrowband signals, including IVHS signals of the same general type as our desired IVHS signal, as well as a low level background from sources such as automotive ignition noise. The resulting interference process is likely to be non-Gaussian. As we shall see, this means that detection techniques exist for obtaining performance improvement over the standard case of matched filter or correlation receivers (optimum of Gaussian noise) in Gaussian noise. Also, when conventional receivers are used in non-Gaussian noise, the performance can be drastically degraded, when compared to the performance in Gaussian interference. Here, for completeness, we want to briefly review an appropriate model for our case, and note what is required for appropriate interference environment measurement.

In order to guard against unacceptable performance, the true characteristics of the interference must be taken into account. To do so, we need to develop a model for the interference that fits available measurements, is physically meaningful when the nature of the noise sources, their distribution in time and space, propagation, etc., are taken into account, is directly relatable to the physical mechanisms giving rise to the interference, and is tractable for signal detection problems. One way of categorizing the EM interference environment is by defining three classes, A, B, and C as follows: Class A interference is narrowband in that it produced negligible transients in the receiver (coherent pulse trains also produce Class A interference), whereas Class B interference is “impulsive” and is characterized by overlapping transients. Class C is the sum of interferences of the other two types. Statistical-physical models for all three interference classes have been derived by Middleton. In addition to satisfying the above requirements, the models treat both narrowband and broadband interference processes. The models are parametric with parameters explicitly determined by the underlying physical mechanisms, and are canonical in that the mathematical forms do not change with changing

physical conditions. A complete description of these models, including their derivation, further motivation, and taxonomy, can be found in [22, 23, 24, and 25]. It is the Middleton Class A model that is appropriate for our cases of interest. It is of interest to note that Prasad, et al. [27] has recently used the Class A model to represent the interference environment for Personal Communications Services (PCS) and analyzed the performance of Differential Phase Shift Keying (DPSK) modulation in this interference.

We will give a brief overview of the Class A model. Further details can be found in [23, 24, and 25]. In this model, the received interference is assumed to be a process having two components:

$$X(t) = X_p(t)+X_G(t) \qquad (5)$$

where $X_p(t)$ and $X_G(t)$ are independent processes. The first component, X_p, is represented by:

$$X_p(t) = \sum_j U_j(t, \gamma) \qquad (6)$$

where U denotes the j-th waveform from an interfering source and γ represents a set of random parameters which describes the waveform scale and structure. It is next assumed that only one type of waveform,U, is generated, with variations in the individual waveforms accounted for by appropriate statistical treatment of the parameters in γ. and the generic waveform U(t) is obtained explicitly from the underlying physical mechanisms [23]. Under the assumption that the sources are Poisson-distributed in space and emit their waveforms independently according to the Poisson distribution in time, the first-order characteristic function for X_p is given by (see, e.g., [24]:

$$F(i\xi)_p = \exp\left[<AJ_o(B_o\xi) - A>\right] \qquad (7)$$

where B_o denotes the envelope of U when U is written in envelope and phase form, J_o is the Bessel function of order zero, and $<\cdot>$ denotes required statistical averages over the random epoch representing the time at which the typical j-th source emits. Doppler velocities (if any) are in the random signal parameters in γ. The quantity A is the first basic parameter of the model and will be discussed below. The second component, $X_G(t)$, is an additive stationary Gaussian background process attributable either to receiver noise or to the limit of a high density Poisson process representing the contributions of unresolvable background sources, or both. Hence, under the assumption that this background component has zero mean and variance σ_G^2, its first-order characteristic function is

$$F(i\xi)_G = e^{-\xi^2\sigma_G^2/2} \qquad (8)$$

and the overall characteristic function for the process is then given by:

$$F(i\xi)_{P+G} = F(i\xi)_p F(i\xi)_G \qquad (9)$$

which can be approximated as follows [25]:

$$F(i\xi)_{P+G} = e^{-A} \sum_{m=o}^{\infty} \frac{A^m}{m!} e^{-c_m^2\xi^2/2} \qquad (10)$$

where:

$$c_m^2 = m <B_o^2>/2 + \sigma_G^2 \qquad (11)$$

For computational purposes, it is convenient to consider the normalized variable

$$Z = X/(\langle X_G^2 \rangle + \langle Xp^2 \rangle)^{1/2} \qquad (12)$$

Transforming (10) for the normalized variable Z yields the desired probability density function (pdf):

$$p_Z(z) = e^{-A} \sum_{m=o}^{\infty} \frac{A^m}{m!\sqrt{2\pi}\sigma_m} e^{-\xi^2/2\sigma_m^2} \qquad (13)$$

here:

$$\sigma_m^2 \triangleq \frac{\frac{m}{A} + \Gamma}{1 + \Gamma} . \qquad (14)$$

The quantity Γ' is the second basic parameter of the model, and will be discussed below. Note that $P_Z(z)$ is a weighted sum of zero-mean Gaussians with increasing variance. The m=O term corresponds to the background component of the interference, whereas; all remaining terms correspond to the Poisson (impulsive) component.

The corresponding envelope exceedance probability distribution is given by:

$$Prob[E>E_o] = e^{-A} \sum_{m=o}^{\infty} \frac{A^m}{m!} e^{-E_o^2/\sigma_m^2} \qquad (15)$$

Since the phase process is uniformly distributed, it is the envelope statistics which are stressed for measurements and for the estimation of the model parameters.

As stated above, A and Γ', are the basic parameters of the model. Let us consider their definitions and physical significance:

I) A is the "Overlap Index" or "Nonstructure Index," Specifically.

$$A \triangleq \nu T_s \qquad (16)$$

where ν is the average number of emission events impinging on the receiver per second and T_s is the mean duration of a typical interfering source emission. Note that ν is simply the rate of the Poisson process underlying the impulsive part of the interference. Thus, A is a measure of the amount of temporal overlap among the interfering signals. The smaller A is, the fewer the number of emission "events" and/or their durations so that the (instantaneous) noise properties are dominated by the waveform characteristics of individual events. As A is made larger, the noise becomes less structured, i.e., the statistics of the instantaneous amplitude approach the Gaussian distribution (asymptotically as $A \to \infty$, although $A \cong 10$ is considered a large value for A). Hence, A is a measure of the "non-Gaussianness" of the noise input to the receiver.

ii) Γ' is called the "Gaussian factor." It is the ratio of the intensity of the independent Gaussian component of the input interference, σ_G^2 to the intensity Ω_{2A} of the non-Gaussian component, i.e.,

$$\Gamma' \triangleq \langle X_G^2 \rangle / \langle X_p^2 \rangle = \frac{\sigma_G^2}{\Omega_{2A}} \quad \text{where } \Omega_{2A} \triangleq A \langle B_o^2 \rangle / 2 \; . \qquad (17)$$

By adjusting the parameters A and T', the density (13) or the envelope distribution (15) can be made to fit a great variety of non-Gaussian noise distributions. In particular, the Class A model is appropriate for interference caused by collections of intentionally radiated signals, including coherent pulse trains. Figure 39 shows an example of the Class A interference envelope distribution from (15) for $T' = 10^{-4}$ and various A. It also shows the Rayleigh (envelope of Gauss) limit.

When performing measurements of the interference environment, it is usually the envelope distribution that is measured. As noted earlier, other needed statistics for system design and analysis can be obtained for the envelope distribution. These include the pdf of the instantaneous amplitude, the rms level (relatable to field strength), etc. Also, a great deal of effort has gone into developing efficient estimation methods of the Class A parameters from measured data [28, 29, and 30].

Figure 39 shows the envelope distribution for Class A interference for $T' = 10^{-4}$ and various A from (15). The exceedence distributions are given relative to their rms levels. As noted above, as A increases, we approach the Rayleigh (envelope of the Gaussian process) limit. Figure 40 shows the performance of the "standard" (optimum for Gaussian noise) CPSK receiver in Class A noise, again for $T' = 10^{-4}$ and various A.When we have a non-Gaussian noise process, improvement, sometime great improvement can be achieved. In developing "optimum" systems, the threshold signal approach is taken in that if the signal is "small enough" and the time bandwidth product large enough optimum receivers can be realized. These receivers generally take the form of current receivers (based on white Gaussian noise) proceeded by one or more particular adaptive nonlinearities. Such receivers approach true optimality for small signal levels and often perform 20 or 30 dB better than current receivers at all signal levels [31]. Figures 40 and 41 show examples of the performance improvement achievable for one sample of Class A non-Gaussian interference. The first figure gives the probability of detection for various false alarm probabilities. On Figure 40, the parameter L denotes the limiting performance gain achievable [31]. Figure 41 shows results (simulation)

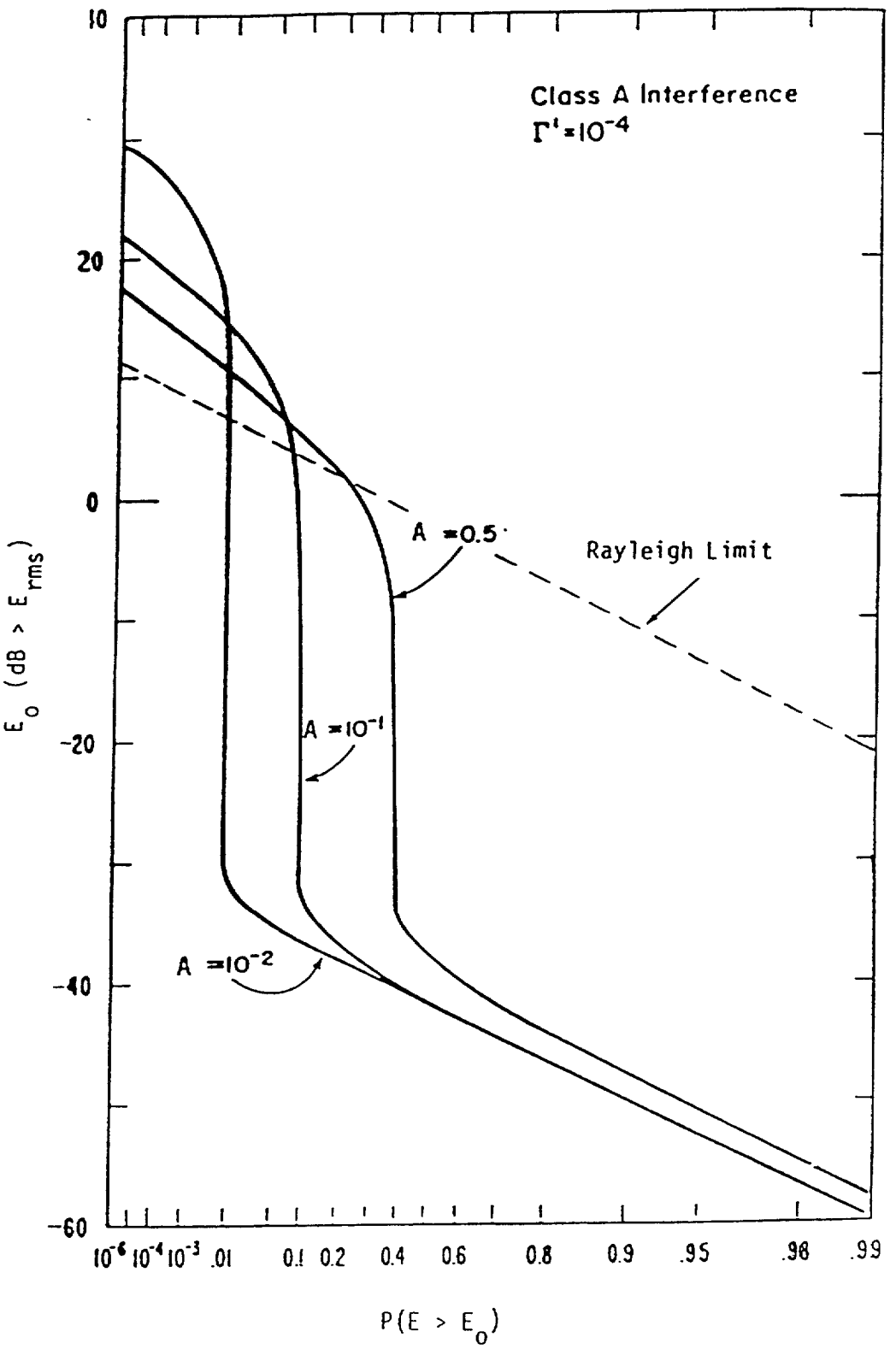

Figure 39. The envelope distribution for Class A interference for $\Gamma' = 10^{-4}$ and various A from (15)

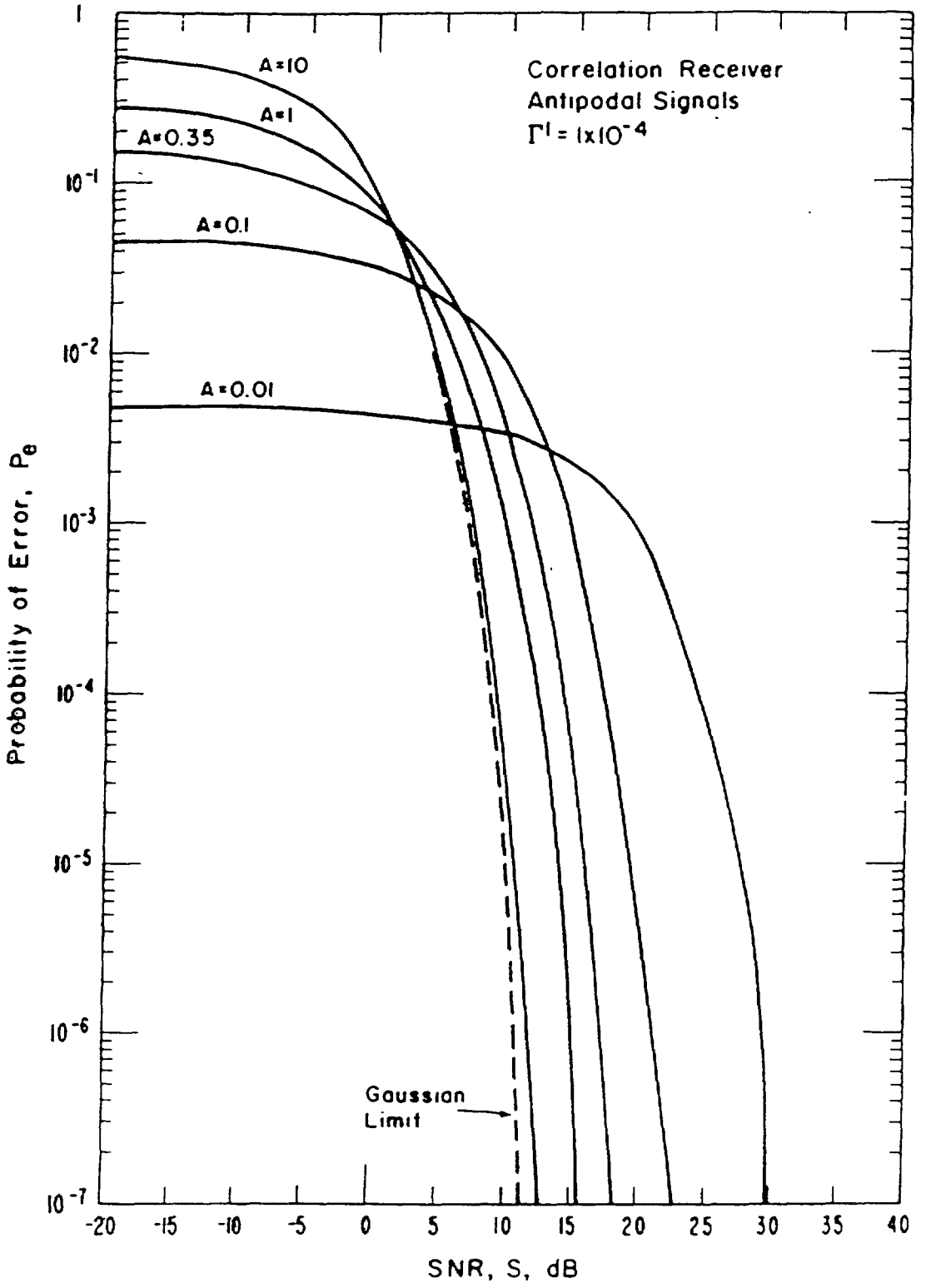

Figure 40. Performance of the correlation receiver (Gaussian optimum receiver) in Class A interference for $\Gamma' = 10^{-4}$ for various values of the impulsive index A

for a binary CPSK system including results for various suboptimum detectors for the case of N= 10 and 100 independent samples in each detection interval (baud). Note that here the performance can quickly degrade if the signal is not “small enough.”

Large gains are achievable only if the number of independent received waveform samples is relatively large for each detection interval. One way to overcome the requirement for a large number of temporal samples is to use both spatial and time sampling. This has required the development of detection and extraction algorithms appropriate for interference fields and the expansion of the earlier, physical-statistical, non-Gaussian interference models to vector/tensor nonuniform electromagnetic signal and interference field (both near and far) models. These models play the central role in the structure of optimal threshold detection, extraction, and estimation algorithms.

In many applications of threshold, or weak-signal detection theory, it is reasonable to postulate independent interference samples, particularly for time-sampling procedures. In addition, independent samples are often postulated in order to avoid intractable analytic difficulties when the interference is non-Gaussian, and attempts are made to approximate such idealized situations. The problem becomes acute in many cases when spatial sampling in nonuniform interference is involved, because it is usually not possible to position the sensors of practical arrays sparsely enough to achieve spatial independence and still maintain coherence in the desired signal field across the array. Account must be taken of the fact of correlated samples in order to obtain optimal or near-optimal processing algorithms. When this is done, improved performance is obtained over that of processors optimized for uncorrelated noise samples when the latter are employed in correlated interference.

When the correlated interference fields cannot be sampled at statistically independent intervals, either in space or time, or both, use of threshold algorithms that are optimal for independent samples can be very suboptimum. Accounting for the first-order correlations can greatly

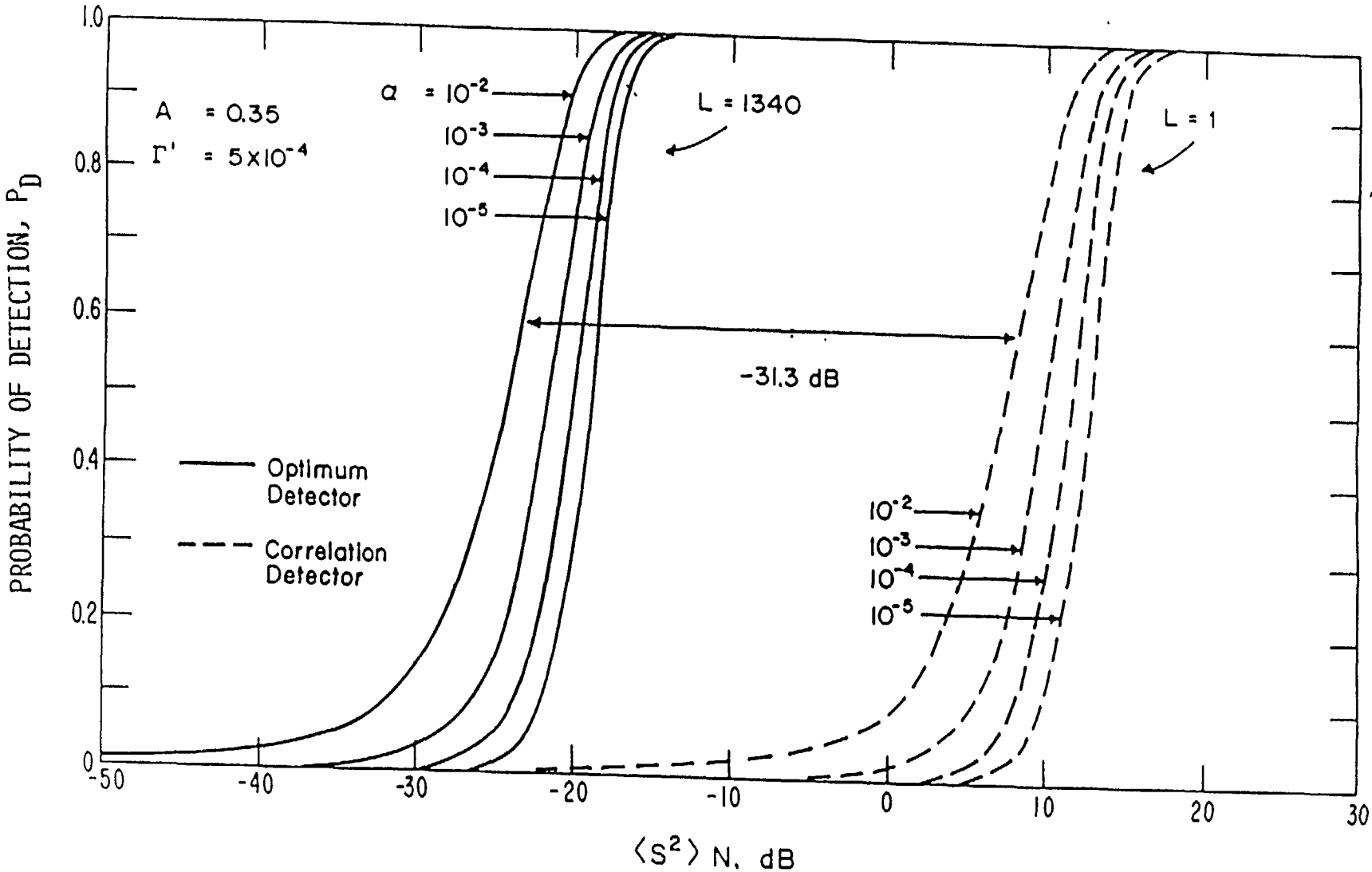

Figure 41. Probability of signal detection P_D for threshold coherent detection with fixed false alarm probabilities $\propto$ for optimum and coherent receivers in a sample of Class A interference

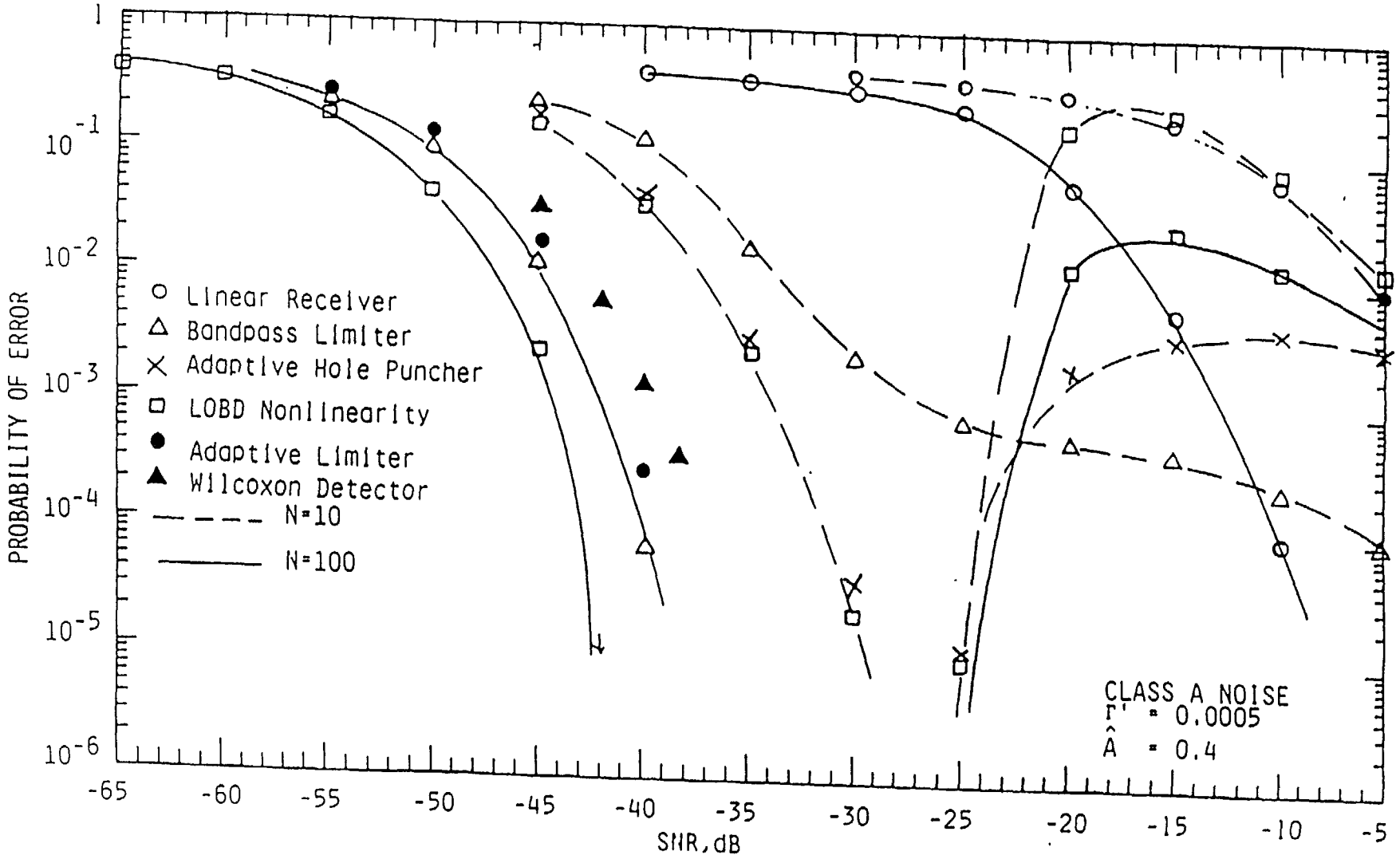

Figure 42. Simulation results with Class A interference, N = 10 and 100, binary CPSK and constant signal, for the linear receiver, various non-linearities (including the optimum, termed LOBD) and nonparametric detectors

improve performance, albeit at the expense of considerably more complex threshold algorithms [31 and 32].

In addition to the gains achievable by the optimal temperal and spatial processes noted above, Personal Communication Systems and IVHS Communication and Toll Collection Systems can utilize the interference reduction and spectrum conservation benefits of adaptive antennas. These systems when using conventional antennas must operate on separate radio frequencies to avoid interfering with each other. If these systems were to use an adaptive antenna, they would be able to operate on the same radio frequency by virtue of the multiple nulls formed by the antennas in the directions of interference. Multiple beam antennas can also provide these advantages.

One type of adaptive antenna is the steerable-nulling antenna processor (SNAP). It consists of an array of radiating elements and a real-time adaptive receiver processor. The array of radiating elements can have a linear, conformal, or circular geometry. When given a beam steering command, the system will simultaneously sample the current environment for interference, jamming, and the desired signal. The system then proceeds to adjust the element control weights in phase and amplitude to attain one form of optimum condition such as maximum signal-to-interference-plus-noise) ratio using a particular adaptive algorithm. The optimum weighting condition produced via this algorithm usually forms some degree of nulling in the directions of interference. This is termed adaptive interference nulling. The complete operation of the adaptive antenna array is equivalent to a spatial filter.

One implementation of an adaptive array is capable of forming n-l nulls where n is the number of array elements of the antenna. It is possible to null more than n-l interferers when either multiple interferers are located at the same angular direction or the interferers possess symmetry in angle. This depends on the scenario, which in general may not provide these conditions most of the time. An N element antenna has N degrees of freedom. Assuming a worst case scenario, one of these degrees of freedom is required to form the mainbeam and the

remaining N-l degrees of freedom can be used to form N-l nulls in the directions of interference. In addition to the interference nulling and mainbeam gain, the correlation in the remaining interference field can also be used to achieve additional gain [32].

6. Summary and Conclusions

It has been the purpose of this report to investigate the suitability of the 2.45 and 5.8 GHz ISM bands for IVHS systems. The study started by summarizing the natural background noise and man-made noise levels in these two bands. The background noise in the 2400-2500 MHZ band is due to automotive ignition systems and microwave oven (and other ISM devices) radiations. These two sources are of comparable levels in urban areas. In urban areas, the peak levels in this band are some 10-20 dB higher than adjacent to this band. Even so, the levels are not high enough to cause any appreciable interference to short range directed communications systems such as those envisioned by IVHS. The background is quite low in the 5725-5875 MHZ band, especially since there is currently no ISM equipment operating in this band.

Interference to IVHS systems in these bands can only come from intentionally radiated signals, i.e., from authorized (licensed) transmissions, or from a combination of the intentional signal, and the background. The main source of potential interference within the bands are radiolocation (radar) signals. However, both bands are reserved for radiolocation use by the military services. These radars are located in remote areas and operate intermittently. Even so, these were broadly treated by our EMC analysis. There are numerous S-band weather radars located immediately above the 2400-2500 MHZ ISM band and C-band radars located immediately below the 5725-5875 MHZ ISM band. The majority of these radars, both Government and non-Government, use magnetron output tubes and have the potential of causing interference within our bands via spurious emissions. The majority of new Government ground-based weather radars will use klystron output tubes, which typically have spurious emissions levels 50 dB lower than the existing radars using magnetron output tubes.

The Government is procuring two new types of radars, the Next Generation Radar (NEXRAD, WSR-88D) (2700-2900 MHZ) and the Terminal Doppler Weather Radar (TDWR) (5600-5650 MHZ). The NEXRAD is replacing the majority of the existing Government weather radars, both S-band and C-band. The NEXRAD and TDWR will be deployed in the 1994-1996 time frame. The majority of new (as well as old) non-Government ground-based weather radars are expected to use magnetron output tubes, so will continue to have the potential to cause interference.

An EMC analysis was performed considering primarily a non-Government WSDR-88CTV radar, although the existing C-band and S-baud Government radars as well as the inband military radars were covered. The analysis was to determine a worst case separation distance required between the radar and a generic IVHS receiver. For the military radar (on frequency) this worst case distance was 40 miles. For the non-Government WSDR-88CTV, an example of the required separation distance was 7 miles and for an example Government WSR-74C radar the required distance was 17 miles. If the IVHS system was within the derived worst case separation distance, a more detailed analysis for the particular case is required. An example of this was shown for the "17 mile" WSR-74C radar. The analysis using actual terrain in the propagation model, etc., showed, in the example case at least, the IVHS system could, in general, be quite close to the radar, well within the "17 miles." The main objective was to give an EMC analysis technique for IVHS systems and pulsed radar interference.

We have seen that both ISM bands considered are suitable for IVHS systems. For the 2400-2500 MHZ band, presently the lower sub-band is the most suitable, the middle sub-band being occupied by microwave ovens. After the NWS S-band radars are replaced by NEXRAD, the upper segment of this band should be much more usable. The 5725-5875 MHZ band is very suitable, being in general, free of interference. No ISM equipment are currently operating in this band, and the out-of-band radars produce interference only for quite near systems. This will be especially true when the NWS C-band radars are replaced by NEXRAD. Also, this band is to be used by Europe for its IVHS systems.

In order to analyze or design communications systems for the real-world non-Gaussian interference environment, such as exists in the two ISM bands, an appropriate interference model is required. This report included a summary of such a model (Middleton's Class A Model) along with measurement specifications required to determine the physical-statistical parameter of the model. Examples of generic system performance using the model were included along with signal processing techniques (both temper-al and spatial) to improve performance in the non-Gaussian interference.

References

[1] Spaulding, A.D., The roadway natural and man-made noise environment, IVHS Journal, Vol. 2, No. 2, April, 1995.

[2] Shumpert, T.H., M.A. Hannell, and G.K. Lott, Jr., Measured Spectral amplitude of lightning Sferics in the HF, VHF, and VHF bands, IEEE Transactions of Electromagnetic Compatibility. Vol. EMC-24, pp. 368-369, August 1982.

[3] Yamanaka, Y., and A. Sugiura, Measurements of automotive radio noise in lower frequency microwave bands (l-3 GHz), Symposium Record, International Symposium on Electromagnetic Compatibility, pp. 352-357, September 8-10, 1989, Nagoya 464, Japan.

[4] Shepherd, R. A., J.C. Gaddie, and Aki Shohara, Measurement parameters for automobile ignition noise, Final Report, SRI Project 3950, June 1975.

[5] Osepchuk, J.M., A history of microwave heating applications, IEEE Transactions on Microwave Theory and Techniques, Vol. MTT-32, No.9, September 1984.

[6] Watson, R.T., Spectrum Resource Assessment in the 2300-2450 MHZ Band, NTIA Report 81-78, Natural Telecommunications and Information Administration, Washington, D. C., September 1981.

[7] Gawthrop, P.E., F.H. Sanders, K.B. Nebbia and J.J. Sell, Radio Spectrum Measurements of Individual Microwaves Ovens, Vol. 1, NTIA Report 94-303-l) March 1994.

[8] Gawthrop, P.E., F.H. Sanders, K.B. Nebbia and J.J. Sell, Radio Spectrum Measurements of Individual Microwave Ovens, Vol. 2, NTIA Report 94-303-2, March 1994.

[9] Watson, R.T., Spectrum Resource Assessment in the 2300-2450 MHZ Band, NTIA Report 81-78, National Telecommunications and Information Administration, Washington, D. C., September 1980.

[10] Hoffman, J.R., A.D. Spaulding, and M.G. Cotton, IVHS Roadway Environment, informal ITS Report.

[11] Matheson, R.J., and F.K. Steele, A preliminary look at spectrum requirements for the fixed services, ITS Staff Study, May 1993.

[12] Grant, W.B., et al. Spectrum Resource Assessment in the 5650-5925, MHZ band, NTIA Report 83-l 16, National Telecommunications and Information Administration, Washington, D. C., January 1983.

[13] ASTM Exxx-xx, Standard for dedicated, short range, two-way vehicle to roadside communications equipment, American Society for Testing and Materials Standards Committee, Draft 4, April 28, 1994.

[14] IVHS America, Electronic Toll and Traffic Management (ETTM) user requirements for future national interoperability, Draft Version 2.0, April 19, 1994.

[15] Scott, H., K. Stouffer and P. Rowe, MST Robot System Division Report, Recommendations on selection of vehicle-to-roadside communications standard for commercial vehicle operations, no date.

[16] Davis, D.T., A vehicle-to-roadside communications national standard for commercial vehicle main line sorting Lawrence Livermore National Laboratory Report, March 1, 1994.

[17] Pietrzyk, M.C. and E.A. Mierzejewski, NCHRP Synthesis of Highway Practice 194, Electronic Toll and Traffic Management (ETTM) systems, Transportation Research Board, National Research Council, National Academy Press, Washington, D. C., 1993.

[18] Gawthrop, P.E. and G.M. Patrick, Ground-based weather radar compatibility with digital radio-relay, microwave systems, NTIA Report 90-260, March 1990.

[19] Berman, T. And T. Kaplan, Advanced coding techniques study for TDRS/TDRS IL systems. Stanford Telecom Report Stel 003R1493, April 23, 1993.

[20] Slcylar, B., Digital Communications, Fundamentals and Applications, Prentice Hall, Englewood Cliffs, NJ 07632, 1988.

[21] Hufford, G.A., A.G. Longley and W.A. Kissick, A guide to the use of the ITS irregular terrain model in the area prediction mode, NTIA Report 82-100, April 1982.

[22] ITS, Telecommunication Analysis Services User Guide, informal NTIA Report, July 1988.

[23] Middleton, D., Statistical-physical models of urban radio-noise environments - Part 1: Foundations, IEEE Transactions Electromagnetic Compatibility, Vol. EMC-14, No. 2, pp. 38-56, 1972.

[24] Spaulding, A.D. and D. Middleton, Optimum reception in an impulsive Interference environment. Office of Telecommunications Technical Report 75-67, June 1975 (NTIS Order #COM75_11097/AS)

[25] Middleton, D., Canonical and quasi-canonical probability models of Class A interference. IEEE Transactions Electromagnetic Compatibility, Vol. EMC-25, No. 2, pp. 76-106,
May 1983.

[26] Middleton, D. And A.D. Spaulding, A tutorial review of elements of weak Signal detection in non-Gaussian EMI environment, National Telecommunication and Information Administration (NTIA), U. S. Department of Commerce, NTIA Report 86-194, May 1986.

[27] Prasad, R., A. Kegal and A DeVos, Performance of Micro cellular mobile radio in a cochannel interference, natural, and man-made noise environment. IEEE Transactions on Vehicular Technology, Vol. 42, No. 1, pp. 3340, February 1993.

[28] Middleton, D., Procedures for determining the parameters of the first-order canonical models of Class A and Class B electromagnetic interference, IEEE Transactions Electromagnetic Compatibility, Vol. EMC-21, No. 3, pp. 190-208, August 1979.

[29] Zabin, S.M. and H.V. Poor, Recursive algorithms for identification of impulsive noise channels, IEEE Transactions on Information Theory, Vol. 36, No. 3, pp. 559-578, May 1990.

[30] Zabin, S.M., and H.V. Poor, Efficient estimation of Class A noise parameters via the EM Algorithm. IEEE Transactions on Information Theory, Vol. 37, No. 2, pp. 60-72, January 1991.

[3 l] Middleton, D. And A.D. Spaulding , Elements of Weak Signal Detection in Non-Gaussian Noise Environments, in Advances in Statistical Signal Processing, V. Poor and J.I. Thomas editions, Vol. 2, Signal Detection, JAI Press, Inc, Greenwich, Connecticut, 1993.

[32] Middleton, D. Threshold detection and estimation in correlated interference, proceedings of the 10th International Symposium on Electromagnetic Compatibility, Zurich, March 12-14, 1991.

NTIA FORMAL PUBLICATION SERIES

NTIA MONOGRAPH

A scholarly, professionally oriented publication dealing with state-of-the-art research or an authoritative treatment of a broad area. A monograph is expected to have a long lifespan.

NTIA SPECIAL PUBLICATION

Information derived from or of value to NTIA activities such as conference proceedings, bibliographies, selected speeches, course and instructional materials, and directories.

NTIA HANDBOOK

Information pertaining to technical procedures: reference and data guides, and formal user's manuals that are expected to be pertinent for a long time.

NTIA REPORT

Important contributions to existing knowledge but of less breadth than a monograph, such as results of completed projects and major activities, specific major accomplishments, or NTIA-coordinated activities.

NTIA RESTRICTED REPORT

Contributions that fit the NTIA Report classification but that are limited in distribution because of national security classification or Departmental constraints. This material receives full review and quality control equivalent to the open-literature report series.

NTIA CONTRACTOR REPORT

Information generated under an NTIA contract or grant and considered an important contribution to existing knowledge.

SPONSOR-ISSUED REPORTS

NTIA authors occasionally produce reports issued under an other-agency sponsor's cover. These reports generally embody the criteria of the NTIA Report series.

For information about NTIA publications. contact the Executive Office at 325 Broadway, Boulder, Colorado 80303 (telephone: 303-497-3572).